



**UiT** The Arctic University of Norway

Department of Pharmacy

## **Mercaptoalkonol-derived self-immolative linkers for bioconjugates**

Synthesis and analysis

Myagmarsuren Sengee

Master's thesis in Pharmacy FAR-3911 December 2020





## **Acknowledgements**

I would like to thank Associate Professor Terje Vasskog for being an excellent supervisor and for helping and guiding me to the advanced instruments at Barents Biocentre Lab.

My thank also goes to Dr. Johann Eksteen for the valuable discussions we had during the project and for helping me in solid phase peptide synthesis.

I would also like to express my gratitude towards my seniors and leaders at my employer Norce Norwegian Research Centre AS for giving me flexibility to combine the work and the pharmacy study over long period of time.

## Abstract

This project was a part of research project run at Norce Norwegian Research Centre As in collaboration with UiT-The Arctic University of Norway.

Many of the anticancer compounds discovered through synthesis or bioprospecting activities are found to be equally toxic to healthy cells and tumors. Consequently, these compounds are not considered as promising drug candidates worthy of further study. This project seeks to develop a novel chemical toolkit that can be utilized to increase the therapeutic value of such toxic compounds by decreasing the number of potential anticancer compounds that are sidelined. Several prodrug strategies exist whereby compounds can be chemically modified in such a manner that their selective transport and delivery to cancer cells becomes possible. However, a key requirement is that these modifications are temporary in their nature. One such strategy is to reversibly link cytotoxic compounds to a tumor homing delivery vector via a self-eliminating linker. The focus of this project was on the design and synthesis of a set, or toolkit, of heterobifunctional self-eliminating linkers that can be utilized in prodrug synthesis. A series of self-immolative linkers containing a thiol-reactive group at one end and a hydroxyl- or amine-reactive group at the other have been prepared from mercaptoalkonols. The utility of these reagents for preparations of bioconjugates has been explored by reacting the linkers with appropriately functionalized model drugs and peptides. Degradation studies of a series of conjugates with different linkers reveal that the structure of the linkers has a significant impact on their stability.

# Table of contents

ACKNOWLEDGEMENTS	i
ABSTRACT	ii
TABLE OF CONTENTS	iii
<b>1. INTRODUCTION</b>	
1.1. Brief about cancer	1
1.2. Cancer chemotherapy	1
<b>2. THEORETICAL BACKGROUND</b>	
2.1. Prodrug strategy in cancer therapy	3
2.2. Types of delivery vectors	3
2.3. Types of linkers	4
2.4. Biological basis of tripartite prodrug strategy	5
2.5. Principles of the analytical techniques used in this study	7
<b>3. AIM OF THE THESIS</b>	11
<b>4. METHODS AND MATERIALS</b>	
4.1. General	14
4.2. Synthesis of peptide	15
4.3. Synthesis of linkers	15
4.4. Synthesis of Cargo-Linker conjugates	17
4.5 Synthesis of Cargo-Linker-Vector conjugates	19
4.6. Degradation analysis	20

<b>5. RESULTS AND DISCUSSIONS</b>	
5.1. Preparation of linkers and conjugates	21
5.2. Cargo release analysis	38
<b>6. CONCLUSION</b>	46
<b>REFERENCES</b>	47
<b>APPENDIX</b>	
Appendix I: NMR spectra for characterized compounds	53
Appendix II: Data for degradation analysis	78

# **1. Introduction**

## **1.1. Brief about cancer**

Cancer is a disease caused by an uncontrolled division of abnormal cells in a part of the body and it can affect almost all part of the human body. Normally, human cells grow and divide to form new cells as the body needs them. When cells grow old or become damaged, they die, and new cells take their place. When cancer develops, however, this orderly process breaks down. As cells become more and more abnormal, old or damaged cells survive when they should die, and new cells form when they are not needed. These extra cells can divide without stopping and may form growths called tumors. Many cancers form solid tumors, which are masses of tissue. Cancers of the blood, such as leukemias, generally do not form solid tumors. Cancerous tumors are malignant, which means they can spread into, or invade, nearby tissues.<sup>1</sup> In addition, as these tumors grow, some cancer cells can break off and travel to distant places in the body through the blood or the lymph system and form new tumors far from the original tumor. This is called metastasis.<sup>2</sup>

Cancer cells differ from normal cells in many ways that allow them to grow out of control and become invasive. One important difference is that cancer cells are less specialized than normal cells. That is, whereas normal cells mature into very distinct cell types with specific functions, cancer cells do not. This is one reason that, unlike normal cells, cancer cells continue to divide without stopping.

According to World Health Organization, cancer is the second leading cause of death globally, and is responsible for an estimated 9.6 million deaths in 2018. Globally, about 1 in 6 deaths is due to cancer.<sup>3</sup>

## **1.2. Cancer chemotherapy**

The therapeutic strategy of cancer has been changed over time. For example, radical mastectomy was used to treat breast cancer for 90 years, between 1891 and 1981. However, the use of radical surgery was immediately reduced after it was confirmed that systemic adjuvant therapy, in combination with local surgery, showed similar results. Systemic adjuvant therapies include radiation and the application of cytostatic drugs (chemotherapy), and are required for the treatment of cancer dissemination and metastasis.<sup>4</sup>

Chemotherapy, the use of cytotoxic compounds, is currently considered to be a type of standard cancer therapy.<sup>5</sup> In the late 1970s, bleomycin, vinblastine and cisplatin were novel drugs used in chemotherapy. Despite side effects and low effectivity, several cytostatic small molecular drugs have been approved since then.<sup>6</sup>

As discoveries have been made in molecular biology and immunology and the scientific basis of cancer metastasis has been thoroughly explored, novel types of cancer treatment have been developed.<sup>7</sup> These include targeted therapies via small molecule inhibitors or monoclonal antibodies (mAbs). However, chemotherapy is still dominating in cancer therapy and the searches for cytotoxic or cytostatic compounds that effectively kill cancer cells or stop cell division are done through different activities such as bioprospecting.

Many compounds possessing cytotoxicity towards cancerous cells are found to be equally toxic to healthy cells. Consequently, these compounds are not considered as promising drug candidates worthy of further study. However, the therapeutic value of such toxic compounds can be increased by utilizing bioconjugate strategies, in other words, by temporary chemical modifications.



## **2. Theoretical background**

### **2.1. Prodrug strategy in cancer therapy**

It has been shown that the cytotoxicity of some anticancer drugs can be modulated by masking certain functional groups. For example, when the hydroxyl group of camptothecin is masked nearly all cytotoxic activity is lost.<sup>8</sup> These temporarily modified and inactivated drugs are often referred to as prodrugs. After parenteral administration (e.g. intravenous injection), the inactive prodrug will be distributed throughout the body without killing healthy cells. However, once the prodrug reaches its target and is taken up by the tumor, the temporary modifications are removed by reactions with compounds in the tumor and the toxicity of the anticancer drug is fully restored, resulting in the selective killing of cancer cells. This strategy has already been validated and currently there are several anticancer prodrugs in clinical use.<sup>9</sup>

In such prodrug strategies, drug compounds can be chemically modified in such a manner that their selective transport and delivery to cancer cells becomes possible. However, a key requirement is that these modifications are temporary in their nature. One of such strategies is the conjugation of a therapeutic cargo (drug) to a delivery vector that is capable of homing to a desired site of action. These bioconjugates have taken many forms which include antibody-drug conjugates (ADC),<sup>10,11</sup> peptide-drug conjugates (PDC)<sup>12,13</sup> and small ligand-drug conjugates (LDC).<sup>14-16</sup> Structurally, they can be described as tripartite compounds that consist of (i) a delivery vector, (ii) a therapeutic cargo, and (iii) a linker moiety to conjugate the aforementioned components. Despite having similarities in their general architecture, there is considerable variation in the individual components in existing therapeutic bioconjugates.

### **2.2. Types of delivery vectors**

Several types of delivery vectors are being investigated. Antibodies remain the most common type of delivery vector. But, despite committing enormous resources to research and development, few anticancer ADCs are currently enjoying market approval.<sup>17,18</sup>

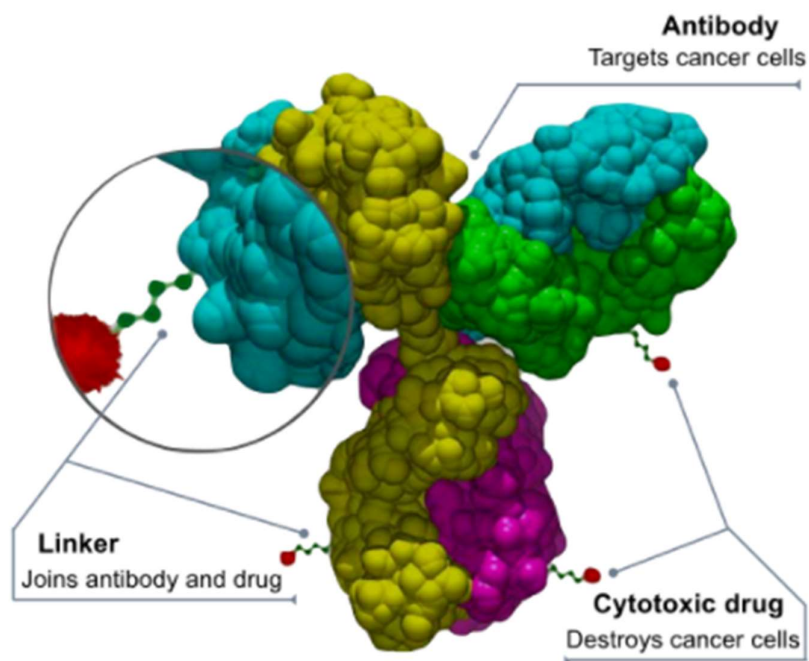


**Figure 1.** Schematic structure of an ADC (adopted from reference 19)

Peptides offer several advantages over antibodies<sup>20</sup> and PDCs have consequently become an emerging class of bioconjugates<sup>13</sup> with applications within drug delivery and theranostics. Usually peptides are used for their ability to cross cellular<sup>21-23</sup> and mitochondrial<sup>24</sup> membranes whilst conjugated to a cargo. Ligands of receptors that are overexpressed on cancer cells have also received a fair amount of attention. Prominent examples of such receptors are folate,<sup>25-28</sup> integrin,<sup>29</sup> and transferrin.<sup>30</sup> LDCs have not yet made it into the clinic, but several are being assessed in clinical trials.<sup>15</sup>

Cargo types reported in the literature also vary greatly. Although cytotoxic payloads for cancer therapy continue to dominate, probes for imaging purposes<sup>21,24</sup> and non-toxic therapeutic agents such as protein kinase agonists,<sup>31</sup> enzyme inhibitors,<sup>32</sup> and antibiotics<sup>33</sup> are also being investigated.

### 2.3. Types of linkers

The choice of linker obviously influences the therapeutic effect of the bioconjugates and since a “one-size-fits-all” solution does not exist a plethora of different linkers have been developed.<sup>34-41</sup> Broadly speaking, linkers can be classified as non-cleavable<sup>35</sup> and cleavable.<sup>36</sup> For cargoes that must be in a free unmodified form<sup>21,37-39</sup> to induce the desired effect, the latter type is the only viable option. Several options are available, with pH-sensitive, enzymatically-cleavable and thiol-sensitive linkers most commonly used.<sup>40</sup>

In many ways, thiol-sensitive linkers, in particular those containing a disulfide bond, offer a good solution for cargo-releasing bioconjugates.<sup>41</sup> Plasma is an oxidative environment with low amounts of free thiols, while the cytoplasm of the (target) cells contains high levels of thiols, e.g. reduced glutathione (GSH).<sup>42,43</sup> This large difference in thiol concentration can be exploited to trigger cargo release at the target site, thereby ensuring an improved therapeutic index. In reality, though, disulfide linkers appear to be prone to premature cleavage, resulting in unwanted side effects.<sup>42</sup> Recent efforts have, therefore, focused on improving the stability of disulfide linkers. It has been demonstrated that by introducing steric hindrance next to the disulfide bond, premature thiol-disulfide exchange reactions become slower and linker stability subsequently increased.<sup>44-46</sup> Similarly, it was reported in the case of ADCs that the site of conjugation can significantly affect the plasma stability of the disulfide bond.<sup>47,48</sup> It should be noted that although disulfide bonds are cleavable, their use does not necessarily result in the release of the native cargo. However, it has previously been shown that disulfide linkers can be designed as self-immolative moieties which yield the free cargo in its native form following a tandem process, whereby an initial thiol-disulfide exchange is followed by an intramolecular reaction.<sup>15,22,23,39</sup>

## **2.4. Biological basis of tripartite prodrug strategy**

Many prodrug strategies, each with their own advantages and disadvantages, have so far been developed. A prodrug approach based on a tripartite model (i.e. consists of the three components, vector, linker and drug) is proposed, where the active drug is attached to a delivery vector via a releasable linker.

- The vector. This component acts as a homing device that directs the prodrug to the target site, the tumor. The vector can, for example, be an antibody that specifically targets a certain tumor antigen that is only found on tumor cells. Antibodies attach themselves to the antigens on the surface of cancerous cells. This can also be a peptide, for example a histidine-rich peptide that is capable of homing to the low pH conditions found in solid tumors.
- The linker. This component has three functions. Firstly, it is a releasable connection between the vector and drug. Secondly, by attaching the linker to an essential functional group it should mask the drug cytotoxicity until the prodrug reaches the tumor. Thirdly, it will facilitate the drug's transport across the target cell membrane towards its intracellular target.
- The drug. This component is responsible for the anticancer activity. The ideal candidates for this study are highly cytotoxic, small compounds (< 1000 Da) containing either a hydroxyl or

an amino group in its structure. Although the cytotoxic activity does not need to be selective (i.e. killing only cancer cells), it is required that the compound's mechanism of action is dependent on the aforementioned hydroxyl group or amino group to be free and that the site of action is intracellular. Based on previous studies,<sup>49</sup> the proposed mechanism of action for a peptide tripartite prodrug can be summarized in a stepwise manner, in Figure 2.

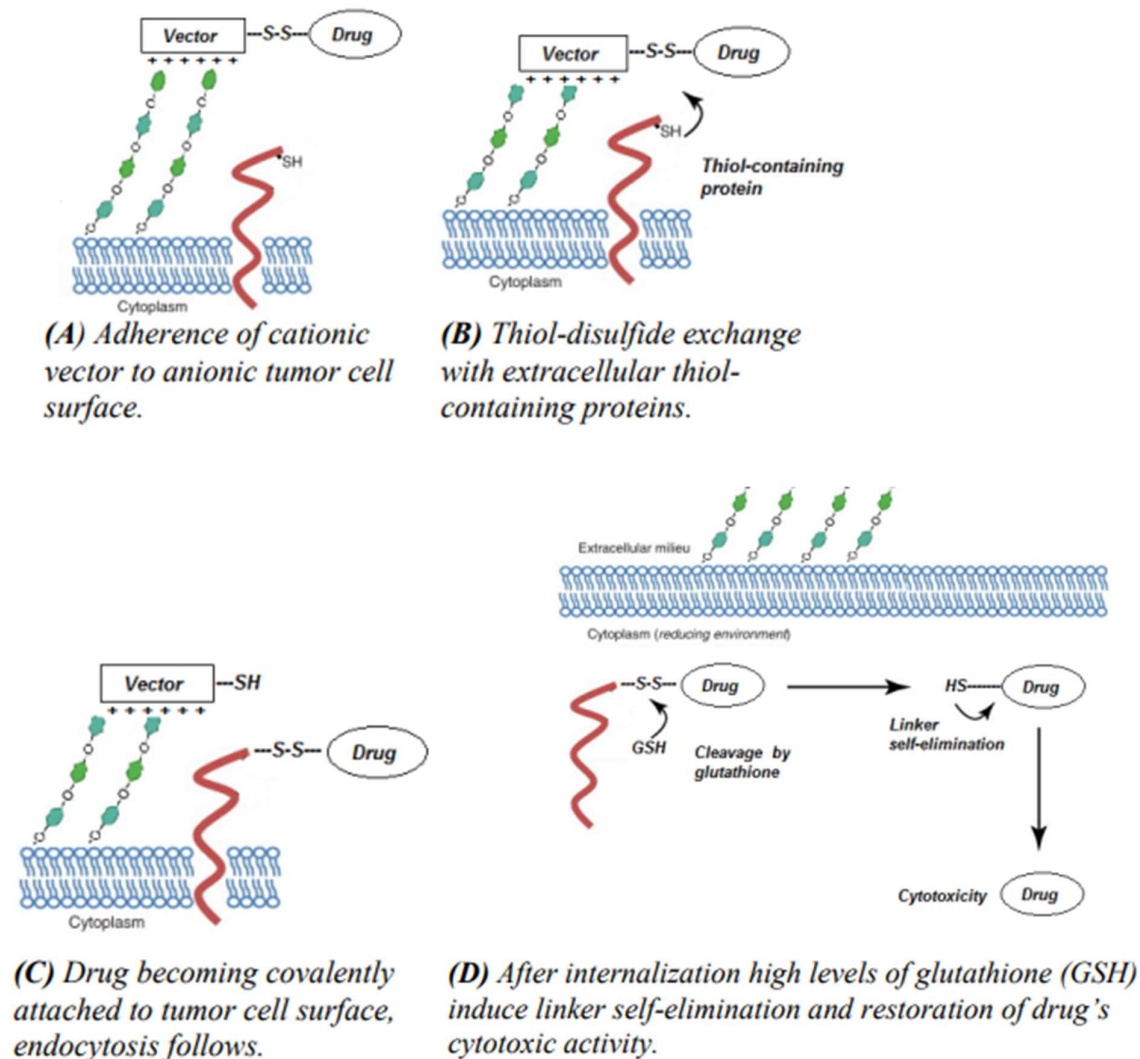


**Figure 2.** Proposed mechanism for the intracellular delivery of cytotoxic compounds using a tripartite prodrug strategies.

As illustrated in Figure 2, the mechanism of action of a tripartite PDC consists of following four steps.

1. Prodrug adherence to the target cell surface. Once the prodrug reaches the low pH conditions of the solid tumor, the histidine-rich vector becomes cationic (via protonation), allowing for electrostatic interaction with anionic macromolecules present on the tumor cell surface. (Figure 2, A)
2. Thiol-disulfide exchange reaction. Cell adherence allows for thiol-disulfide exchange reactions between prodrug and extracellular thiol-containing proteins. This results in the drug being covalently attached to target cell membrane via a newly formed disulfide bond. (Figure 2, B)
3. Internalization of drug. Subsequent endocytosis will facilitate the, still inactive, drug's transport across the cell membrane towards close proximity to its intracellular target (e.g. DNA, enzymes, etc). (Figure 2, C)
4. Linker self-elimination and restoration of activity. The high level of intracellular glutathione (GSH) ensures that the disulfide bond between the linker and thiol-containing protein is cleaved. This cleavage reaction will catalyze a self-elimination reaction that will yield the drug in its native and active form. The released drug will then be able to interact with its target and subsequently induce cell death. (Figure 2, D)

A similar stepwise mechanism of action can be envisaged for an antibody tripartite prodrug (ADC). The antibody part of the ADC binds selectively to the antigen on tumor, followed by internalization. After the conjugate is degraded in the cell, the cytotoxic drug is liberated leading to cytotoxic cell death.

## **2.5. Principles of the analytical techniques used in this study**

### *High Pressure Liquid Chromatography (HPLC)*

In HPLC, the mobile phase is a liquid delivered under high pressure to ensure a constant flow rate, and thus reproducible chromatography, while the stationary phase is packed into a column capable of withstanding the high pressures which are necessary. A chromatographic separation occurs if the components of a mixture interact to different extents with the mobile and/or stationary phases and therefore take different times to move from the position of sample introduction to the position at which they are detected. There are two extremes, as it follows: (i) All analytes have total affinity for the mobile phase and do not interact with the stationary phase – all analytes move at the same rate as the mobile phase, they reach the detector very quickly and are not separated. (ii) All analytes have total affinity for the stationary phase and

do not interact with the mobile phase – all analytes are retained on the column and do not reach the detector. Therefore, one should carry out analysis/separation based on a knowledge of the analytes in order to manipulate the properties of the stationary and/or mobile phases to move from these extremes and effect the desired separation. This principle applies both to preparative and analytical HPLC. Recently, higher pressure version of HPLC, the Ultra High Pressure Liquid Chromatography (UPLC) techniques are commonly used for analytical purposes. Based on the stationary phases, HPLC can be divided into two main types, normal phase and reverse phase HPLC. In normal phase chromatography, the stationary phase consists of very polar particles such as pure silica, and the mobile phase is a non-aqueous solvents, while the stationary phase of the reverse phase HPLC is a non-polar particles such as modified silica substrate with long hydrophobic aliphatic chains, for instance silica modified with octadecyl moiety. The mobile phase for the reverse phase HPLC is mainly polar solvents such as water, acetonitrile or methanol which carry polar analytes and the less polar analytes have a high retention time in the column. Columns for reverse phase HPLC are less prone to damage compared to normal phase HPLC columns.

The detector is an important part of an HPLC system. A number of detectors may be used in conjunction with HPLC depending on the type of chosen analytes and the type of analysis being undertaken. UV and visible light absorbing detector is the most commonly used for vast majority of HPLC systems. Most organic analytes gives absorption in the ultraviolet range 190 - 350 nm. For HPLC with normal UV detector, a couple of user-selectable specific wavelengths are measures simultaneously. So, confirmation of the specific analyte is based on its retention time in the chromatography.

The photo diode array (PDA) detector has advantage and can in turn measure the entire wavelength range in real time. A full spectral profile is obtained by PDA and it is useful in distinguishing between analytes based on their absorbance spectra and in determining an unknown peak in the chromatograms. For full confirmation, analyses should be performed by mass spectrometry.

#### *Mass spectrometric detector*

The use of an HPLC coupled with mass spectrometer allows analysis at molecular level with high sensitivity, specificity and precision. The individual components in a mixture separated by HPLC are ionized and the resulting ions are separated on the basis of their mass/charge ratio in

a mass analyzer which makes it possible to identify ions. The separated ions are then directed to a photo or electron multiplier tube detector, which can contribute to quantification of ions. The advantage of having a mass spectrometric detector is that in many cases it can provide that absolute identification. It provides not only the molecular weight of the analyte, but it may also provide structural information from the molecule under investigation. This is, in most cases, the single most important and discriminating piece of information available to the analyst which, when determined, immediately reduces, dramatically, the number of possible structures for the analyte. Another advantage of mass spectrometry is its sensitivity – a full-scan spectrum, and potentially an identification, can be obtained from picogram (pg) amounts of analyte. In addition, it may be used to provide quantitative information, usually to low levels, with good accuracy and precision.

The ion source is an important component in any MS analysis, as this basically aids in efficient generation of ions for analysis. To ionize intact molecules, the ion source could be for instance Atmospheric Pressure Chemical Ionization (APCI) or Electrospray Ionization (ESI). The choice of ion source also depends on the chemical nature of the analyte of interest i.e. polar or non-polar. ESI is an important soft ionization technique in which the analytes are ionized at atmospheric pressure and then reaches the low pressure region of the MS instrument. The mobile phase with the sample from the HPLC column is nebulized and the resulting aerosol is ionized with a high voltage up to 5 kV. In a positive mode,  $\text{H}_3\text{O}^+$  derived from water acts as a proton donor. The analyte is transported in and through the MS by electric voltage. High intensity signal can be achieved if the analyte is already ionized in the mobile phase. The mobile phase and any added compounds for pH adjustment of the mobile phase, for example formic acid should be volatile. Ionized analytes then enter the mass filter, the low pressure region of the instrument. In time-of-flight (ToF), one of the most commonly used mass analyzer, the ions are accelerated by a set of plates with opposite charges and drift down a flight path before they hit the detector. The time of flight is proportional to the mass of ions so that heavier ions drift more slowly than lighter ions. Therefore it is possible to calculate the mass based on the time of flight as long as the length of the flight path is known.

### *Infrared (IR) spectroscopy*

Almost any compound having covalent bond absorbs various frequencies of electromagnetic radiation in the infrared region (400-800 nm) of the electromagnetic spectrum. These absorbances correspond to different modes of vibrational motion in a molecule. The most important modes of motions for infrared active molecules are stretching of a covalent bond and

bending motion of two atoms separated by two covalent bonds. IR spectroscopy provides information about what type of chemical bond the molecule has. Since every type of bond has a different natural frequency of vibration, and two of the same bond in two different compounds are in two slightly different environments, no two molecules of different structure have exactly the same infrared absorption pattern. Although some of the frequencies absorbed in the two cases might be the same, in no case of two different molecules will their infrared spectra be identical. IR spectroscopy is a standard tool for full characterization of new organic compounds.

#### *Nuclear Magnetic Resonance (NMR) spectroscopy*

Nuclear magnetic resonance (NMR) is a spectroscopic method important for elucidation of structure of organic molecules. NMR gives information about the number of magnetically distinct nuclei. Many nuclei may be studied by NMR techniques, but hydrogen and carbon are most commonly available. When hydrogen nuclei (proton) is studied, one can determine the number of each of the distinct types of hydrogen nuclei as well as obtain information regarding the nature of the immediate environment of each type. Similar information can be determined for the carbon nuclei. Proton and carbon NMR spectral data is requirement in characterization of new organic molecules. The combination of IR and NMR data and elemental composition analysis is often sufficient to determine completely the structure of organic molecule. Elemental composition analysis used to be carried out by combustion chemical analysis, but nowadays elemental composition calculated from high resolution mass spectral data is frequently used.



### 3. Aim of the thesis

In this study the focus was to develop a self-eliminating heterobifunctional crosslinker toolkit that could be used to produce prodrugs by spontaneous reactions between a hydroxyl group or a primary amine group in the drug and a thiol moiety in the vector. Due to an inherent propensity to react with itself, self-eliminating linkers present certain synthetic challenges. In conventional prodrug synthesis these issues are normally circumvented by following a laborious, multistep synthesis resulting in low yields, long preparation times, and high production costs. Heterobifunctional and self-eliminating linkers offer an alternative to this approach. By modifying both ends of a linker with compatible activating groups it is possible to fully control the conjugation chemistry as illustrated in Figure 3, as well as prevent intramolecular cyclization (self-elimination).

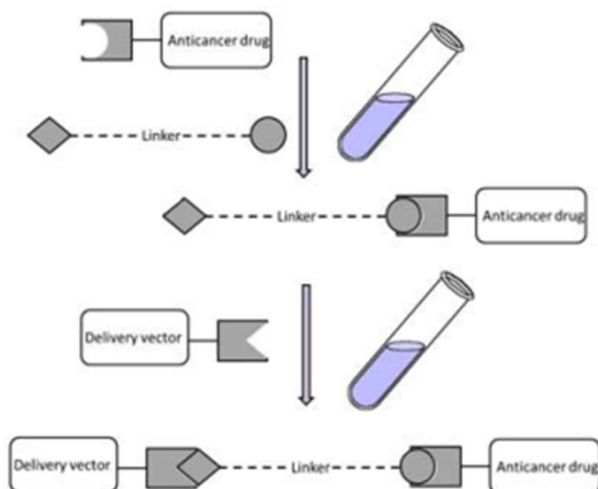


**Figure 3.** Using heterobifunctional linker technology to ensure the correct connection between the prodrug components. By simplifying the conjugation chemistry, this toolkit allows for a higher throughput in tripartite prodrug synthesis and eventual testing.

#### *Linker design aspects*

Ideally, heterobifunctional and self-eliminating linkers should have the following characteristics: The linkage they form between the drug and the delivery vector should (i) be able to rapidly self-eliminate following chemical impact inside the tumor; (ii) be stable enough to exist as individual compounds; (iii) be able to conjugate selectively with both drug and delivery vectors. Taking the abovementioned requirements together, the most suitable

compounds for this purpose are envisaged to be modified mercaptoalkyl carbonates and linkers with the overall structure shown in Figure 4 should therefore be synthesized.

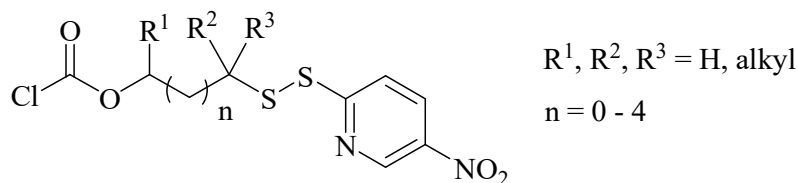
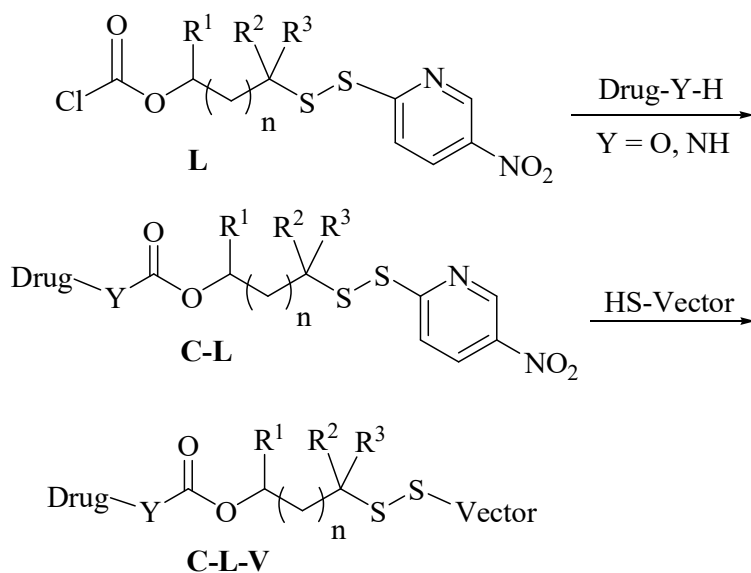


**Figure 4.** The general structure of the heterobifunctional linkers investigated.

The agents depicted in Figure 4 are envisaged to be reactive towards hydroxyl- and amino-containing cargoes and yield Cargo-Linker (C-L) conjugates forming carbonate or carbamate linkages between the cargo and the linker. The pyridinesulfenyl group in C-L is then able to react with thiols and form disulfide. If the vector contains a thiol group, reaction with C-L conjugate is envisaged to afford the Cargo-Linker-Vector (C-L-V) conjugate which completes the prodrug synthesis. (Scheme 1)



**Scheme 1.** Synthesis of the conjugate from heterobifunctional linker

The linkage between the drug and the linker is also important in therapeutic bioconjugates. A stable carbamate linkage can be formed with amine-containing cargoes while hydroxyl-containing cargoes will form a carbonate linkage.

These linkers will be evaluated for the ability to form the desired prodrug conjugates between cargo (drug) and delivery vectors. The resulting drug-linker-peptide conjugate was therefore subjected to glutathione-rich conditions, and the release kinetics were studied by means of chromatographic and mass spectrometric techniques by using a series of model conjugates, made by conjugating hydroxyl- and amino-containing drugs to short peptides with different linkers.

## 4. Methods and Materials

### 4.1. General

Chemicals and solvents were purchased from Sigma-Aldrich or VWR and used as received. Reactions were monitored by thin layer chromatography (TLC) on a silica gel plate on aluminum coated with fluorescent indicator F254 and visualized by UV light at 254 nm. The analyses of the products were performed on a Waters Ultra Performance Liquid Chromatography (UPLC) instrument with an Acquity UPLC BEH C18 1.7  $\mu\text{m}$ , 2.1 x 50 mm column and with a photodiode array (PDA) detector of wavelength range between 200 and 500 nm by using a gradient of water (purified by a Milli-Q Water Purification System) and acetonitrile (HPLC-grade) containing 0.1% trifluoroacetic acid (TFA). The sample temperature was at room temperature (approximately 26 °C), and the column temperature was set to 50 °C. Chromatographic data was processed by MassLynx v4.1 software from Waters.

The purification of the reaction products was performed on Waters Preparative High Performance Liquid Chromatography (HPLC) with 2767 sample manager, 2998 PDA detector and 2545 pump using XBridge Prep C18 5  $\mu\text{m}$  OBD, 19 x 250 mm column from Waters. Mixture of water (purified by a Milli-Q Water Purification System) and acetonitrile (HPLC-grade) containing 0.1% trifluoroacetic acid (TFA) were used as eluent. For some crude products, preliminary purification was performed on column flash chromatography using 230-400 mesh silica gel and mixture of hexane and ethyl acetate as eluent.

Melting points were determined on a calibrated Büchi 535 apparatus.

IR spectra were recorded on an Avatar 360 FT-IR spectrometer.

NMR spectra were recorded on a Bruker Avance III 400 spectrometer at 25 °C using  $\text{CDCl}_3$  or  $\text{DMSO-}d_6$  as solvents. Chemical shifts are reported as  $\delta$  in parts per million, for  $^1\text{H}$  NMR relative to the signal of TMS at 0.00 ppm or dimethylsulfoxide at 2.50 ppm, and for  $^{13}\text{C}$  NMR relative to the center-line signal of the  $\text{CDCl}_3$  triplet at 77.16 ppm or the DMSO multiplet at 39.52 ppm. The multiplicity is given as s (singlet), doublet (d), dd (doublet of doublet), t (triplet), q (quartet), p (pentet), and m (multiplet). Coupling constants,  $J$ , are reported in hertz (Hz).

High resolution mass spectra were run on a Waters Acquity UPLC Xevo G2 QToF system with an Acquity UPLC BEH C18 1.7  $\mu\text{m}$ , 2.1 x 100 mm column from Waters by using a gradient of water (purified by a Milli-Q Water Purification System) and acetonitrile (HPLC-MS grade) containing 0.1% formic acid (FA). The sample temperature was set to 5 °C, and the column

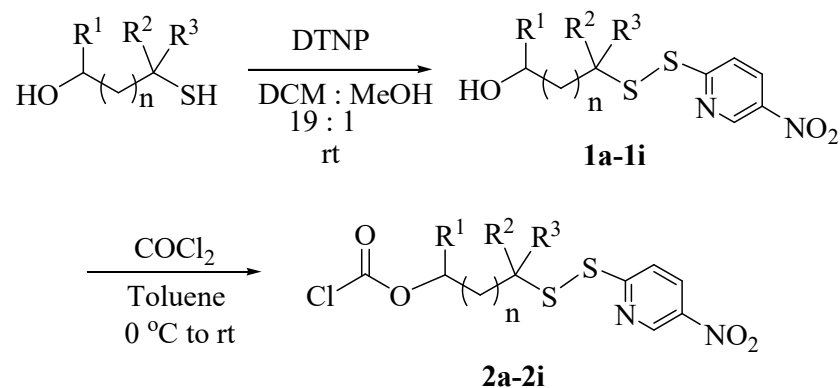
temperature was set to 65 °C. The mass spectra were recorded in full scan mode with  $m/z$  100 – 5000, in an electrospray positive mode and processed by using MassLynx v4.1 software from Waters.

## 4.2. Synthesis of peptide

The peptide C(Ac)GHHPHGHHPH-amide were synthesized on a PTI Prelude instrument using well-established solid-phase Fmoc-methodologies, reagents and solvents. Rink amide resin and standard Fmoc-amino acid derivatives were used in all syntheses. Coupling reactions were done with HCTU/DIPEA activation, while Fmoc-groups were removed with piperidine. Following the final coupling and Fmoc-removal, the peptides were cleaved from the resin using TFA and the fully deprotected peptide precipitated with diethyl ether. The crude peptides were purified (>95% purity) using preparative HPLC.

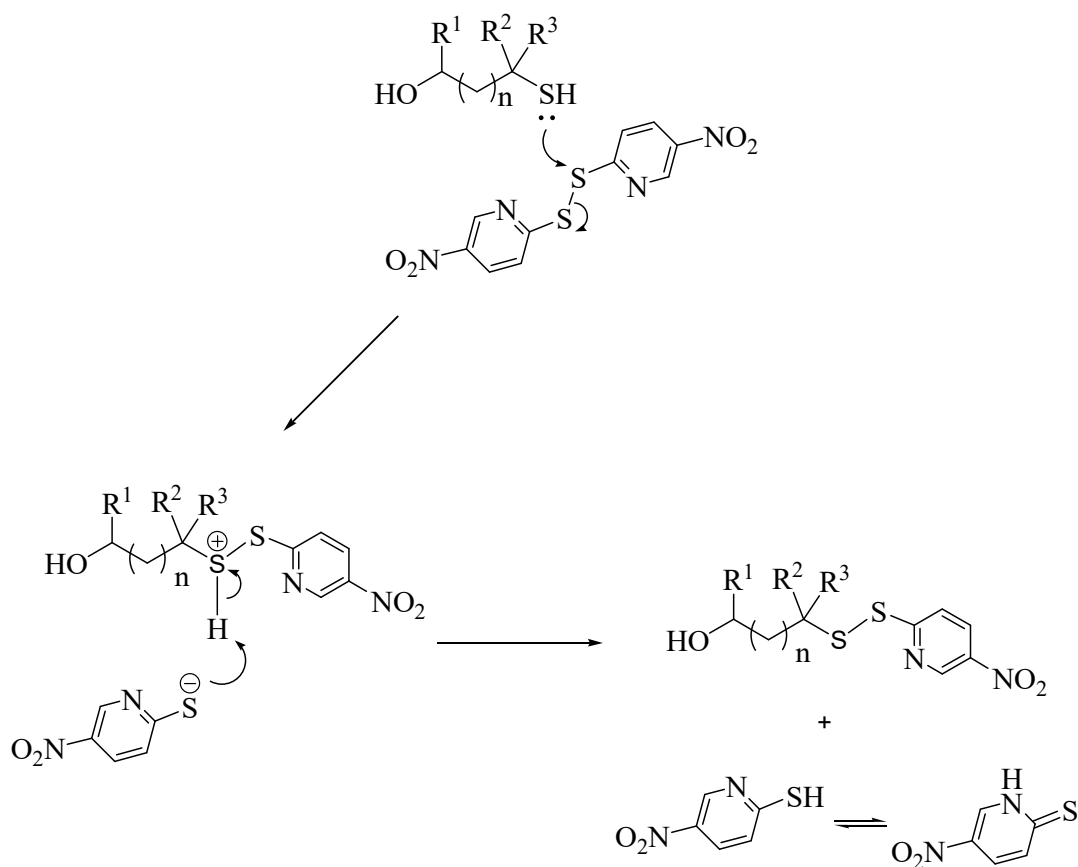
## 4.3. Synthesis of the linker

The heterobifunctional linkers (**2a-2i**) were synthesized from the corresponding mercaptoalcohol in two steps as shown in Scheme 2. All the chiral alcohols were mixtures of racemates.



**Scheme 2.** Synthesis of self-eliminating heterobifunctional linkers, DTNP = 2,2'-Dithiobis(5-nitropyridine)

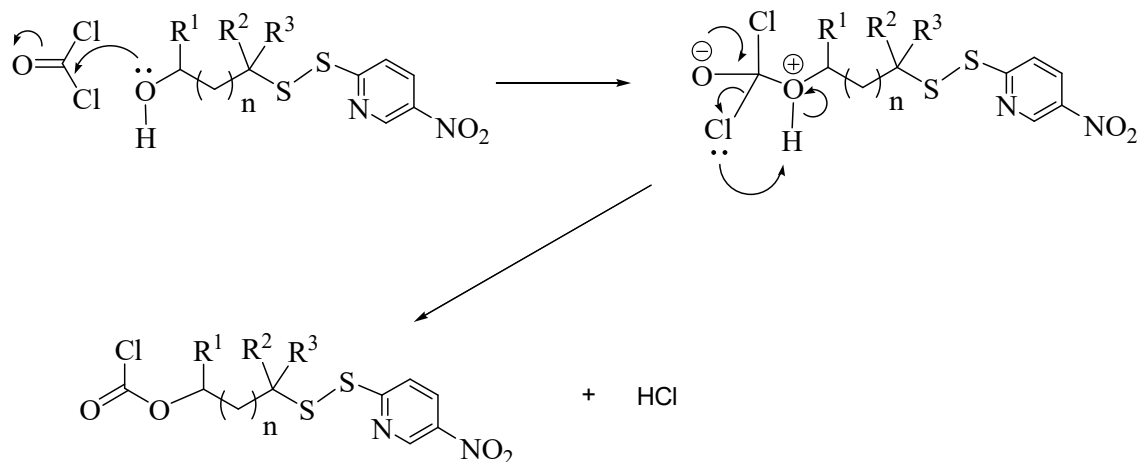
This two-step synthesis involves reactions that take place through disulfide exchange (Scheme 3) and nucleophilic addition (Scheme 4) mechanisms.



**Scheme 3.** Mechanism of the disulfide exchange between DTNP and mercaptoalkanol

### Step 1. Synthesis of $\omega$ -[2-(5-nitropyridin-2-yl)disulfanyl]-alkanols (**1**)

*General procedure:* A solution of mercaptoalkanol (1.0 mmol) in dichloromethane (5.0 mL) was added to a solution of 2,2'-dithiobis(5-nitropyridine) (0.46 g, 1.50 mmol) in dichloromethane (20 mL) containing 5% methanol (v/v). The resulting mixture was stirred at room temperature (1-5 h). The solvent was removed and the residue was mixed with 10% ethyl acetate in hexane (20 mL), and the resulting suspension was filtered on a sintered glass filter. The filtrate was concentrated on a rotary evaporator and the residue was purified by reverse phase preparative HPLC by gradient elution using acetonitrile and water containing 0.1% TFA as eluent. The fractions were collected and lyophilized to give **1a-1i**.



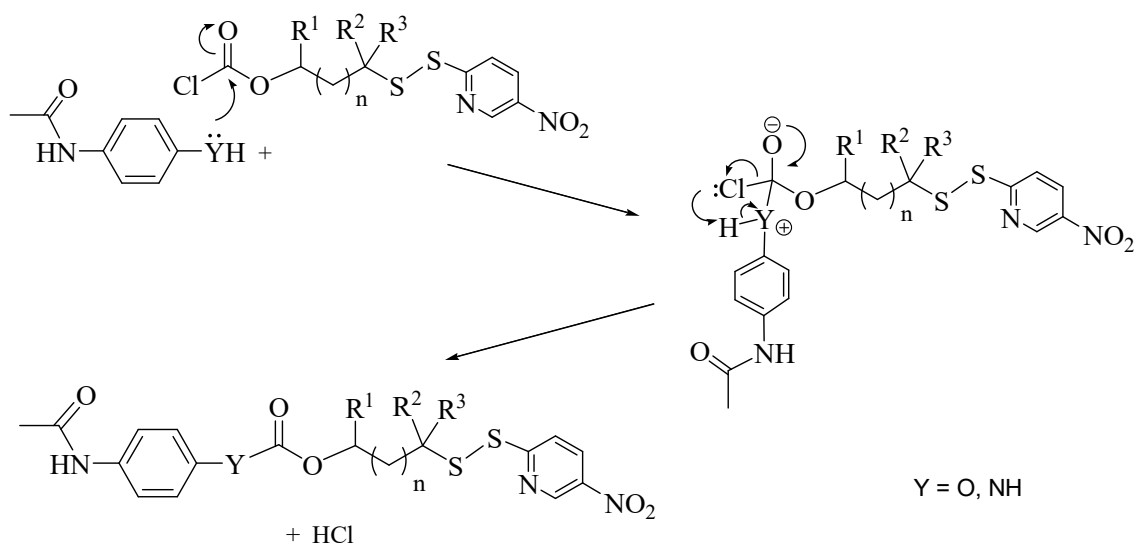
**Scheme 4.** Mechanism of the nucleophilic addition of alcohols to phosgene

#### Step 2. Synthesis of chloroformates (2)

*General procedure:* A 15% solution of phosgene (0.18 mL,  $d = 0.924$  g/mL, 0.25 mmol) in toluene was added to a solution of alkanol **1** (0.20 mmol) in toluene (1.0 mL). The reaction mixture was stirred at 0 °C for 1 h and then at room temperature for 18 h. The solvent was removed under reduced pressure and the crude product was purified by reverse phase preparative HPLC with acetonitrile containing 0.1% TFA as eluent. The collected fractions were lyophilized to give chloroformate **2**.

#### **4.4. Synthesis of cargo-linker conjugate**

Conjugation of hydroxyl and amine containing cargoes with the linkers **2** are envisaged to take place through nucleophilic addition mechanism illustrated in Scheme 5. The reaction is initiated by attack of the Nucleophilic group (hydroxyl or amine) to carbonyl carbons of the chloroformates followed by elimination of chloride ion as a leaving group.



**Scheme 5.** Mechanism of conjugation between cargo and linker

#### Synthesis of cargo-linker conjugate **3** (carbonate type)

*General procedure:* To a solution of 4-acetamidophenol (0.0151 g, 0.100 mmol) in acetonitrile (2.00 mL) was added 0.100 M solution of triethylamine in acetonitrile (1.00 mL). The resulting mixture was added to a solution of linker (0.100 mmol) in acetonitrile (1.00 mL) and the reaction mixture was stirred at room temperature. When the reaction was complete (UPLC analysis), the mixture was concentrated under reduced pressure and the remaining crude was purified by reverse phase preparative HPLC with a gradient of acetonitrile and water containing 0.1% TFA as eluent to give conjugate **3** after lyophilization. The syntheses of **3a** and **3h** were carried out following this procedure.

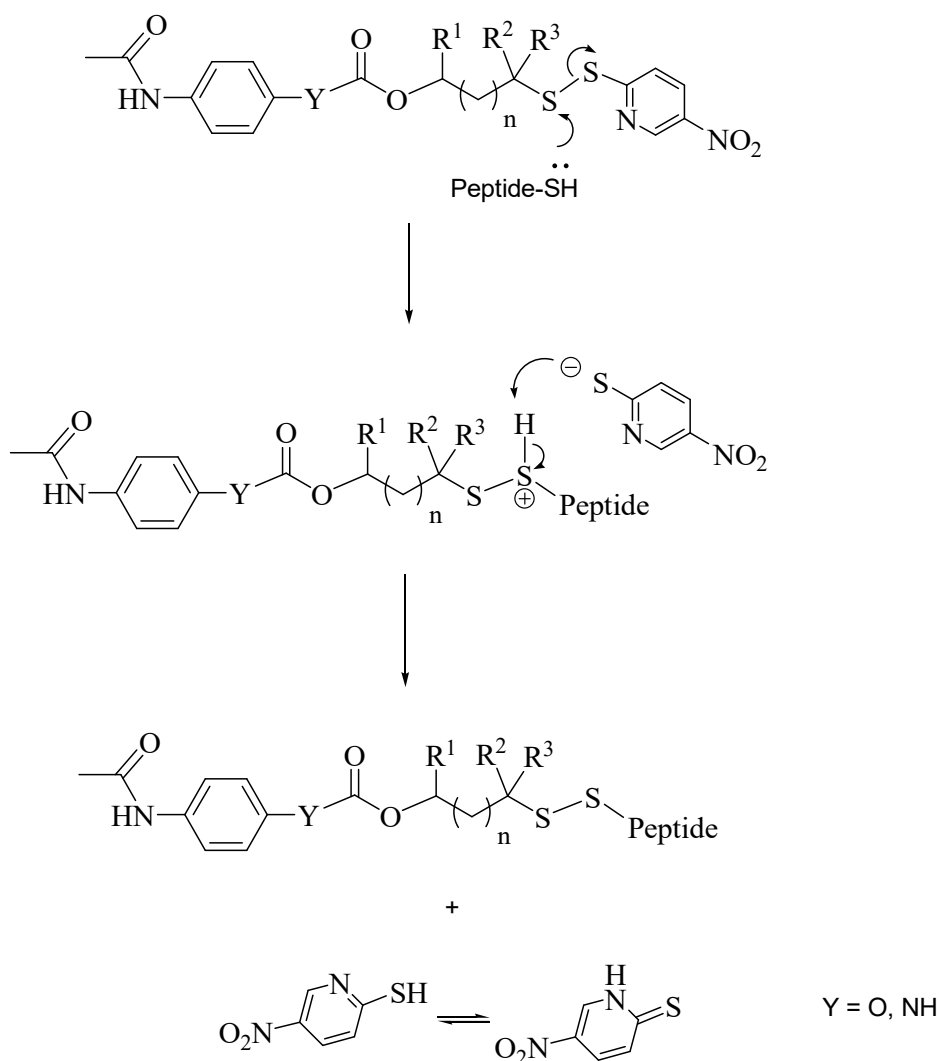
#### Synthesis of cargo-linker conjugate **4** (carbamate type)

*General procedure:* To a solution of 4-acetamidoaniline (0.0150 g, 0.100 mmol) in acetonitrile (4.0 mL) was added 0.100 M solution of triethylamine in acetonitrile (0.500 mL) and the resulting mixture was added to a solution of linker (0.100 mmol) in acetonitrile (1.00 mL) and the reaction mixture was stirred at room temperature. When the reaction was complete (UPLC analysis), the mixture was concentrated under reduced pressure and the residue was purified by reverse phase preparative HPLC with a gradient of acetonitrile and water containing 0.1% TFA as eluent to give conjugate **4** after lyophilization. The synthesis of **4a-4d** and **4h** are carried out following this procedure.



## 4.5. Synthesis of cargo-linker-vector conjugates 5 and 6

*General procedure:* A solution of cargo-linker conjugate (0.050 mmol) in a 2:1 mixture of acetonitrile and water (0.5 mL) is added to a solution of the histidine rich peptide (Ac)CGHHPHGHHHPH-amide (0.050 mmol, 65 mg) in a 1:4 mixture of acetonitrile and water (0.5 mL) and the reaction mixture is stirred at room temperature. The color of the reaction mixture turns to more intense yellow due to the release of pyridinethiol. When reaction is complete (UPLC), the mixture is directly purified by performing reverse phase preparative HPLC with a gradient of acetonitrile and water containing 0.1% TFA as eluent to give the drug-linker-peptide conjugate as a white solid after lyophilization. Reaction is based disulfide exchange mechanism. (Scheme 6)



**Scheme 6.** Mechanism of the conjugation between peptide and cargo-linker conjugates.

#### **4.6. Degradation analysis**

To a 0.20 mM solution (0.50 mL) of a C-L-V conjugate (**5** or **6**) in a 1.0 mM phosphate buffer (adjusted to the physiological pH = 7.4 with 0.10 M NaOH) placed in a chromatography vial was added 10/1.0 mM solution of reduced/oxidized glutathione solution (0.50 mL) in the same buffer and the mixture was placed at 25°C. The reaction was analyzed over time by analytical UPLC with photodiode array (PDA) detector by using C18 column and a gradient of acetonitrile and water containing 0.1% TFA as eluent. Relative proportions of the reaction products containing the cargo were then determined by measuring the peak areas of the respective signals at 242 nm (the absorption maximum for the cargoes). The signals detected by UPLC-PDA were identified with help of mass spectrometer coupled with UPLC system using the same column and chromatographic condition.

## 5. Results and Discussions

### 5.1. Preparation of linkers and conjugates

**Peptide vectors.** A histidine-rich decapeptide, which was investigated as a candidate for tumor-homing peptide<sup>50</sup> was used in this study as the vector component. In order to facilitate disulfide-bond formation, a thiol group was introduced by adding a cysteine at the N-terminus of the peptide to finally yield a vector peptide. The N-terminus of this undecapeptide was acetylated to yield Ac-CGHHPHGHHPH-amide. Purity and the correct molecular weight were confirmed with UPLC-PDA and UPLC-MS, respectively. The purified peptides were lyophilized as TFA salts. Mass spectrometric analysis of the product provides following data. HRMS: Calculated mass for  $C_{55}H_{73}N_{24}O_{12}S^+ [M+H]^+$  1293.5506, found 1293.5538. (Figure 5)

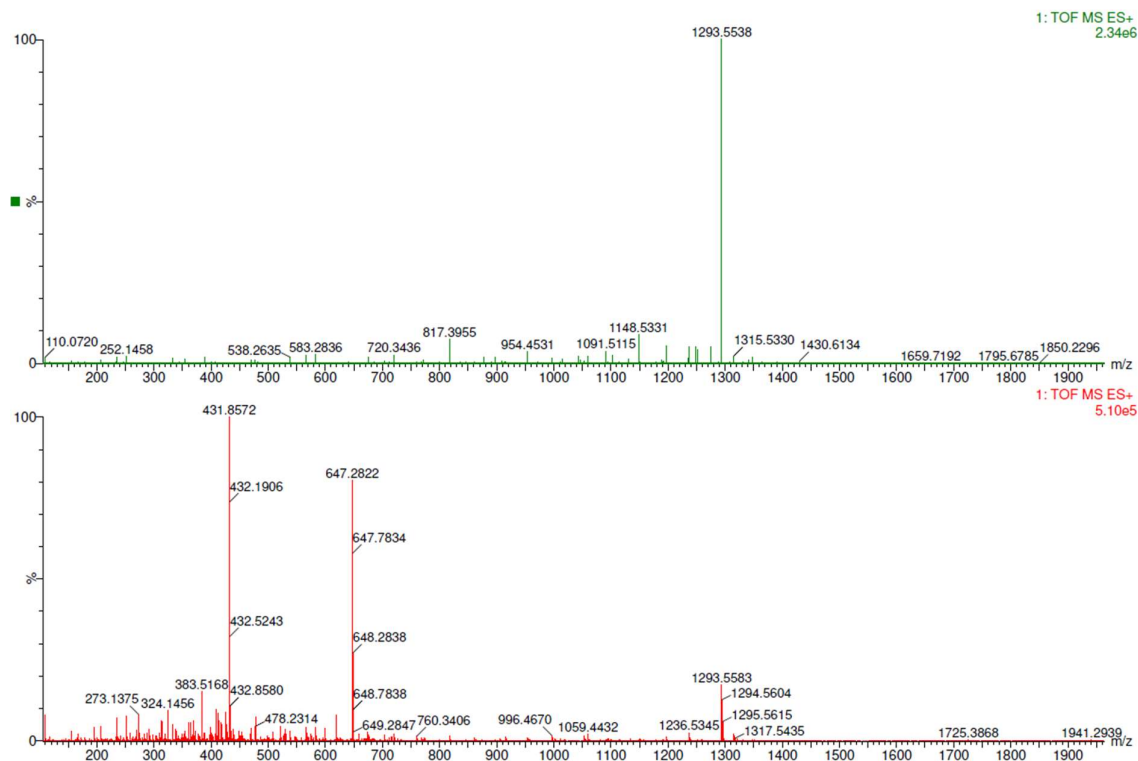
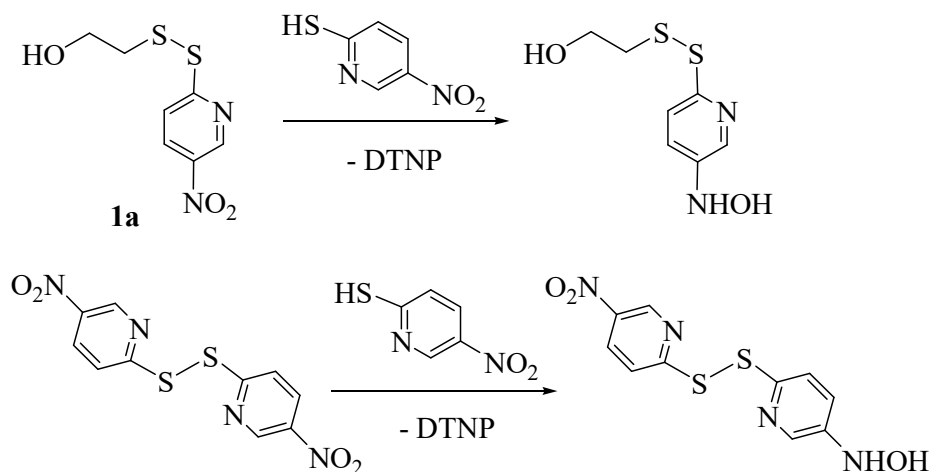


**Figure 5.** Mass spectra of the peptide vector. The lower part is the original spectrum, the upper part is the processed spectrum by using Transform function in MassLynx 4.1 software to display m/z spectrum of true molecular mass based on charge states assigned to each peak.

**Linkers.** Synthesis of the target heterobifunctional crosslinkers have been carried out in two steps as illustrated in Scheme 2. In the first step, mercaptoalcohol was reacted with different dipyridyldisulfides. Preliminary experiments using 2-mercaptoethanol with 2,2'-

dipyridyldisulfide, 4,4'-dipyridyldisulfide and 2,2'-dithiobis(5-nitropyridine) (DTNP) showed that all reactions took place at room temperature and gave the corresponding pyridinyl disulfanyl ethanols in 43-72% yields. However, the isolated yields of the alcohols from 2,2'-dipyridyldisulfide and 4,4'-dipyridyldisulfide were significantly lower than those obtained from DTNP. Significant amounts of the pyridinyl disulfanyl ethanols appeared to be lost during lyophilization when the two former disulfides were used, possibly due to their relatively high volatility. Therefore, the syntheses of pyridinyl disulfanyl alkanols **1a-1i** were carried out using DTNP and mercaptoalkanols as reactants. These reactions took place at room temperature and appeared to be reversible. The larger the excess of DTNP, the better the conversion, but use of excess DTNP, for example 3 equivalents, made the purification of the products quite tedious. The use of 1.5 equivalents seemed to be optimal in terms of the purification conditions and conversion rates. The reaction time also influenced the outcome the most; the best yields were obtained with a reaction time of 1-6 hours. When longer reaction times were applied, byproducts containing a hydroxylamino group were formed by reduction of the nitro group. UPLC-MS investigations of the crude products obtained from several alkanols reacted with DTNP for 24 hours showed several such byproducts. The formation of two conceivable reduced products from **1a** and DTNP is shown in Scheme 7.



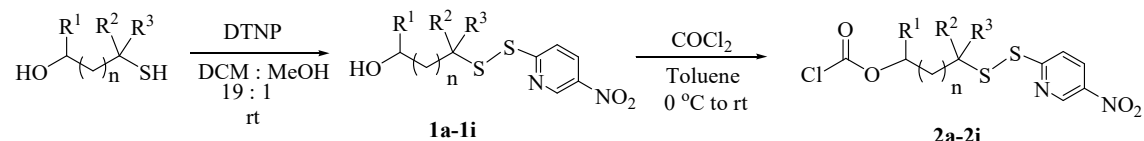
**Scheme 7.** Reduction of nitro compounds by free thiol using mercaptoethanol and DTNP as examples

Synthesis of **2** was then completed by reacting alkanols **1** with phosgene in toluene. This reaction was uneventful and gave the corresponding chloroformates in 72-84% yields. Samples

of **2a** and **2e** stored under air at 2 °C for three months showed no signs of degradation according to UPLC analyses. Thus, these chloroformates can be synthesized in advance, stored, and utilized as heterobifunctional linkers when required.

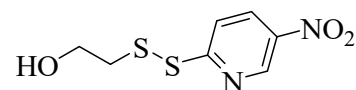
Yields of each step are summarized in Table 1.

**Table 1.** Yields in each step of the synthesis shown in Scheme 2.



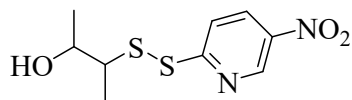
R <sup>1</sup>	R <sup>2</sup>	R <sup>3</sup>	n	Stepwise results; compound/yield (%)	
H	H	H	0	<b>1a</b> /72	<b>2a</b> /84
Me	Me	H	0	<b>1b</b> /62	<b>2b</b> /81
Me	H	H	0	<b>1c</b> /69	<b>2c</b> /77
H	H	H	1	<b>1d</b> /70	<b>2d</b> /72
H	Me	Me	1	<b>1e</b> /68	<b>2e</b> /78
Me	Me	Me	1	<b>1f</b> /70	<b>2f</b> /81
H	Pr	H	1	<b>1g</b> /65	<b>2g</b> /77
H	H	H	2	<b>1h</b> /72	<b>2h</b> /76
H	H	H	4	<b>1i</b> /70	<b>2i</b> /80

Descriptions of the synthesis and characterization of each compound outlined in Table 1, are detailed as follows.



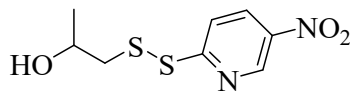
2-(2-(5-Nitropyridin-2-yl)disulfanyl)ethanol (**1a**): 2-Mercapto-1-

ethanol (0.078 g, 1.0 mmol) was reacted for 1 h to give **1a** (0.167 g, 72%) as a yellowish powder. M.p. 52.1-52.5 °C; IR (neat): 3353 (m), 3085 (m), 2929 (m), 2873 (m), 2508 (w), 1592 (s), 1566 (s), 1514 (s), 1439 (s), 1369 (m), 1343 (s), 1272 (s), 1223 (m), 1138 (m), 1100 (s), 1063 (s), 1011 (s), 940 (m), 858 (s), 754 (s) cm<sup>-1</sup>; <sup>1</sup>H NMR (400 MHz, CDCl<sub>3</sub>) δ 9.33 (dd, *J* = 2.6, 0.7 Hz, 1H), 8.37 (dd, *J* = 8.9, 2.6 Hz, 1H), 7.67 (dd, *J* = 8.9, 0.7 Hz, 1H), 3.79 (t, *J* = 7.2 Hz, 2H), 3.01 (t, *J* = 7.2 Hz, 2H); <sup>13</sup>C NMR (100 MHz, CDCl<sub>3</sub>) δ 167.7, 145.5, 142.7, 131.6, 121.0, 58.9, 42.7; HRMS: Calculated for C<sub>7</sub>H<sub>9</sub>O<sub>3</sub>N<sub>2</sub>S<sub>2</sub><sup>+</sup> [M+H]<sup>+</sup> 232.9976, found 233.0048.



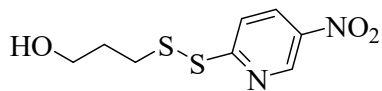
3-(2-(5-Nitropyridin-2-yl)disulfanyl)butan-2-ol (**1b**):

Diastereomeric mixture of 3-mercapto-2-butanol (0.106 g, 1.00 mmol) was reacted for 3 h to give **1b** (0.144 g, 62%) as a yellow oil. IR (neat): 3350 (w), 3087 (w), 2972 (m), 2929 (w), 2507 (w), 1587 (s), 1563 (s), 1514 (s), 1440 (s), 1368 (m), 1348 (s), 1268 (s), 1254 (s), 1218 (s), 1133 (m), 1117 (m), 1095 (s), 1060 (m), 1007 (s), 971 (m), 937 (m), 912 (m), 854 (s), 748 (s)  $\text{cm}^{-1}$ ;  $^1\text{H}$  NMR (400 MHz,  $\text{CDCl}_3$ )  $\delta$  9.32 (ddd,  $J = 3.5, 2.6, 0.7$  Hz, 1H), 8.36 (ddd,  $J = 8.9, 3.5, 2.6$  Hz, 1H), 7.65 (td,  $J = 8.9, 0.7$  Hz, 1H), 3.96 and 3.48 (2 qd in a 3:2 ratio,  $J = 6.5$  Hz, 2.5 Hz, 1H), 3.08 and 2.86 (2 qd in a 3:2 ratio,  $J = 7.1, 2.5$  Hz, 1H), 1.39 and 1.31 (2 d in a 2:3 ratio,  $J = 6.9$  Hz, 3H), 1.26 and 1.22 (2 d in a 2:3 ratio,  $J = 6.9$  Hz, 3H);  $^{13}\text{C}$  NMR (100 MHz,  $\text{CDCl}_3$ )  $\delta$  168.0 and 167.8 (in a 3:2 ratio), 145.5 and 145.4 (in a 3:2 ratio), 142.7 and 142.6 (in a 2:3 ratio), 131.6 and 131.5 (in a 3:2 ratio), 121.0 and 120.8 (in a 2:3 ratio), 69.0 and 66.7 (in a 2:3 ratio), 55.7 and 54.3 (in a 2:3 ratio), 20.0 and 19.2 (in a 2:3 ratio), 17.9 and 12.5 (in a 2:3 ratio); HRMS: Calculated for  $\text{C}_9\text{H}_{13}\text{N}_2\text{O}_3\text{S}_2^+$   $[\text{M}+\text{H}]^+$  261.0362, found 261.0368.



1-(2-(5-Nitropyridin-2-yl)disulfanyl)propan-2-ol (**1c**):

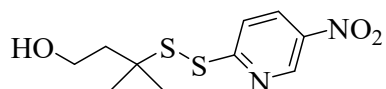
A racemic mixture of 3-mercapto-2-propanol (0.092 g, 1.00 mmol) was reacted for 5 h to give **1c** (0.169 g, 69%) as a yellowish powder. M.p. 54.5-55.0  $^\circ\text{C}$ ; IR (neat): 3400 (w), 3086 (w), 2970 (w), 1587 (s), 1564 (s), 1513 (s), 1437 (s), 1389 (m), 1366 (m), 1339 (s), 1269 (m), 1254 (m), 1127 (m), 1096 (s), 1076 (m), 1041 (m), 1008 (m), 936 (m), 854 (s), 749 (s)  $\text{cm}^{-1}$ ;  $^1\text{H}$  NMR (400 MHz,  $\text{CDCl}_3$ )  $\delta$  9.34 (dd,  $J = 2.6, 0.7$  Hz, 1H), 8.37 (dd,  $J = 8.8, 2.6$  Hz, 1H), 7.65 (dd,  $J = 8.8, 0.7$  Hz, 1H), 4.35 (bs, 1H), 3.85 (m, 1H), 3.04 (dd,  $J = 13.9, 2.7$  Hz, 1H), 2.72 (dd,  $J = 13.9, 9.5$  Hz, 1H), 1.28 (d,  $J = 6.3$  Hz, 3H);  $^{13}\text{C}$  NMR (100 MHz,  $\text{CDCl}_3$ )  $\delta$  167.6, 145.5, 142.7, 131.6, 120.8, 64.7, 48.9, 21.7; HRMS: Calculated for  $\text{C}_8\text{H}_{11}\text{N}_2\text{O}_3\text{S}_2^+$   $[\text{M}+\text{H}]^+$  247.0206, found 247.0213.



3-(2-(5-Nitropyridin-2-yl)disulfanyl)propan-1-ol (**1d**):

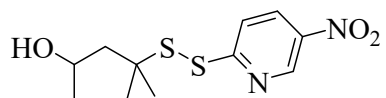
3-Mercapto-1-ethanol (0.092 g, 1.0 mmol) was reacted for 4 h to give **1d** (0.172 g, 70%) as a white powder. M.p. 50.1-50.7  $^\circ\text{C}$ ; IR (neat): 3353 (m), 3085 (m), 3065 (m), 2930 (m), 2878 (m), 1586 (s), 1564 (s), 1512 (s), 1436 (s), 1343 (s), 1267 (s), 1254 (s), 1134 (s), 1095 (s), 1052 (s), 937 (m), 902 (m), 854 (s), 748 (s)  $\text{cm}^{-1}$ ;  $^1\text{H}$  NMR (400 MHz,  $\text{CDCl}_3$ )  $\delta$  9.22 (d,  $J = 2.4$  Hz,

1H), 8.34 (dd,  $J = 8.9, 2.4$  Hz, 1H), 7.82 (d,  $J = 8.9$  Hz, 1H), 3.73 (t,  $J = 6.0$  Hz, 2H), 2.92 (t,  $J = 7.1$  Hz, 2H), 1.90 (p,  $J = 6.6$  Hz, 2H), 1.58 (s, 1H);  $^{13}\text{C}$  NMR (100 MHz,  $\text{CDCl}_3$ )  $\delta$  168.8, 145.3, 142.2, 131.8, 119.5, 60.9, 35.7, 31.6; HRMS: Calculated for  $\text{C}_8\text{H}_{11}\text{N}_2\text{O}_3\text{S}_2^+$   $[\text{M}+\text{H}]^+$  247.0206, found 247.0207.



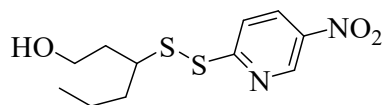
3-Methyl-3-(2-(5-nitropyridin-2-yl)disulfanyl)butan-1-ol (**1e**):

3-Mercapto-3-methyl-1-butanol (0.120 g, 1.0 mmol) was reacted for 4 h to give **1e** (0.186 g, 68%) as a white powder. M.p. 52.2-52.3 °C; IR (neat): 3350 (m), 3088 (w), 3065 (w), 2960 (m), 2923 (m), 1587 (s), 1564 (s), 1514 (s), 1437 (s), 1366 (s), 1339 (s), 1267 (s), 1253 (m), 1211 (m), 1122 (m), 1095 (s), 1057 (m), 1021 (m), 1008 (m), 979 (m), 937 (w), 854 (s), 749 (s)  $\text{cm}^{-1}$ ;  $^1\text{H}$  NMR (400 MHz,  $\text{CDCl}_3$ )  $\delta$  9.26 (dd,  $J = 2.6, 0.7$  Hz, 1H), 8.38 (dd,  $J = 8.9, 2.6$  Hz, 1H), 7.93 (dd,  $J = 8.9, 0.7$  Hz, 1H), 3.84 (t,  $J = 6.8$  Hz, 2H), 1.93 (t,  $J = 6.8$  Hz, 2H), 1.38 (s, 6H);  $^{13}\text{C}$  NMR (100 MHz,  $\text{CDCl}_3$ )  $\delta$  169.72, 145.03, 142.18, 131.57, 119.72, 59.72, 52.34, 43.64, 28.12 (2C); HRMS: Calculated for  $\text{C}_{10}\text{H}_{15}\text{N}_2\text{O}_3\text{S}_2^+$   $[\text{M}+\text{H}]^+$  275.0519, found 275.0532.



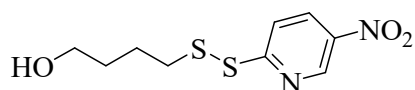
4-Methyl-4-(2-(5-nitropyridin-2-yl)disulfanyl)pentan-2-ol (**1f**):

A racemic mixture of 4-mercapto-4-methyl-2-pentanol (0.134 g, 1.0 mmol) was reacted for 5 h to give **1f** (0.201 g, 70%) as a yellowish powder. M.p. 58.0-58.2 °C; IR (neat): 3399 (m), 3085 (w), 2967 (m), 2926 (m), 1590 (s), 1568 (s), 1520 (s), 1439 (m), 1371 (m), 1344 (s), 1278 (m), 1134 (m), 1099 (s), 854 (s), 753 (m)  $\text{cm}^{-1}$ ;  $^1\text{H}$  NMR (400 MHz,  $\text{CDCl}_3$ )  $\delta$  9.26 (dd,  $J = 2.7, 0.7$  Hz, 1H), 8.37 (dd,  $J = 8.9, 2.7$  Hz, 1H), 7.90 (dd,  $J = 8.9, 0.7$  Hz, 1H), 4.10 (m, 1H), 1.81 (dd,  $J = 15.0, 8.8$  Hz, 1H), 1.73 (dd,  $J = 15.0, 2.7$  Hz, 1H), 1.43 (s, 3H), 1.40 (s, 3H), 1.21 (d,  $J = 6.2$  Hz, 3H);  $^{13}\text{C}$  NMR (100 MHz,  $\text{CDCl}_3$ )  $\delta$  169.6, 145.0, 142.2, 131.5, 119.9, 65.6, 52.9, 49.7, 28.8, 28.0, 25.7; HRMS: Calculated for  $\text{C}_{11}\text{H}_{17}\text{N}_2\text{O}_3\text{S}_2^+$   $[\text{M}+\text{H}]^+$  289.0675, found 289.0681.



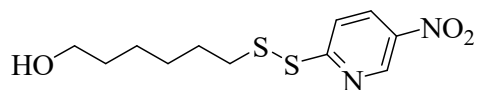
3-(2-(5-Nitropyridin-2-yl)disulfanyl)hexan-1-ol (**1g**): A racemic mixture of 3-mercapto-1-hexanol (0.134 g, 1.0 mmol) was reacted for 4 h to give **1g** (0.187 g, 65%) as a white powder. M.p. 55.4-55.7 °C; IR (neat): 3350 (m), 3083 (w), 2957 (m),

2930 (m), 2871 (m), 1587 (s), 1564 (s), 1515 (s), 1436 (s), 1367 (m), 1338 (s), 1267 (s), 1219 (m), 1133 (m), 1095 (s), 1045 (s), 1007 (s), 938 (m), 854 (s), 749 (s)  $\text{cm}^{-1}$ ;  $^1\text{H NMR}$  (400 MHz,  $\text{CDCl}_3$ )  $\delta$  9.28 (dd,  $J = 2.6, 0.7$  Hz, 1H), 8.39 (dd,  $J = 8.9, 2.6$  Hz, 1H), 7.83 (dd,  $J = 8.9, 0.7$  Hz, 1H), 3.97-3.91 (m, 1H), 3.83-3.77 (m, 1H), 3.14-3.07 (m, 1H), 2.10 (bs, 1H), 2.00 – 1.88 (m, 1H), 1.88 – 1.76 (m, 1H), 1.73 – 1.62 (m, 2H), 1.55 – 1.44 (m, 2H), 0.91 (t,  $J = 7.3$  Hz, 3H);  $^{13}\text{C NMR}$  (100 MHz,  $\text{CDCl}_3$ )  $\delta$  169.1, 145.2, 142.3, 131.6, 120.1, 60.2, 50.3, 37.1, 36.6, 20.1, 14.0; HRMS: Calculated for  $\text{C}_{11}\text{H}_{17}\text{N}_2\text{O}_3\text{S}_2^+ [\text{M}+\text{H}]^+$  289.0675, found 289.0682.



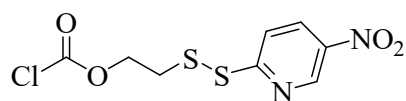
4-(2-(5-Nitropyridin-2-yl)disulfanyl)butan-1-ol (**1h**):

4-Mercapto-1-butanol (0.106 g, 1.0 mmol) was reacted for 5 h to give **1h** (0.187 g, 72%) as a white powder. M.p. 56.0-56.4  $^\circ\text{C}$ ; IR (neat): 3309 (m), 3085 (m), 2933 (m), 2862 (m), 2504 (w), 1592 (s), 1566 (s), 1518 (s), 1439 (s), 1369 (m), 1343 (s), 1272 (s), 1138 (m), 1100 (s), 1052 (s), 1011 (s), 940 (m), 858 (s), 754 (s)  $\text{cm}^{-1}$ ;  $^1\text{H NMR}$  (400 MHz,  $\text{CDCl}_3$ )  $\delta$  9.28 (dd,  $J = 2.6, 0.7$  Hz, 1H), 8.41 (dd,  $J = 8.9, 2.6$  Hz, 1H), 7.91 (dd,  $J = 8.9, 0.7$  Hz, 1H), 3.68 (t,  $J = 6.2$  Hz, 2H), 2.95 – 2.79 (m, 2H), 1.95 – 1.77 (m, 2H), 1.77 – 1.61 (m, 2H), 1.43 (s, 2H);  $^{13}\text{C NMR}$  (100 MHz,  $\text{CDCl}_3$ )  $\delta$  169.2, 145.3, 142.1, 131.7, 119.3, 62.3, 38.9, 31.4, 25.6; HRMS: Calculated for  $\text{C}_9\text{H}_{13}\text{N}_2\text{O}_3\text{S}_2^+ [\text{M}+\text{H}]^+$  261.0362, found 261.0360.



6-(2-(5-Nitropyridin-2-yl)disulfanyl)hexan-1-ol (**1i**):

6-Mercapto-1-hexanol (0.134 g, 1.0 mmol) was reacted for 6 h to give **1i** (0.202 g, 70%) as a white powder. M.p. 59.4-59.5  $^\circ\text{C}$ ; IR (neat): 3368 (m), 3089 (w), 2933 (s), 2858 (m), 1592 (s), 1570 (s), 1521 (s), 1439 (s), 1346 (s), 1272 (m), 1138 (m), 1100 (s), 1056 (m), 1011 (w), 858 (s), 755 (s)  $\text{cm}^{-1}$ ;  $^1\text{H NMR}$  (400 MHz,  $\text{CDCl}_3$ )  $\delta$  9.28 (dd,  $J = 2.6, 0.6$  Hz, 1H), 8.41 (dd,  $J = 8.9, 2.6$  Hz, 1H), 7.92 (dd,  $J = 8.9, 0.6$  Hz, 1H), 3.64 (t,  $J = 6.5$  Hz, 2H), 2.88 – 2.80 (m, 2H), 1.79 – 1.67 (m, 2H), 1.63 – 1.51 (m, 2H), 1.49-1.33 (m, 4H);  $^{13}\text{C NMR}$  (100 MHz,  $\text{CDCl}_3$ )  $\delta$  169.4, 145.3, 142.1, 131.7, 119.2, 62.9, 39.0, 32.6, 29.1, 28.4, 25.5; HRMS: Calculated for  $\text{C}_{11}\text{H}_{17}\text{N}_2\text{O}_3\text{S}_2^+ [\text{M}+\text{H}]^+$  289.0675, found 289.0692.

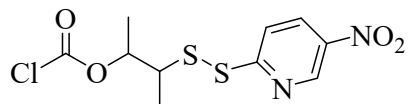


2-(2-(5-Nitropyridin-2-yl)disulfanyl)ethyl chloroformate

(**2a**): Alkanol **1a** (0.0464 g, 0.200 mmol) was reacted to give **2a** (0.0495 g, 84% ) as yellowish

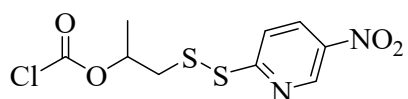


white powder. M.p. 45.0-45.3 °C; IR (neat): 3089 (w), 2962 (w), 1774 (s), 1592 (s), 1570 (s), 1521 (s), 1443 (m), 1340 (s), 1302 (m), 1275 (m), 1257 (m), 1138 (s), 1100 (s), 1015 (m), 948 (m), 858 (s), 754 (s)  $\text{cm}^{-1}$ ;  $^1\text{H}$  NMR (400 MHz,  $\text{CDCl}_3$ )  $\delta$  9.31 (d,  $J = 2.6$  Hz, 1H), 8.43 (dd,  $J = 8.8, 2.6$  Hz, 1H), 7.84 (d,  $J = 8.8$  Hz, 1H), 4.57 (t,  $J = 6.4$  Hz, 2H), 3.17 (t,  $J = 6.4$  Hz, 2H);  $^{13}\text{C}$  NMR (100 MHz,  $\text{CDCl}_3$ )  $\delta$  167.3, 150.7, 145.5, 142.5, 131.9, 119.8, 68.8, 36.6; HRMS: Calculated for  $\text{C}_8\text{H}_8\text{ClN}_2\text{O}_4\text{S}_2^+$   $[\text{M}+\text{H}]^+$  294.9614, found 294.9617.



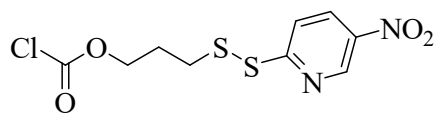
3-(2-(5-Nitropyridin-2-yl)disulfanyl)butan-2-yl

chloroformate (**2b**): Alkanol **1b** (0.0520 g, 0.200 mmol) was reacted to give **2a** (0.0524 g, 81% ) as yellowish oil. IR (neat): 3130 (w), 3089 (w), 1774 (s), 1592 (s), 1570 (s), 1521 (s), 1447 (m), 1372 (m), 1270 (m), 1171 (s), 1130 (s), 1100 (s), 858 (s), 754 (s)  $\text{cm}^{-1}$ ;  $^1\text{H}$  NMR (400 MHz,  $\text{CDCl}_3$ )  $\delta$  9.29 (d,  $J = 2.6$  Hz, 1H), 8.41 (dd,  $J = 8.9, 2.6$  Hz, 1H), 7.84 (d,  $J = 8.9$ , 1H), 5.20-5.08 (m, 1H), 3.30-3.18 (m, 1H), 1.48 (d,  $J = 6.5$  Hz, 3H), 1.43-1.39 (m, 3H);  $^{13}\text{C}$  NMR (100 MHz,  $\text{CDCl}_3$ )  $\delta$  168.0 and 167.9 (in 3:2 ratio), 150.2 and 150.0 (in 3:2 ratio), 145.3, 142.4, 131.8, 119.8 and 119.7 (in 2:3 ratio), 81.2 and 80.5 (in 2:3 ratio), 51.0 and 49.7 (in 3:2 ratio), 17.0 and 15.9 (in 3:2 ratio), 15.7 and 15.1 (in 2:3 ratio); HRMS: Calculated for  $\text{C}_{10}\text{H}_{12}\text{ClN}_2\text{O}_4\text{S}_2^+$   $[\text{M}+\text{H}]^+$  322.9922, found 322.9937.



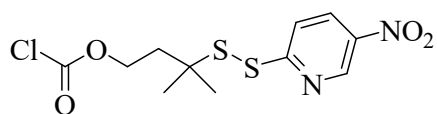
1-(2-(5-Nitropyridin-2-yl)disulfanyl)propan-2-yl

chloroformate (**2c**): Alkanol **1c** (0.0492 g, 0.200 mmol) was reacted to give **2c** (0.0498 g, 77%) as an off-white powder. M.p. 47.8-48.2 °C; IR (neat): 3089 (w), 2988 (w), 2936 (w), 1774 (s), 1592 (s), 1570 (s), 1521 (s), 1443 (m), 1346 (s), 1272 (m), 1164 (s), 1123 (s), 1100 (s), 1019 (s), 884 (m), 858 (s), 754 (m)  $\text{cm}^{-1}$ ;  $^1\text{H}$  NMR (400 MHz,  $\text{CDCl}_3$ )  $\delta$  9.30 (dd,  $J = 2.6, 0.7$  Hz, 1H), 8.41 (dd,  $J = 8.8, 2.6$  Hz, 1H), 7.80 (dd,  $J = 8.9, 0.7$  Hz, 1H), 5.18 (dq,  $J = 7.3, 6.3, 4.8$  Hz, 1H), 3.14 (dd,  $J = 14.4, 7.3$  Hz, 1H), 3.05 (dd,  $J = 14.4, 4.8$  Hz, 1H), 1.50 (d,  $J = 6.3$  Hz, 3H);  $^{13}\text{C}$  NMR (100 MHz,  $\text{CDCl}_3$ )  $\delta$  167.3, 150.1, 145.5, 142.5, 131.8, 119.8, 77.9, 43.8, 19.1; HRMS: Calculated for  $\text{C}_9\text{H}_{10}\text{ClN}_2\text{O}_4\text{S}_2^+$   $[\text{M}+\text{H}]^+$  308.9765, found 308.9775.



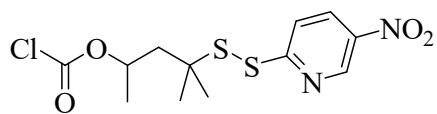
3-(2-(5-Nitropyridin-2-yl)disulfanyl)propyl

chloroformate (**2d**): Alkanol **1d** (0.0492 g, 0.20 mmol) was reacted to give **2d** (0.0444 g, 72% ) as yellowish white powder. M.p. 46.2-46.5 °C; IR (neat): 3089 (w), 2962 (m), 2925 (w), 1774 (s), 1592 (s), 1570 (s), 1521 (s), 1443 (m), 1346 (s), 1272 (m), 1156 (s), 1100 (s), 1015 (m), 858 (m), 754 (m) cm<sup>-1</sup>; <sup>1</sup>H NMR (400 MHz, CDCl<sub>3</sub>) δ 9.30 (d, *J* = 2.6 Hz, 1H), 8.42 (dd, *J* = 8.9, 2.6 Hz, 1H), 7.85 (d, *J* = 8.9 Hz, 1H), 4.46 (t, *J* = 6.1 Hz, 2H), 2.95 (t, *J* = 7.0 Hz, 2H), 2.17 (p, *J* = 6.5 Hz, 2H); <sup>13</sup>C NMR (100 MHz, CDCl<sub>3</sub>) δ 167.99, 150.76, 145.42, 142.36, 131.83, 119.58, 69.82, 34.71, 27.78; HRMS: Calculated for C<sub>9</sub>H<sub>10</sub>ClN<sub>2</sub>O<sub>4</sub>S<sub>2</sub><sup>+</sup> [M+H]<sup>+</sup> 308.9765, found 308.9777.



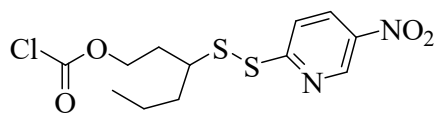
3-Methyl-3-(2-(5-nitropyridin-2-yl)disulfanyl)butyl

chloroformate (**2e**): Alkanol **1e** (0.0548 g, 0.20 mmol) was reacted to give **2e** (0.0525 g, 78% ) as yellowish white powder. M.p. 48.0-48.2 °C; IR (neat): 3089 (w), 2974 (m), 2933 (w), 1778 (s), 1595 (s), 1570 (s), 1521 (s), 1443 (m), 1346 (s), 1272 (m), 1153 (s), 1100 (s), 858 (s), 754 (m) cm<sup>-1</sup>; <sup>1</sup>H NMR (400 MHz, CDCl<sub>3</sub>) δ 9.27 (s, 1H), 8.40 (d, *J* = 7.9 Hz, 1H), 7.90 (d, *J* = 7.9 Hz, 1H), 4.50 (t, *J* = 6.2 Hz, 2H), 2.08 (t, *J* = 6.2 Hz, 2H), 1.39 (s, 6H); <sup>13</sup>C NMR (100 MHz, CDCl<sub>3</sub>) δ 168.9, 150.7, 145.2, 142.3, 131.7, 119.8, 68.8, 51.5, 39.1, 27.9 (x2C); HRMS: Calculated for [M+H]<sup>+</sup> C<sub>11</sub>H<sub>14</sub>ClN<sub>2</sub>O<sub>4</sub>S<sub>2</sub><sup>+</sup> 337.0078, found 337.0097.



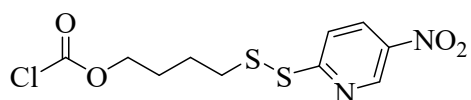
4-Methyl-4-(2-(5-nitropyridin-2-yl)disulfanyl)pentan-2-

yl chloroformate (**2f**): Alkanol **1f** (0.0576 g, 0.20 mmol) was reacted to give **2f** (0.0568 g, 81% ) as yellowish white powder. M.p. 49.0-49.5 °C; IR (neat): 3089 (w), 2970 (m), 2933 (w), 1774 (s), 1595 (s), 1570 (s), 1521 (s), 1443 (m), 1346 (s), 1273 (w), 1171 (s), 1119 (s), 1100 (s), 1033 (s), 1011 (m), 858 (s), 754 (m) cm<sup>-1</sup>; <sup>1</sup>H NMR (400 MHz, CDCl<sub>3</sub>) δ 9.26 (d, *J* = 2.6 Hz, 1H), 8.40 (dd, *J* = 8.9, 2.6 Hz, 1H), 7.94 (d, *J* = 8.9 Hz, 1H), 5.34 – 5.11 (m, 1H), 2.12 (dd, *J* = 15.6, 8.8 Hz, 1H), 1.89 (dd, *J* = 15.6, 2.3 Hz, 1H), 1.39-1.36 (m, 9H); <sup>13</sup>C NMR (100 MHz, CDCl<sub>3</sub>) δ 169.3, 150.1, 145.0, 142.2, 131.7, 119.7, 77.8, 52.0, 46.4, 28.6, 27.3, 21.5; HRMS: Calculated for C<sub>12</sub>H<sub>16</sub>ClN<sub>2</sub>O<sub>4</sub>S<sub>2</sub><sup>+</sup> [M+H]<sup>+</sup> 351.0235, found 351.0240.



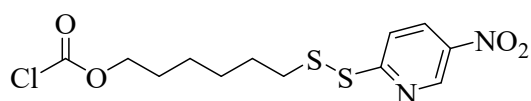
3-(2-(5-Nitropyridin-2-yl)disulfanyl)hexyl chloroformate

(**2g**): Alkanol **1g** (0.0576 g, 0.20 mmol) was reacted to give **2g** (0.0540 g, 77% ) as yellowish white powder. M.p. 49.2-49.6 °C; IR (neat): 3089 (w), 2962 (m), 2933 (m), 2877 (w), 1778 (s), 1595 (s), 1570 (s), 1521 (s), 1443 (m), 1346 (s), 1272 (m), 1156 (s), 1100 (s), 1011 (m), 858 (s), 754 (m)  $\text{cm}^{-1}$ ;  $^1\text{H}$  NMR (400 MHz,  $\text{CDCl}_3$ )  $\delta$  9.27 (d,  $J = 2.6$  Hz, 1H), 8.40 (dd,  $J = 8.8, 2.6$  Hz, 1H), 7.83 (d,  $J = 8.8$  Hz, 1H), 4.61-4.47 (m, 2H), 3.03-2.96 (m, 1H), 2.15 – 1.98 (m, 2H), 1.71 – 1.43 (m, 4H), 0.92 (t,  $J = 7.2$  Hz, 3H);  $^{13}\text{C}$  NMR (100 MHz,  $\text{CDCl}_3$ )  $\delta$  168.5, 150.7, 145.2, 142.3, 131.6, 119.9, 69.4, 49.1, 36.3, 32.6, 20.2, 13.9; HRMS: Calculated for  $\text{C}_{12}\text{H}_{16}\text{ClN}_2\text{O}_4\text{S}_2^+$   $[\text{M}+\text{H}]^+$  351.0235, found 351.0242.



4-(2-(5-Nitropyridin-2-yl)disulfanyl)butyl

chloroformate (**2h**): Alkanol **1h** (0.0520 g, 0.20 mmol) was reacted to give **2h** (0.0490 g, 76% ) as yellowish white powder. M.p. 50.3-50.5 °C; IR (neat): 3089 (w), 2936 (m), 2858 (w), 1774 (s), 1595 (s), 1570 (s), 1521 (s), 1443 (m), 1346 (s), 1273 (m), 1149 (s), 1100 (s), 1011 (m), 858 (s), 754 (m)  $\text{cm}^{-1}$ ;  $^1\text{H}$  NMR (400 MHz,  $\text{CDCl}_3$ )  $\delta$  9.29 (dd,  $J = 2.6, 0.7$  Hz, 1H), 8.42 (dd,  $J = 8.9, 2.6$  Hz, 1H), 7.88 (dd,  $J = 8.9, 0.7$  Hz, 1H), 4.34 (t,  $J = 6.1$  Hz, 2H), 2.88 (t,  $J = 6.9$  Hz, 2H), 1.95 – 1.77 (m, 4H);  $^{13}\text{C}$  NMR (100 MHz,  $\text{CDCl}_3$ )  $\delta$  168.6, 150.8, 145.4, 142.2, 131.8, 119.4, 71.4, 38.2, 27.2, 25.3; HRMS: Calculated for  $\text{C}_{10}\text{H}_{12}\text{ClN}_2\text{O}_4\text{S}_2^+$   $[\text{M}+\text{H}]^+$  322.9922, found 322.9935.

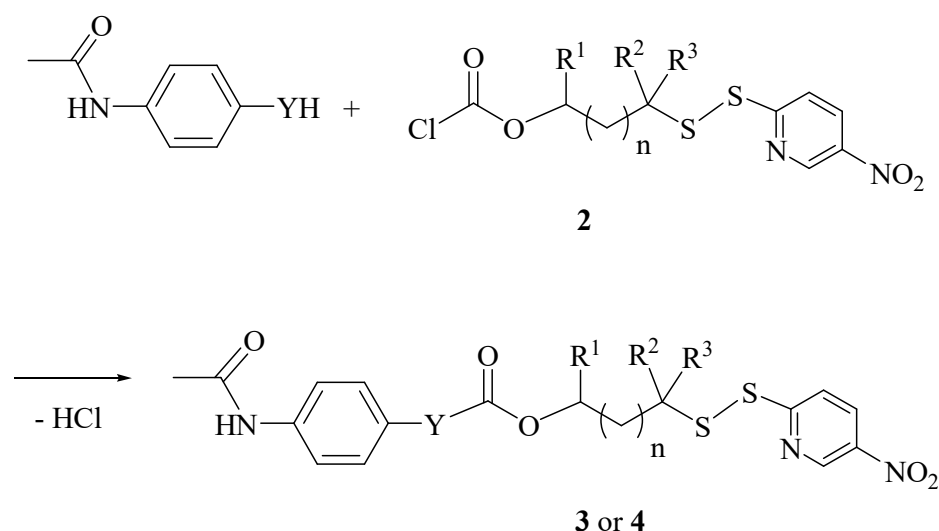


6-(2-(5-Nitropyridin-2-yl)disulfanyl)hexyl

chloroformate (**2i**): Alkanol **1i** (0.0576 g, 0.20 mmol) was reacted to give **2i** (0.0561 g, 80% ) as yellowish white powder. M.p. 53.9-54.2 °C; IR (neat): 3089 (w), 2933 (m), 2862 (m), 1778 (s), 1595 (s), 1570 (s), 1521 (s), 1439 (m), 1346 (s), 1272 (m), 1145 (s), 1100 (s), 1048 (m), 858 (m), 754 (m)  $\text{cm}^{-1}$ ;  $^1\text{H}$  NMR (400 MHz,  $\text{CDCl}_3$ )  $\delta$  9.28 (d,  $J = 2.6$  Hz, 1H), 8.41 (dd,  $J = 8.9, 2.6$  Hz, 1H), 7.90 (dd,  $J = 8.9, 0.7$  Hz, 1H), 4.31 (t,  $J = 6.6$  Hz, 2H), 2.91 – 2.76 (m, 2H), 1.76-1.70 (m, 4H), 1.41-1.25 (m, 4H);  $^{13}\text{C}$  NMR (100 MHz,  $\text{CDCl}_3$ )  $\delta$  169.1, 150.8, 145.3, 142.1, 131.7, 119.3, 72.1, 38.8, 28.9, 28.3, 28.0, 25.3; HRMS: Calculated for  $\text{C}_{12}\text{H}_{16}\text{ClN}_2\text{O}_4\text{S}_2^+$   $[\text{M}+\text{H}]^+$  351.0235, found 351.0240.

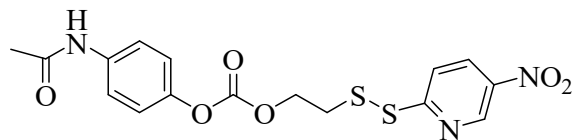
**Preparation of Cargo-Linker semiconjugates.** Many cancer drugs contain one or several hydroxyl and amino groups which are instrumental for the biological activity. In this study, 4-acetamidophenol (paracetamol) was used as a model compound for hydroxyl-containing drugs and 4-acetamidoaniline as a model for amino-containing drugs. These two structurally related compounds were selected (i) due to their ionization potential making MS detection easy, (ii) good light absorption allowing for UV detection and (iii) unlike cytotoxins used in ADCs, they are cheap and non-hazardous.

These cargoes were conjugated with linkers to give C-L semiconjugates **3** and **4** (Scheme 8). The reactions between 4-acetamidophenol and linkers **2** did not occur in the absence of a base. Triethylamine (TEA) appeared to be a good choice; therefore, this base was added and formation of the C-L semiconjugate **3** was achieved. 4-Acetamidoaniline, on the other hand, reacted with linker **2** giving semiconjugate **4** in the absence of a base. When stoichiometric amount of 4-acetamidoaniline was used, the reaction was not complete due to the hydrogen chloride generated from the reaction formed an ammonium salt with the unreacted 4-acetamidoaniline. Therefore, the use of 0.5 equivalent of TEA appeared to increase the yield of **4**. Using these methods several cargo-MCA semiconjugates were synthesized; the results are summarized in Table 2.



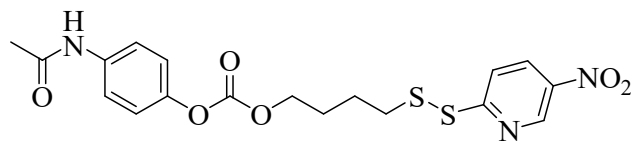
**Scheme 8.** Conjugation of cargo to linkers; **3** when Y is O and **4** when Y is NH

Descriptions of the synthesis and characterization of all semi-conjugates, are detailed as follows  
 Yields of semi-conjugates are summarized in Table 2.



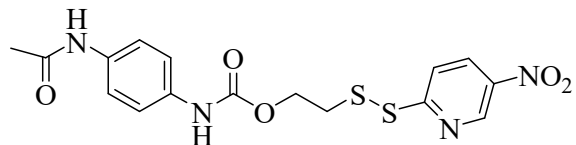
4-Acetamidophenyl 2-(2-(5-nitropyridin-2-

yl)disulfanyl)- ethyl carbonate (**3a**): Linker **2a** (0.0294 g, 0.100 mmol) reacted for 1 h to give **3a** (0.0266 g, 65%) as a white solid. M.p. 104.5-105.0 °C; IR (neat): 3365 (m), 3130 (w), 3089 (w), 2950 (w), 1760 (s), 1674 (m), 1592 (s), 1566 (s), 1510 (s), 1443 (s), 1410 (s), 1346 (s), 1380 (s), 1253 (s), 1205 (s), 1171 (s), 1100 (s), 989 (s), 937 (m), 858 (s), 780 (m)  $\text{cm}^{-1}$ ;  $^1\text{H}$  NMR (400 MHz,  $\text{CDCl}_3$ )  $\delta$  9.29 (d,  $J = 2.6$  Hz, 1H), 8.41 (dd,  $J = 8.9, 2.6$  Hz, 1H), 7.91 (d,  $J = 8.9$  Hz, 1H), 7.58 (s, 1H), 7.52-7.46 (m, 2H), 7.16-7.09 (m, 2H), 4.50 (t,  $J = 6.2$  Hz, 2H), 3.20 (t,  $J = 6.2$  Hz, 2H), 2.23 (s, 3H);  $^{13}\text{C}$  NMR (100 MHz,  $\text{CDCl}_3$ )  $\delta$  170.5, 167.9, 153.5, 147.8, 145.3, 142.4, 135.2, 132.0, 121.8, 121.6, 119.9, 66.0, 37.3, 24.2; HRMS: Calculated for  $\text{C}_{16}\text{H}_{16}\text{N}_3\text{O}_6\text{S}_2^+$   $[\text{M}+\text{H}]^+$  410.0481, found 410.0476



4-Acetamidophenyl 4-(2-(5-nitropyridin-

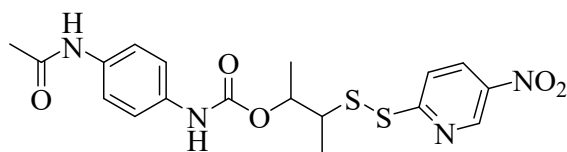
2-yl)disulfanyl) butyl carbonate (**3h**): Linker **2h** (0.0323 g, 0.100 mmol) reacted for 1 h to give **3h** (0.0258 g, 59%) as a white solid. M.p. 106.2-106.8 °C; IR (neat): 3312 (m), 3093 (w), 2981 (w), 2933 (w), 1783 (m), 1666(m), 1592 (s), 1566 (s), 1510 (s), 1443 (s), 1410 (s), 1346 (s), 1380 (s), 1253 (s), 1205 (s), 1179 (s), 1134 (s), 1100 (s), 989 (s), 937 (m), 858 (s), 780 (m)  $\text{cm}^{-1}$ ;  $^1\text{H}$  NMR (400 MHz,  $\text{CDCl}_3$ )  $\delta$  9.29 (dd,  $J = 2.6, 0.7$  Hz, 1H), 8.41 (dd,  $J = 8.9, 2.6$  Hz, 1H), 7.90 (dd,  $J = 8.9, 0.7$  Hz, 1H), 7.54-7.47 (m, 2H), 7.16-7.09 (m, 2H), 4.30-4.23 (m, 2H), 2.90 (t,  $J = 6.6$  Hz, 2H), 2.22 (s, 3H), 1.92-1.85 (m, 4H);  $^{13}\text{C}$  NMR (100 MHz,  $\text{CDCl}_3$ )  $\delta$  169.2, 168.8, 153.3, 147.6, 145.3, 142.3, 135.5, 131.8, 121.7, 121.3, 119.5, 68.2, 38.5, 27.5, 25.5, 24.5; HRMS: Calculated for  $\text{C}_{18}\text{H}_{20}\text{N}_3\text{O}_6\text{S}_2^+$   $[\text{M}+\text{H}]^+$  438.0794, found 438.1315.



2-(2-(5-Nitropyridin-2-yl)disulfanyl)ethyl 4-

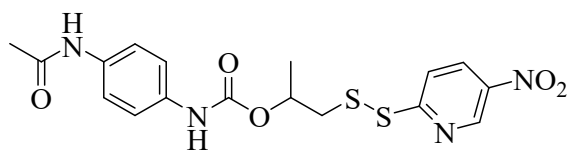
acetamido-phenyl carbamate (**4a**): Linker **2a** (0.0294 g, 0.100 mmol) reacted for 30 min to give **4a** (0.0286 g, 70%) as a white solid. M.p. 108.1-108.7 °C; IR (neat): 3312 (m), 3093 (w), 2985

(w), 2936 (w), 1782 (m), 1711 (m), 1674(m), 1592 (s), 1570 (s), 1521 (s), 1443 (s), 1410 (s), 1346 (s), 1380 (s), 1313 (s), 1253 (s), 1216 (s), 1171 (s), 1100 (s), 1056 (m), 1022 (s), 914 (s), 858 (s), 754(m)  $\text{cm}^{-1}$ ;  $^1\text{H}$  NMR (400 MHz,  $\text{DMSO-}d_6$ )  $\delta$  9.83 (s, 1H), 9.59 (s, 1H), 9.24 (d,  $J = 2.7$  Hz, 1H), 8.53 (dd,  $J = 8.9, 2.7$  Hz, 1H), 8.07 (d,  $J = 8.9$  Hz, 1H), 7.55-7.36 (m, 2H), 7.35-7.31 (m, 2H), 4.30 (t,  $J = 6.0$  Hz, 2H), 3.22 (t,  $J = 6.0$  Hz, 2H), 2.00 (s, 3H);  $^{13}\text{C}$  NMR (100 MHz,  $\text{DMSO-}d_6$ )  $\delta$  167.9, 167.0, 153.1, 144.9, 142.3, 134.4, 134.0, 132.6, 119.7, 119.5, 118.7, 61.6, 37.3, 23.9; HRMS: Calculated for  $\text{C}_{16}\text{H}_{17}\text{N}_4\text{O}_5\text{S}_2^+$   $[\text{M}+\text{H}]^+$  409.0640, found 409.0643.



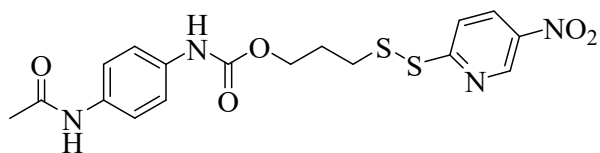
3-(2-(5-Nitropyridin-2-yl)disulfanyl)butan-2-

yl 4-acetamidophenylcarbamate (**4b**): Linker **2b** (0.0323 g, 0.100 mmol) reacted for 90 min to give **4b** (0.0275 g, 63%) as a white solid. M.p. 109.8-110.3  $^{\circ}\text{C}$ ; IR (neat): 3312 (m), 3093 (w), 2985 (m), 2936 (w), 1711 (m), 1674 (m), 1592 (s), 1570 (s), 1521 (s), 1441 (m), 1410 (m), 1313 (m), 1216 (s), 1171 (s), 1056 (s), 1022 (m), 914 (m), 736 (m)  $\text{cm}^{-1}$ ;  $^1\text{H}$  NMR (400 MHz,  $\text{CDCl}_3$ )  $\delta$  9.20 (d,  $J = 2.6$  Hz, 1H), 8.29 (dd,  $J = 8.9, 2.6$  Hz, 1H), 7.87 (d,  $J = 8.9$  Hz, 1H), 7.47 – 7.36 (m, 2H), 7.35 – 7.28 (m, 2H), 6.69 (s, 1H), 5.19 – 5.04 (m, 1H), 3.25 (qd,  $J = 7.1, 3.5$  Hz, 1H), 2.21 (s, 3H), 1.41 (d,  $J = 6.8$  Hz, 3H), 1.36 (d,  $J = 7.1$  Hz, 3H);  $^{13}\text{C}$  NMR (100 MHz,  $\text{DMSO-}d_6$ )  $\delta$  167.9, 167.3, 152.8, 144.8, 142.2, 134.3, 134.1, 132.5, 119.6, 119.4, 118.6, 71.1, 50.7, 23.9, 17.2, 14.7; HRMS: Calculated for  $\text{C}_{18}\text{H}_{21}\text{N}_4\text{O}_5\text{S}_2^+$   $[\text{M}+\text{H}]^+$  437.0953, found 437.0953.



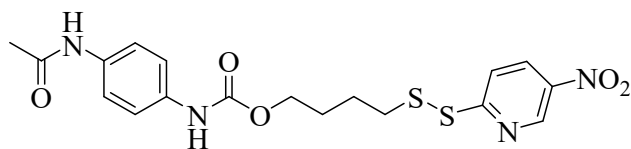
1-(2-(5-Nitropyridin-2-yl)disulfanyl)propan-

2-yl 4-acetamidophenylcarbamate (**4c**): Linker **2c** (0.0309 g, 0.100 mmol) reacted for 90 min to give **4c** (0.0301 g, 71%) as a white solid. M.p. 107.3-107.9  $^{\circ}\text{C}$ ; IR (neat): 3312 (m), 3093 (w), 2981 (m), 2933 (w), 1786 (m), 1666 (m), 1592 (s), 1570 (s), 1521 (s), 1410 (s), 1346 (s), 1223 (s), 1134 (s), 1100 (s), 1056 (s), 1022 (s), 914 (m), 754 (m), 736 (m)  $\text{cm}^{-1}$ ;  $^1\text{H}$  NMR (400 MHz,  $\text{DMSO-}d_6$ )  $\delta$  9.82 (s, 1H), 9.52 (s, 1H), 9.22 (d,  $J = 2.7$  Hz, 1H), 8.50 (dd,  $J = 8.9, 2.7$  Hz, 1H), 8.03 (d,  $J = 8.9$  Hz, 1H), 7.49 – 7.23 (m, 4H), 5.01-4.97 (m, 1H), 3.25-3.13 (m, 2H), 2.00 (s, 3H), 1.32 (d,  $J = 6.3$  Hz, 3H);  $^{13}\text{C}$  NMR (100 MHz,  $\text{DMSO-}d_6$ )  $\delta$  167.9, 167.0, 152.8, 144.9, 142.2, 134.3, 134.1, 132.6, 119.7, 119.4, 118.5, 68.9, 43.7, 23.9, 19.4; HRMS: Calculated for  $\text{C}_{17}\text{H}_{19}\text{N}_4\text{O}_5\text{S}_2^+$   $[\text{M}+\text{H}]^+$  423.0797, found 423.0794.



3-(2-(5-Nitropyridin-2-yl)disulfanyl)propyl

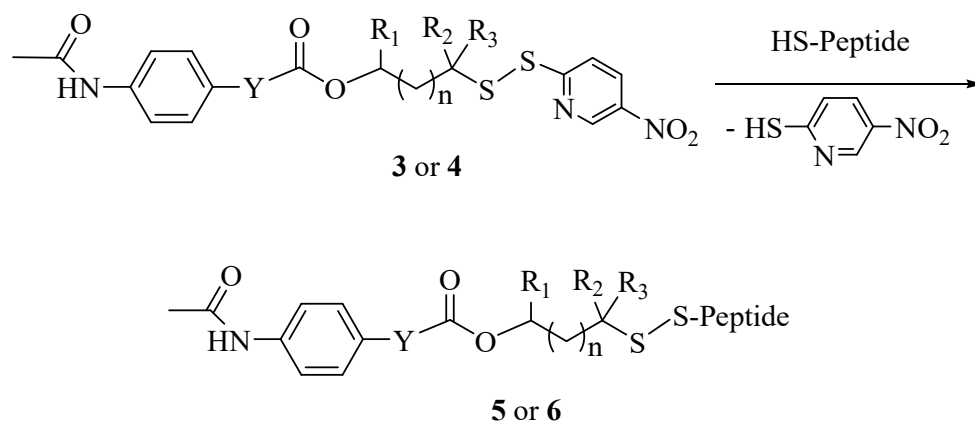
4-acetamidophenylcarbamate (**4d**): Linker **2d** (0.0310 g, 0.100 mmol) reacted for 90 min to give **4d** (0.0305 g, 72%) as a white solid. M.p. 103.0-103.5 °C; IR (neat): 3465 (w), 3320 (w), 3260 (m), 3063 (w), 2959 (m), 2843 (m), 1704 (s), 1674 (s), 1592 (m), 1540 (s), 1514 (s), 1413 (s), 1350 (s), 1223 (s), 1100 (s), 1030 (m), 970 (w), 829 (s), 750 (s)  $\text{cm}^{-1}$ ;  $^1\text{H}$  NMR (400 MHz,  $\text{DMSO-}d_6$ )  $\delta$  9.80 (s, 1H), 9.48 (s, 1H), 9.25 (dd,  $J = 2.7, 0.7$  Hz, 1H), 8.56 (dd,  $J = 8.9, 2.7$  Hz, 1H), 8.05 (dd,  $J = 8.9, 0.7$  Hz, 1H), 7.52 – 7.40 (m, 2H), 7.33 (d,  $J = 8.6$  Hz, 2H), 4.16 (t,  $J = 6.3$  Hz, 2H), 3.01 (dd,  $J = 7.9, 6.6$  Hz, 2H), 2.08-2.01 (m, 2H), 2.01 (s, 3H);  $^{13}\text{C}$  NMR (101 MHz,  $\text{DMSO-}d_6$ )  $\delta$  167.8, 167.2, 153.4, 144.9, 142.3, 134.2, 132.6, 119.6, 119.5, 118.5, 117.9, 62.3, 34.7, 28.2, 23.8; HRMS: Calculated for  $\text{C}_{17}\text{H}_{19}\text{N}_4\text{O}_5\text{S}_2^+$   $[\text{M}+\text{H}]^+$  423.0797, found 423.0801.



4-(2-(5-Nitropyridin-2-yl)disulfanyl)butyl

4-acetamidophenylcarbamate (**4h**): Linker **2h** (0.0323 g, 0.100 mmol) reacted for 90 min to give **4h** (0.0306 g, 70%) as a white solid. M.p. 110.1-110.4 °C; IR (neat): 3298 (m), 3212 (m), 3063 (w), 2940 (m), 2847 (m), 1700 (s), 1674 (s), 1547 (s), 1514 (s), 1413 (s), 1346 (s), 1272 (s), 1246 (s), 1100 (s), 1067 (m), 970 (m), 829 (s), 750 (s)  $\text{cm}^{-1}$ ;  $^1\text{H}$  NMR (400 MHz,  $\text{DMSO-}d_6$ )  $\delta$  9.82 (s, 1H), 9.48 (s, 1H), 9.24 (d,  $J = 2.7$  Hz, 1H), 8.57 (dd,  $J = 8.8, 2.7$  Hz, 1H), 8.04 (d,  $J = 8.8$  Hz, 1H), 7.48 – 7.41 (m, 2H), 7.33 (d,  $J = 9.0$  Hz, 2H), 4.10 – 4.03 (m, 2H), 3.01 – 2.93 (m, 1H), 2.00 (s, 3H), 1.76-1.72 (m, 4H);  $^{13}\text{C}$  NMR (100 MHz,  $\text{DMSO-}d_6$ )  $\delta$  167.9, 167.4, 153.6, 145.0, 142.3, 134.3, 134.2, 132.7, 119.5, 119.5, 118.5, 63.5, 37.5, 27.3, 25.1, 23.9; HRMS: Calculated for  $\text{C}_{18}\text{H}_{21}\text{N}_4\text{O}_5\text{S}_2^+$   $[\text{M}+\text{H}]^+$  437.0953, found 437.0973.

**Preparation of full conjugates.** This was achieved by reacting semi conjugate **3** or **4** with thiol-containing peptide as illustrated in Scheme 9.



**Scheme 9.** Preparation of C-L-V conjugates; **3** and **5** when Y is O, **4** and **6** when Y is NH

Preparation of the first full conjugate was achieved by reacting carbonate **3a** with a cysteine-containing peptide in aqueous acetonitrile at room temperature. The reaction was relatively slow (UPLC monitoring), but what was more important was the regioselective attack of **3a**. This carbonate has two sites that can react with thiols, *viz.* the nitropyridyl disulfide end and the carbonate moiety, but analyses showed that the peptide attacked the former site exclusively and afforded the C-L-V conjugate **5a** only. High resolution mass spectrometric analysis gave four main peaks which correspond to single and multiply charged ions. (Figure 6)



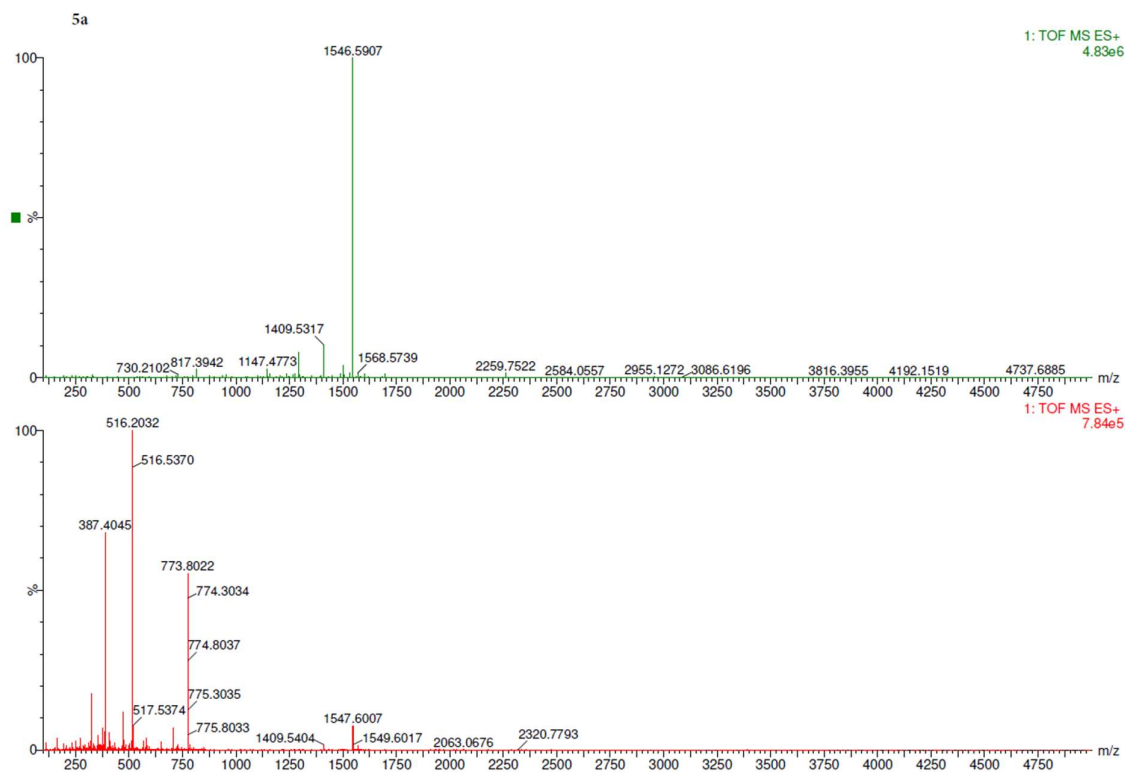


**Figure 6.** High resolution mass spectra of **5a**. The lower part is the original spectrum, the upper part is the spectrum processed in the same way as in Figure 5.

However, in another exploratory experiment a cell-penetrating peptide with sequence of CGRKKRRQRRRPQ (containing free amine on the lysine side chain) reacted with **3a** at both sites; thus, **1a** and paracetamol were formed to some extent and proved that the carbonate moiety had been attacked. Based on these experiments, carbonates **3** and carbamates **4** were reacted with the histidine-rich peptide (Ac)CGHHPHGHHHPH-amide under similar conditions to give the corresponding conjugates **5** and **6** as illustrated in Scheme 5. The yields are summarized in Table 2. Coupling of peptide with semi conjugate were completed within 24 hours. UPLC monitoring of the reaction between **4a** and peptide (Ac)CGHHPHGHHHPH-amide is shown in Figure 7.

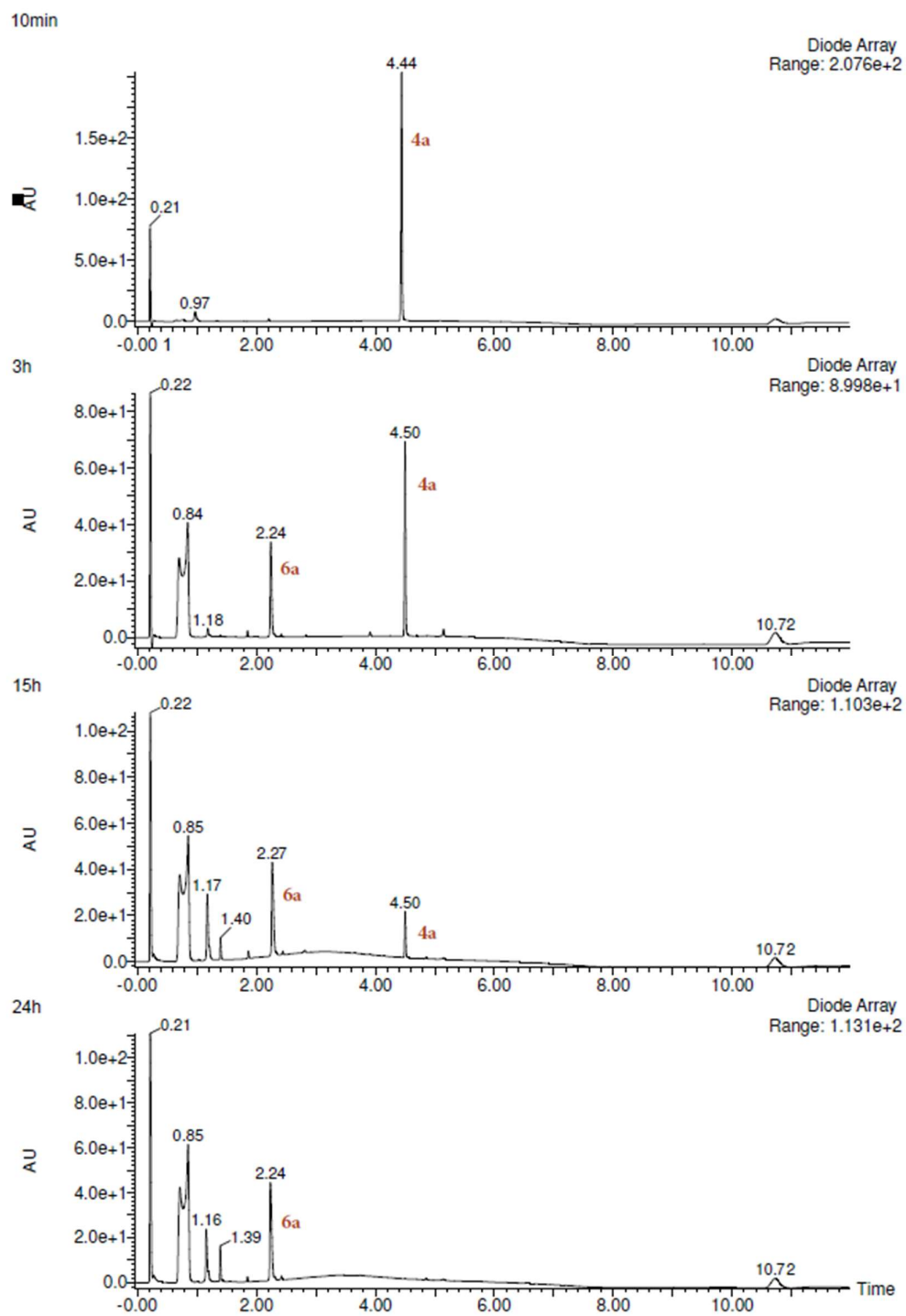


**Figure 7.** UPLC-chromatograms of reaction mixture between **4a** and peptide at 10 min, 3 h, 15 h and 24 h of reaction times.

**Table 2.** Yields of cargo-linker (C-L) semiconjugate and cargo-linker-vector (C-L-V) conjugates

Linker	Cargo	Conjugates/Yield(%)	
		C-L	C-L-V*
<b>2a</b>	4-Acetamidophenol	<b>3a/65</b>	<b>5a</b>
<b>2a</b>	4-Acetamidoaniline	<b>4a/70</b>	<b>6a</b>
<b>2b</b>	4-Acetamidoaniline	<b>4b/63</b>	<b>6b</b>
<b>2c</b>	4-Acetamidoaniline	<b>4c/71</b>	<b>6c</b>
<b>2d</b>	4-Acetamidoaniline	<b>4d/72</b>	<b>6d</b>
<b>2h</b>	4-Acetamidophenol	<b>3h/59</b>	<b>5h</b>
<b>2h</b>	4-Acetamidoaniline	<b>4h/70</b>	<b>6h</b>
<b>2a</b>	4-Acetamidophenol	<b>3a/65</b>	<b>5a</b>

\*Isolated yields were not calculated due to undetermined water content of the peptide which was the limiting reagent

With a number of complete conjugates **5** and **6**, their stability under aqueous conditions could be studied. At pH 2 and lower, all conjugates turned out to be stable, but at physiological pH the conjugates with a carbonate linkage, *i.e* **5a** and **5h**, suffered general hydrolysis and afforded 4-acetamidophenol and linker-peptide fragments.

These results warrant the conclusion that carbonate-containing conjugates are too unstable to be suitable for therapeutic applications. Similar results have been reported previously when a cargo molecule was attempted to be conjugated via a phenolic hydroxyl group.<sup>27</sup> Analysis of conjugates **6a** - **6d** and **6h**, however, showed no degradation at pH 7.4 which means that only carbamate-containing conjugates are stable enough to have a reasonable half-life in plasma. Consequently, the use of mercaptoalkanol linkers would be restricted to amine-containing cargo only.

Conjugate **5a**. Drug-linker conjugate **3a** (0.050 mmol, 20 mg) reacted for 24 h to give **5a** as a white solid (12 mg). HRMS: Calculated for C<sub>66</sub>H<sub>84</sub>N<sub>25</sub>O<sub>16</sub>S<sub>2</sub><sup>+</sup> [M+H]<sup>+</sup> 1546.5969, found 1546.5907.

Conjugate **5h**. Drug-linker conjugate **3h** (0.050 mmol, 22 mg) reacted for 24 h to give **5h** as a white solid (14 mg). HRMS: Calculated for  $C_{68}H_{88}N_{25}O_{16}S_2^+$   $[M+H]^+$  1574.6282, found 1574.5493.

Conjugate **6a**. Drug-linker conjugate **4a** (0.050 mmol, 20 mg) reacted for 24 h to give **6a** as a white solid (11 mg). HRMS: Calculated for  $C_{66}H_{85}N_{26}O_{15}S_2^+$   $[M+H]^+$  1545.6129, found 1545.6139.

Conjugate **6b**. Drug-linker conjugate **4b** (0.050 mmol, 22 mg) reacted for 24 h to give **6b** as a white solid (18 mg). HRMS: Calculated for  $C_{68}H_{89}N_{26}O_{15}S_2^+$   $[M+H]^+$  1573.6442, found 1573.6410.

Conjugate **6c**. Drug-linker conjugate **4c** (0.050 mmol, 21 mg) reacted for 24 h to give **6c** as a white solid (16 mg). HRMS: Calculated for  $C_{67}H_{87}N_{26}O_{15}S_2^+$   $[M+H]^+$  1559.6286, found 1559.6256.

Conjugate **6d**. Drug-linker conjugate **4d** (0.050 mmol, 22 mg) reacted for 24 h to give **6d** as a white solid (14 mg). HRMS: Calculated for  $C_{67}H_{87}N_{26}O_{15}S_2^+$   $[M+H]^+$  1559.6286, found 1559.6169

Conjugate **6h**. Drug-linker conjugate **4h** (0.050 mmol, 22 mg) reacted for 24 h to give **6h** as a white solid (13 mg). HRMS: Calculated for  $C_{68}H_{89}N_{26}O_{15}S_2^+$   $[M+H]^+$  1573.6442, found 1573.6417

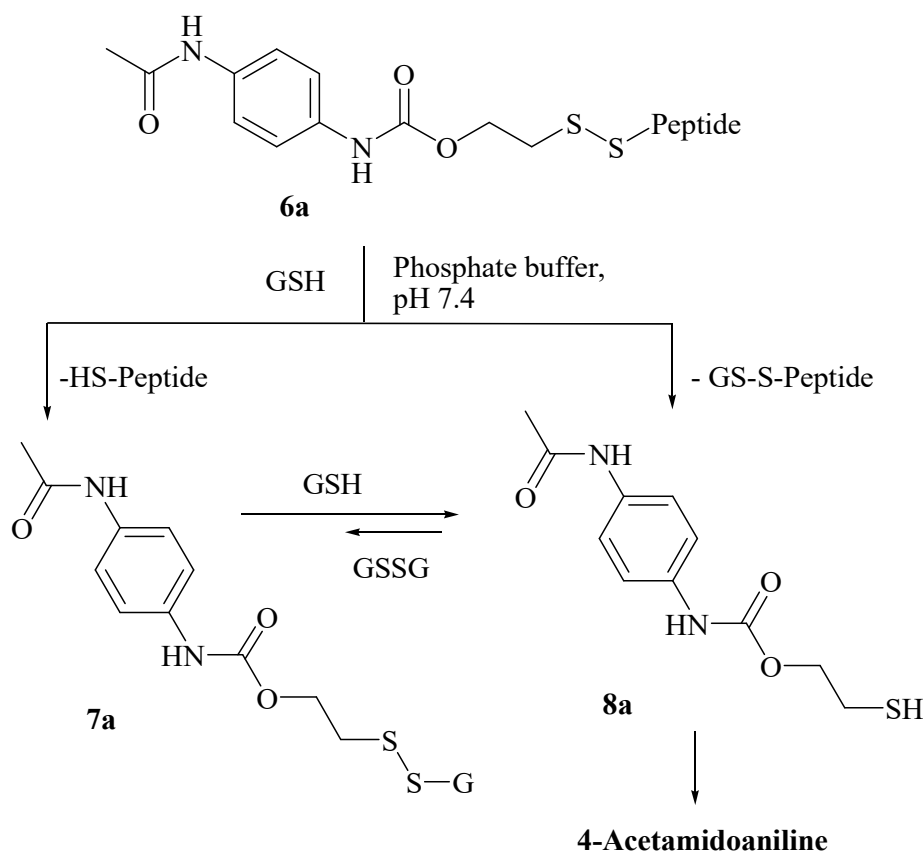
## 5.2. Cargo release analysis

**Cargo release from full conjugates.** In this study the reaction of GSH with conjugates **5** or **6** have been investigated. When **6a** was reacted with GSH at pH 7.4 a cascade of reactions took place releasing the cargo, conceivably via C-L-glutathione conjugate **7a** and cargo-linker adduct **8a** (Scheme 10). The former is the main initial product, but it reacts further with GSH to afford **8a**. Compounds **7a** and **8a** were identified by high resolution mass spectrometer (Figure 8).

In addition, analyses suggested that **8a** was also produced directly from **6a** because the GSH attack on the disulfide moiety is not specific. Thiol **8a** underwent intramolecular reaction to release the free cargo (4-acetamidoaniline), while being generated from **7a**. As Figures 9 and 10 show, the concentration of the released drug increased over time until all **8a** was consumed. However, after approximately 1 hour the rate of cargo release was slightly reduced and the concentration of **7a** increased again whereas that of **8a** constantly decreased. The analysis proved that significant amount of reduced GSH present in the reaction mixture was oxidized to

form oxidized glutathione (GSSG) during the analysis. As the concentration of GSSG surpasses the concentration of GSH, the reverse conversion of the equilibrium between **7a** and **8a** becomes predominant, thus the concentration of **7a** started to increase until **8a** was totally consumed. After this, the concentrations of **7a** and the free drug became nearly constant. However, when a fresh solution of GSH was added after 9 h, **8a** was generated again, thus the release of more cargo took place. This indicates that cargo release is dependent on the concentration of reduced GSH.

This degradation study clearly showed that the free cargo was formed through **8a**. According to the literature,<sup>22,23,28,39</sup> two possible mechanisms of cargo release have been proposed for this type of linkers.



**Scheme 10.** Degradation pattern of **6a** in an aqueous solution of GSH.

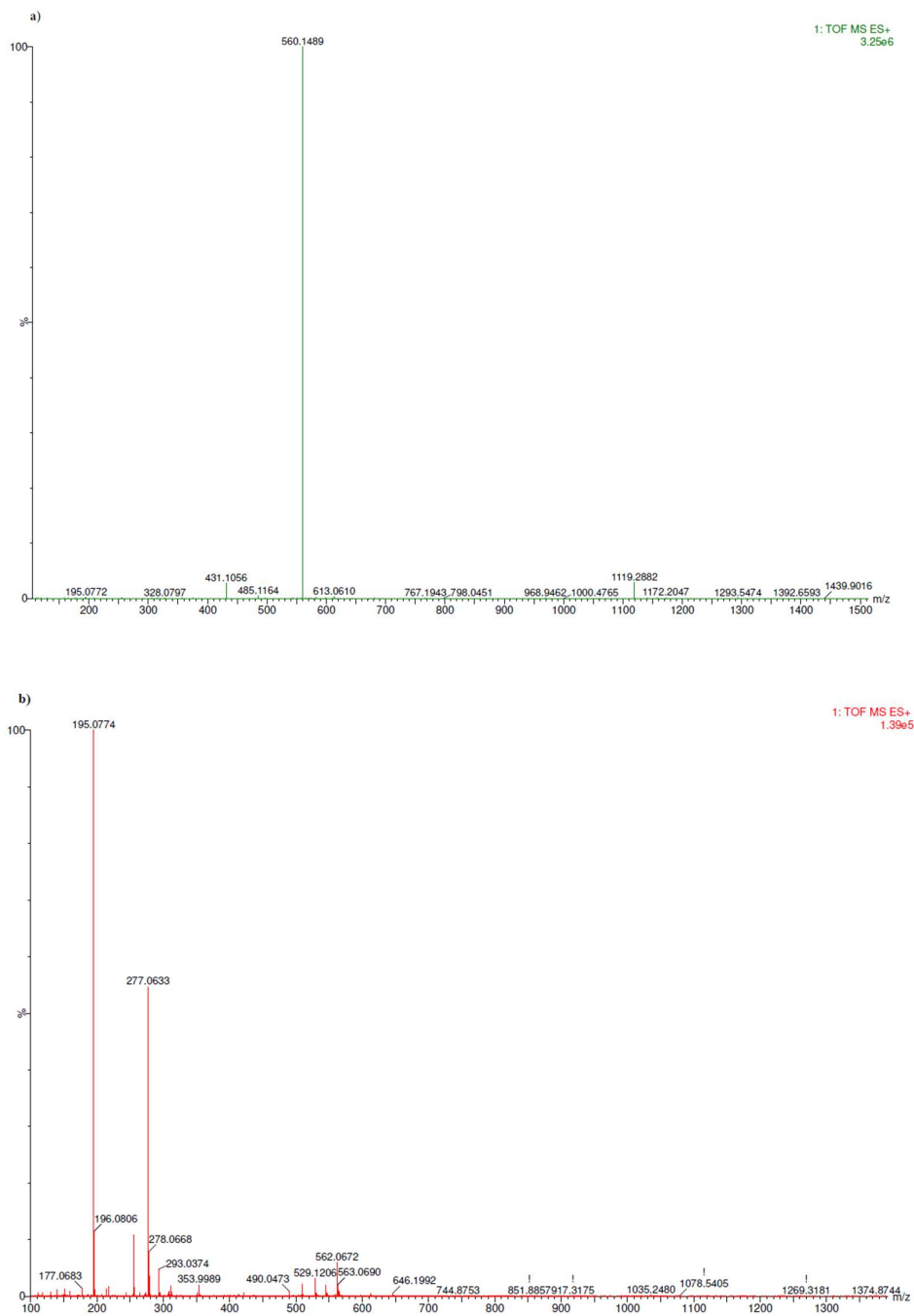


**Figure 8.** Mass spectra of intermediary products of degradation of **6a**: a) **7a**, b) **8a**

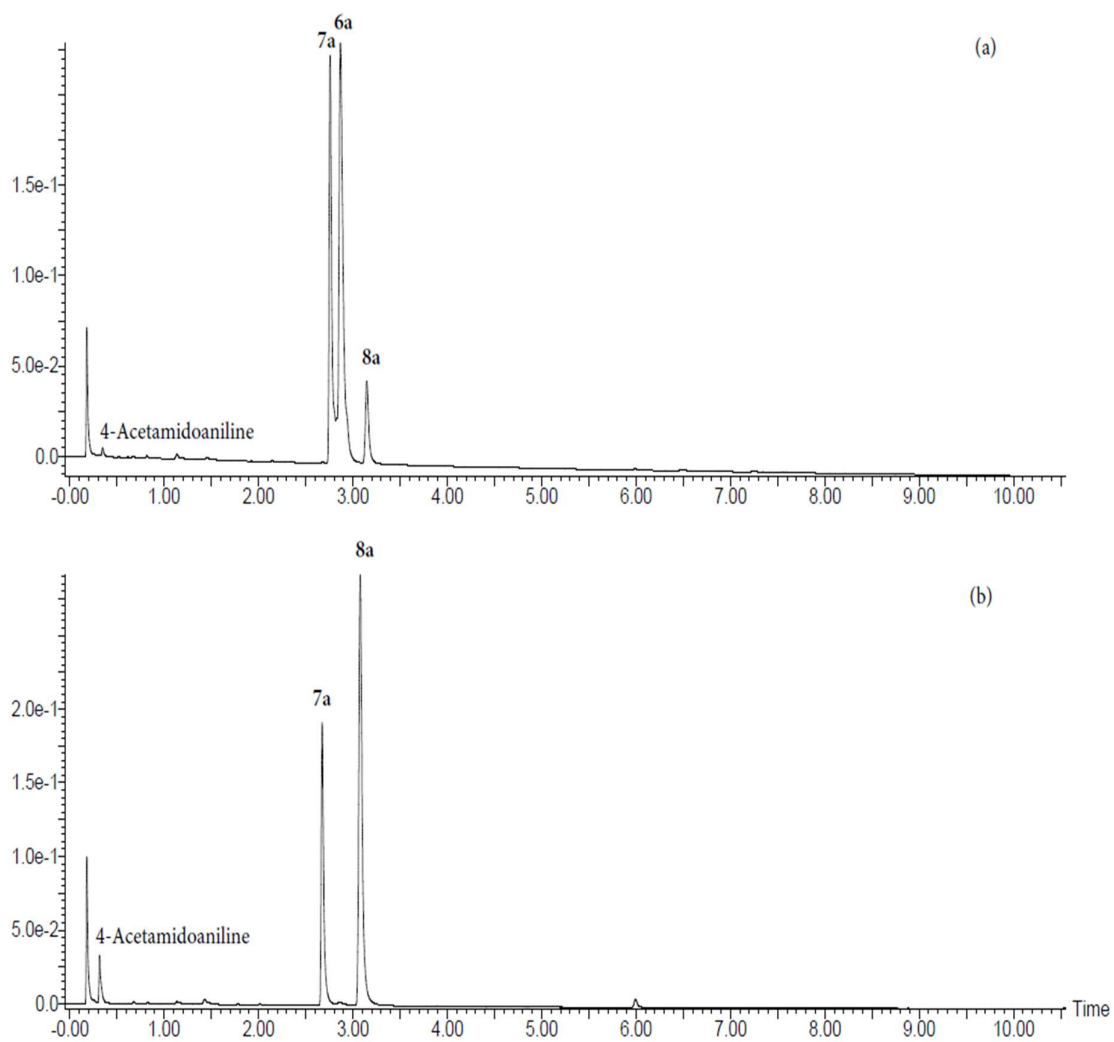


**Figure 9.** UPLC analysis of the degradation products from **6a**. Gradient: acetonitrile 5% to 50% in water in 10 min. a) after 2 min b) after 62 min

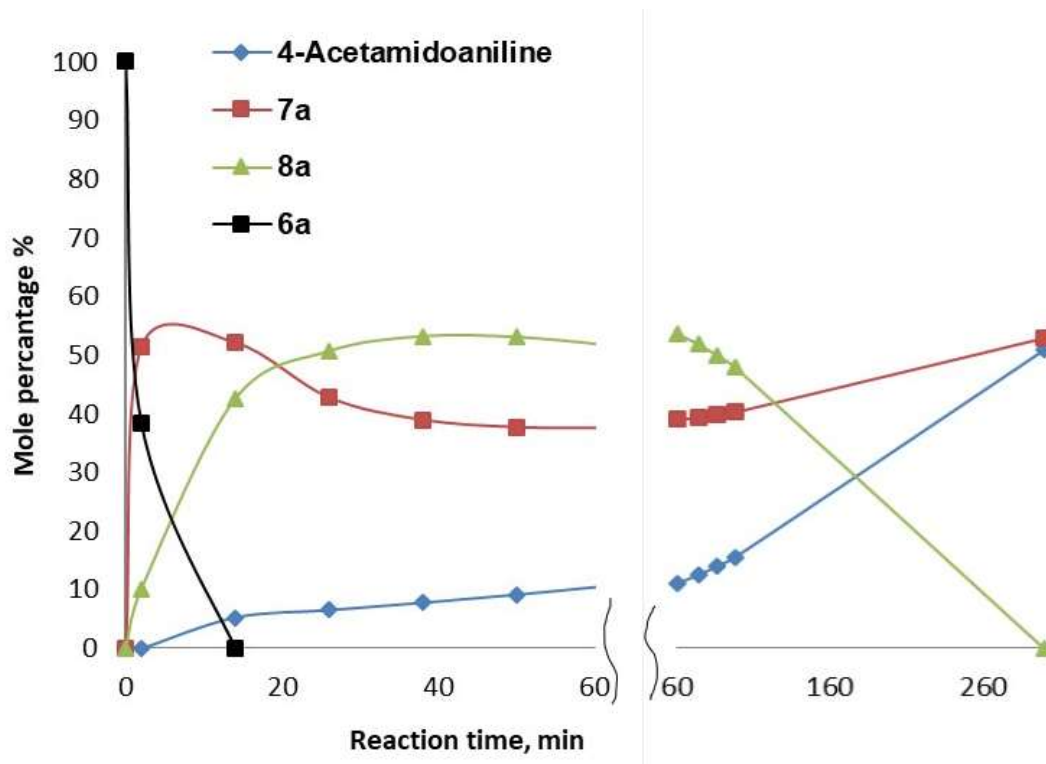
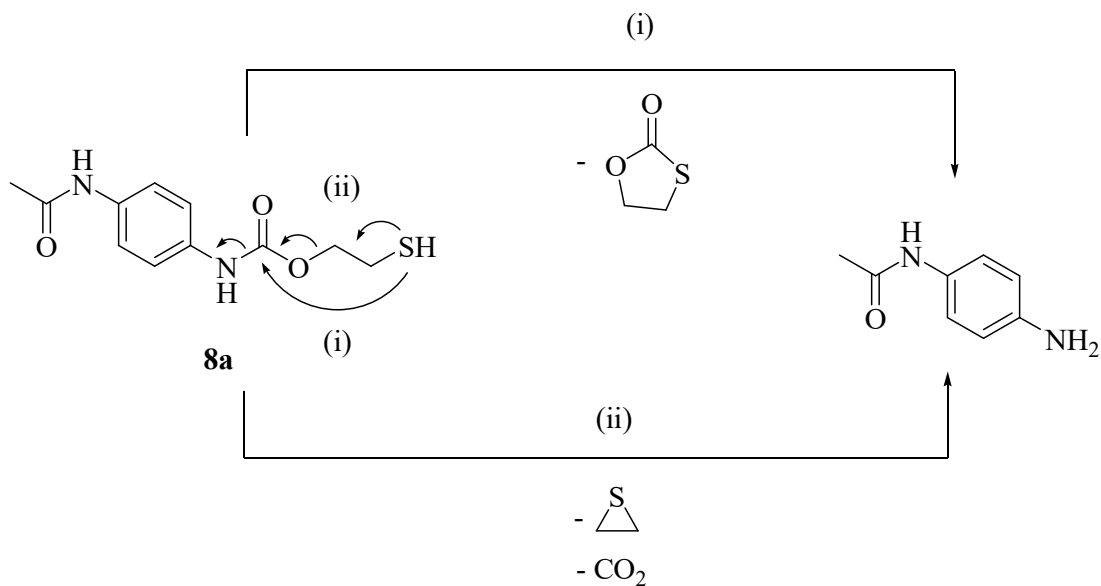


**Figure 10.** Cargo-containing product distribution as function of time for the reaction of **6a**

In the context of this study, these possible degradation pathways for semi-conjugate **8a** are illustrated in Scheme 11.

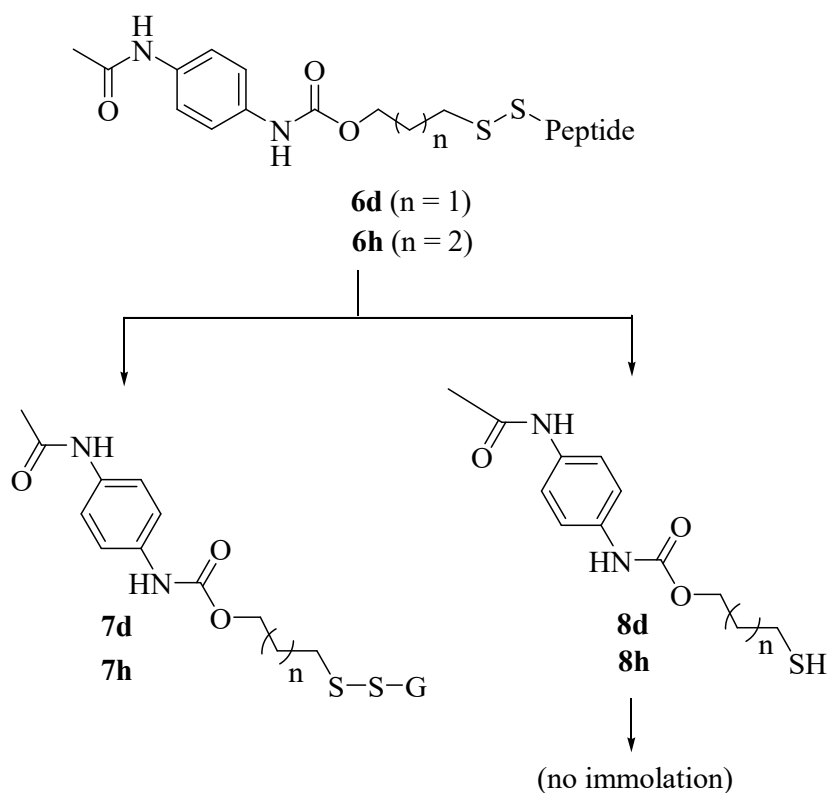


**Scheme 11.** Possible mechanisms for cargo release from **8a**



Based on these mechanisms, the thiol group can attack either the carbamate group directly, yielding cyclic thiocarbonate<sup>22,23</sup> (pathway i), or the neighboring carbon atom, giving thiirane and carbon dioxide,<sup>28,39</sup> (pathway ii).

In order to determine the pathway responsible for the cargo release observed in this study, degradation of other conjugates was studied. When **6h** was reacted with GSH as described for **6a**, no 4-acetamidoaniline was released, only **7h** and **8h**, analogous to **7a** and **8a** from **6a**. These two products were present for a long period of time without any trace of released 4-acetamidoaniline. As time passes, oxidation of **8h** appeared to start and lead to dimeric disulfide. This indicates that **8h** does not undergo self-elimination reaction in a same way as **8a**.



**Scheme 12.** Degradation of **6d** and **6h**

The only possible mechanism of cargo release from **8h** is pathway i as depicted in Scheme 11. However, the fact that the cargo was released from **8a** and not from **8h** strongly indicates that the thiirane pathway is the actual mechanism of the release. Aliphatic thiols have pKa value<sup>51</sup> higher than physiological pH of 7.4 therefore under physiological pH it exists more

likely in thiol form, which is less nucleophilic than its conjugate base thiolate. On the other hand, the carbonyl group of the carbamate is less electrophilic than carbonate. The intramolecular cyclization forming a seven-membered ring is expected to be slower than five-membered ring formation, and this makes the cargo release from **8h** unfavorable. In order to substantiate this hypothesis, the study for degradation was extended to other conjugates **6**. Like in the case of **6h**, no released cargo was observed when **6d** was reacted with GSH (Scheme 12).

Since no self-immolation took place for the conjugates that have longer-than-two-carbon-atom chains between oxygen and sulfur atoms ( $n \geq 1$ ), cargo release was only envisaged to occur for conjugates derived from the linker (**2a-2c**). As the degradation study of **6a** suggested, the concentration of reduced GSH was an important factor on the rate of the cargo release and the intramolecular reaction of **8** to release the free cargo was the rate-determining step.

Next, the effect of variation of substituents ( $R^1$ ,  $R^2$  and  $R^3$ ) of the linker chain on the cargo release rate was investigated by using conjugates **6a**, **6b** and **6c**. (Figure 11)

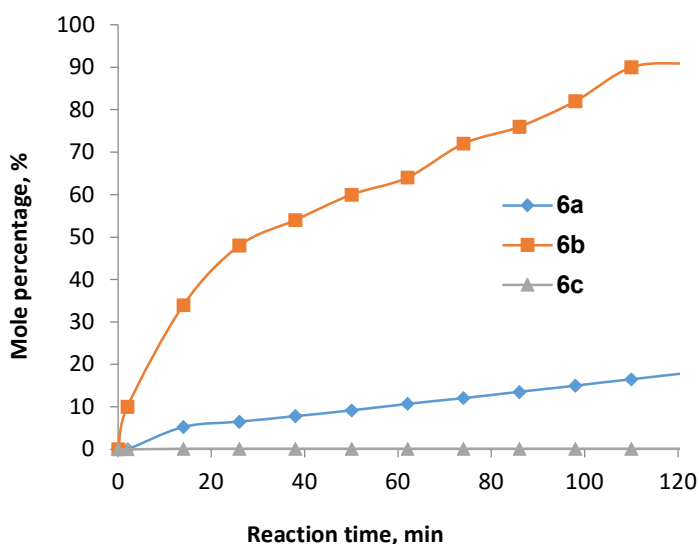


**Figure 11.** Release of the 4-acetamidoaniline from **6a** and **6b**

As previously discussed, conjugate **6a** released 4-acetamidoaniline in a linear fashion until it reaches equilibrium after ca 5 hours in which 51% of the cargo is released whereas 49% of the cargo is remained in the form of C-L-glutathione (**7a**). Analysis after 9 hours showed more or less the same composition as after 5 hours. However, when **6b** was treated with GSH under the

same conditions, a much faster process took place and 90% of the cargo was released within 110 minutes via C-L-glutathione (**7b**) and C-L-SH fragment (**8b**), after which 10% of the cargo remained unchanged in the form of **7b**. Methyl substituent on the sulfur-bearing carbon atom appeared to play an important role to facilitate formation of expected three-membered ring. Surprisingly, when **6c** was studied, cargo release was extremely slow and only a trace amount (below the limit of quantification) of the free cargo was detected. The peptide component was replaced by GSH instantly and the resulting C-L-glutathione adduct (**7c**) and C-L fragment (**8c**) did not yield the released drug. Over time **8c** became oxidized giving rise to a dimer (C-L-L-C). Substitution at oxygen-bearing carbon atom appeared to have hindering effect, which further supports the thiirane-elimination theory (pathway ii).

## 6. Conclusion

Numerous examples of self-immolative disulfide linkers have been prepared based on mercaptoalcohol. When they are used to prepare bioconjugates with amine-containing cargo they yield carbamate linkage that is sufficiently stable for therapeutic applications. In this study it was shown that mercaptoalcohol linkers can be prepared as heterobifunctional reagents that are stable upon storage.

Mercaptoalkanol-derived linkers are easy to synthesize and are amenable to long term storage. The release rate of free cargo from conjugates is reasonable. The cargo release from **6a** was 17%. It should be noted that higher percentages of cargo release can be expected *in vivo* because *in vitro* GSH is depleted by oxidation to form GSSG. In **6b**, the presence of a methyl substituent on the sulfur-bearing carbon atom increased the release rate 5 times than that of **6a**. Thus, a slight difference in the substituent pattern and therefore structure influences cargo release rate significantly.

The carbonate linkage formed between a hydroxyl-containing cargo and linker is prone to general hydrolysis as well as being susceptible to unwanted reactions with amine groups present in the delivery vector. These linkers might, therefore, not be suitable for hydroxyl-containing cargo in many cases. Since carbamate linkage turned out to be stable, future plan should focus on the development of linkers that form carbamate linkage with hydroxyl-containing cargoes.

A GSH-triggered degradation study of the conjugates further revealed that self-immolation of the linker is effective when sulfur and oxygen/nitrogen atoms are only on neighboring carbon atoms. The substitution pattern on these two carbon atoms turned out to be essential factor in the cargo release kinetics.

## REFERENCES

1. "Defining Cancer". National Cancer Institute. Retrieved 19 November 2020. <https://www.cancer.gov/about-cancer/understanding/what-is-cancer>
2. "Definition of metastasis" NCI Dictionary of Cancer Terms, National Cancer Institute Retrieved 19 November 2020, <https://www.cancer.gov/publications/dictionaries/cancer-terms/def/metastasis>
3. "Cancer". World Health Organization. 12 September 2018. Retrieved 19 November 2020. <https://www.who.int/en/news-room/fact-sheets/detail/cancer>
4. Fisher, B.; Wolmark, N. The current status of systemic adjuvant therapy in the management of primary breast cancer. *Surg. Clin. North. Am.* **1981**, *61*, 1347–1360
5. Schirmmacher, V. From chemotherapy to biological therapy: A review of novel concepts to reduce the side effects of systemic cancer treatment. *Int. J. Oncol.* **2019**, *54*, 407-419
6. Mukherjee S. *The Emperor of All Maladies: A Biography of Cancer*. Scribner, a Division of Simon and Schuster Inc.; New York: **2011**
7. Schirmmacher V. Quo Vadis Cancer Therapy? Fascinating discoveries of the last 60 years. Lambert Academic Publishing; **2017**. pp. 1–353
8. Zhang, W.; Song, J.; Zhang, B.; Liu, L.; Wang, K.; Wang, R. Design of Acid-Activated Cell Penetrating Peptide for Delivery of Active Molecules into Cancer Cells. *Bioconjugate Chem.* **2011**, *22*, 1410-1415
9. Engel, J.; Emons, G.; Pinski, J.; Schally, A. V. AEZS-108: a targeted cytotoxic analog of LHRH for the treatment of cancers positive for LHRH receptors *Expert Opin. Investig. Drugs* **2012**, *21*, 891-899
10. Ducry, L.; Stump, B. Antibody–drug conjugates: Linking cytotoxic payloads to monoclonal antibodies. *Bioconjugate Chem.* **2010**, *21*, 5-13
11. Gebleux, R.; Casi, G. Antibody-drug conjugates: Current status and future perspectives. *Pharmacol. Ther.* **2016**, *167*, 48-59
12. Ma, L.; Wang, C.; He, Z.; Cheng, B.; Zheng, L.; Huang, K. Peptide-drug conjugate: A novel drug design approach. *Curr. Med. Chem.* **2017**, *24*, 3373-3396

13. Wang, Y.; Cheetham, A. G.; Angacian, G.; Su, H.; Xie, L.; Cui, H. Peptide-drug conjugates as effective prodrug strategies for targeted delivery. *Adv. Drug Delivery Rev.* **2017**, *110-111*, 112-126
14. Casi, G.; Neri, D. Antibody-drug conjugates and small molecule-drug conjugates: Opportunities and challenges for the development of selective anticancer cytotoxic agents. *J. Med. Chem.* **2015**, *58*, 8751-8761
15. Srinivasarao, M.; Low, P. S. Ligand-targeted drug delivery. *Chem. Rev.* **2017**, *117*, 12133-12164
16. Vlahov, I. R.; Leamon, C. P. Engineering folate–drug conjugates to target cancer: From chemistry to clinic. *Bioconjugate Chem.* **2012**, *23*, 1357-1369
17. Jackson, D.; Stover, D. Using the lessons learned from the clinic to improve the preclinical development of antibody drug conjugates. *Pharm. Res.* **2015**, *32*, 3458-3469
18. Drake, P. M.; Rabuka, D. Recent developments in adc technology: Preclinical studies signal future clinical trends. *BioDrugs* **2017**, *31*, 521-531
19. "Antibody drug conjugate", Wikipedia Foundation, Retrieved on 20 November 2020. [https://en.wikipedia.org/wiki/Antibody-drug\\_conjugate](https://en.wikipedia.org/wiki/Antibody-drug_conjugate)
20. Gilad, Y.; Firer, M.; Gellerman, G. Recent innovations in peptide based targeted drug delivery to cancer cells. *Biomedicines* **2016**, *4*, 11
21. Jones, L. R.; Goun, E. A.; Shinde, R.; Rothbard, J. B.; Contag, C. H.; Wender, P. A. Releasable luciferin-transporter conjugates: Tools for the real-time analysis of cellular uptake and release. *J. Am. Chem. Soc.* **2006**, *128*, 6526-6527
22. Wender, P. A.; Goun, E. A.; Jones, L. R.; Pillow, T. H.; Rothbard, J. B.; Shinde, R.; Contag, C. H. Real-time analysis of uptake and bioactivatable cleavage of luciferin-transporter conjugates in transgenic reporter mice. *Proc. Natl. Acad. Sci. U. S. A.* **2007**, *104*, 10340-10345
23. Zhang, W., Song, J., Zhang, B., Liu, L., Wang, K., and Wang, R. (2011) Design of acid-activated cell penetrating peptide for delivery of active molecules into cancer cells. *Bioconjugate Chem.* *22*, 1410-1415
24. Lei, E. K.; Kelley, S. O. Delivery and release of small-molecule probes in mitochondria using traceless linkers. *J. Am. Chem. Soc.* **2017**, *139*, 9455-9458

25. Satyam, A. Design and synthesis of releasable folate-drug conjugates using a novel heterobifunctional disulfide-containing linker. *Bioorg. Med. Chem. Lett.* **2008**, *18*, 3196-3199.
26. Vlahov, I. R.; Santhapuram, H. K.; Kleindl, P. J.; Howard, S. J.; Stanford, K. M.; Leamon, C. P. Design and regioselective synthesis of a new generation of targeted chemotherapeutics. Part 1: Ec145, a folic acid conjugate of desacetylvinblastine monohydrazide. *Bioorg. Med. Chem. Lett.* **2006**, *16*, 5093-5096
27. Vlahov, I. R.; Wang, Y.; Kleindl, P. J.; Leamon, C. P. Design and regioselective synthesis of a new generation of targeted chemotherapeutics. Part ii: Folic acid conjugates of tubulysins and their hydrazides. *Bioorg. Med. Chem. Lett.* **2008**, *18*, 4558-4561
28. Vlahov, I. R.; You, F.; Santhapuram, H. K.; Wang, Y.; Vaughn, J. F.; Hahn, S. J.; Kleindl, P. J.; Fan, M.; Leamon, C. P. Design and regioselective synthesis of a new generation of targeted therapeutics. Part 3: Folate conjugates of aminopterin hydrazide for the treatment of inflammation. *Bioorg. Med. Chem. Lett.* **2011**, *21*, 1202-1205
29. Lee, M. H.; Sessler, J. L.; Kim, J. S. Disulfide-based multifunctional conjugates for targeted theranostic drug delivery. *Acc. Chem. Res.* **2015**, *48*, 2935-2946
30. Weaver, M.; Laske, D. W. Transferrin receptor ligand-targeted toxin conjugate (Tf-CRM107) for therapy of malignant gliomas. *J. Neuro-oncol.* **2003**, *65*, 3-13
31. Chen, L.; Wright, L. R.; Chen, C. H.; Oliver, S. F.; Wender, P. A.; Mochly-Rosen, D. Molecular transporters for peptides: Delivery of a cardioprotective epsilonpkc agonist peptide into cells and intact ischemic heart using a transport system, r(7). *Chem. Biol.* **2001**, *8*, 1123-1129
32. Geng, Q.; Sun, X.; Gong, T.; Zhang, Z.-R. Peptide–drug conjugate linked via a disulfide bond for kidney targeted drug delivery. *Bioconjugate Chem.* **2012**, *23*, 1200-1210
33. Brezden, A.; Mohamed, M. F.; Nepal, M.; Harwood, J. S.; Kuriakose, J.; Seleem, M. N.; Chmielewski, J. Dual targeting of intracellular pathogenic bacteria with a cleavable conjugate of kanamycin and an antibacterial cell-penetrating peptide. *J. Am. Chem. Soc.* **2016**, *138*, 10945-10949
34. Meng, X.; Gao, M.; Deng, J.; Lu, D.; Fan, A.; Ding, D.; Kong, D.; Wang, Z.; Zhao, Y. Self-immolative micellar drug delivery: The linker matters. *Nano Res.* **2018**, *11*, 6177-6189
35. Walles, M.; Connor, A.; Hainzl, D. Adme and safety aspects of non-cleavable linkers in drug discovery and development. *Curr. Top. Med. Chem.* **2017**, *17*, 3463-3475

36. Leriche, G.; Chisholm, L.; Wagner, A. Cleavable linkers in chemical biology. *Bioorg. Med. Chem.* **2012**, *20*, 571-582
37. Burke, P. J.; Senter, P. D.; Meyer, D. W.; Miyamoto, J. B.; Anderson, M.; Toki, B. E.; Manikumar, G.; Wani, M. C.; Kroll, D. J.; Jeffrey, S. C. Design, synthesis, and biological evaluation of antibody-drug conjugates comprised of potent camptothecin analogues. *Bioconjugate Chem.* **2009**, *20*, 1242-1250
38. Walker, M. A.; Dubowchik, G. M.; Hofstead, S. J.; Trail, P. A.; Firestone, R. A. Synthesis of an immunoconjugate of camptothecin. *Bioorg. Med. Chem. Lett.* **2002**, *12*, 217-219
39. Zhang, D.; Pillow, T. H.; Ma, Y.; Cruz-Chuh, J. D.; Kozak, K. R.; Sadowsky, J. D.; Lewis Phillips, G. D.; Guo, J.; Darwish, M.; Fan, P. Linker immolation determines cell killing activity of disulfide-linked pyrrolbenzodiazepine antibody-drug conjugates. *ACS Med. Chem. Lett.* **2016**, *7*, 988-993
40. Jain, N.; Smith, S. W.; Ghone, S.; Tomczuk, B. Current adc linker chemistry. *Pharm. Res.* **2015**, *32*, 3526-3540
41. Riber, C. F.; Smith, A. A. A.; Zelikin, A. N. Self-immolative linkers literally bridge disulfide chemistry and the realm of thiol-free drugs. *Adv. Healthcare Mater.* **2015**, *4*, 1887-1890
42. Brulisauer, L.; Gauthier, M. A.; Leroux, J. C. Disulfide-containing parenteral delivery systems and their redox-biological fate. *J. Controlled Release* **2014**, *195*, 147-154
43. Saito, G.; Swanson, J. A.; Lee, K. D. Drug delivery strategy utilizing conjugation via reversible disulfide linkages: Role and site of cellular reducing activities. *Adv. Drug Delivery Rev.* **2003**, *55*, 199-215
44. Thorpe, P. E.; Wallace, P. M.; Knowles, P. P.; Relf, M. G.; Brown, A. N.; Watson, G. J.; Knyba, R. E.; Wawrzynczak, E. J.; Blakey, D. C. New coupling agents for the synthesis of immunotoxins containing a hindered disulfide bond with improved stability in vivo. *Cancer Res.* **1987**, *47*, 5924-5931
45. Greenfield, L., Bloch, W., and Moreland, M. Thiol-containing crosslinking agent with enhanced steric hindrance. *Bioconjugate Chem.* **1990**, *1*, 400-410
46. Arpicco, S.; Dosio, F.; Brusa, P.; Crosasso, P.; Cattel, L. New coupling reagents for the preparation of disulfide cross-linked conjugates with increased stability. *Bioconjugate Chem.* **1997**, *8*, 327-337



47. Pillow, T. H.; Sadowsky, J. D.; Zhang, D.; Yu, S. F.; Del Rosario, G.; Xu, K.; He, J.; Bhakta, S.; Ohri, R.; Kozak, K. R. Decoupling stability and release in disulfide bonds with antibody-small molecule conjugates. *Chem. Sci.* **2017**, *8*, 366-370
48. Dorywalska, M.; Strop, P.; Melton-Witt, J. A.; Hasa-Moreno, A.; Farias, S. E.; Galindo Casas, M.; Delaria, K.; Lui, V.; Poulsen, K.; Loo, C. Effect of attachment site on stability of cleavable antibody drug conjugates. *Bioconjugate Chem.* **2015**, *26*, 650-659
49. Torres, A. G.; Gait, M. J. Exploiting cell surface thiols to enhance cellular uptake. *Trends Biotechnol.* **2012**, *4*, 185-190
50. Eksteen, J. J.; Ausbacher, D.; Vasskog, T.; Rekdal, O.; Svendsen, J. S. Selective intracellular delivery of thiolated cargo to tumor and neovasculature cells using histidine-rich peptides as vectors. *ACS Omega* **2020**, *5*, 4937-4942
51. Tadj, S. G.; Tolbert, B. S.; Basavappa, R.; Miller, B. L. Direct determination of thiol pKa by isothermal titration microcalorimetry. *J. Am. Chem. Soc.* **2004**, *126*, 10508-10509

# **APPENDIX**

**APPENDIX I.** NMR spectra for characterized compounds

**APPENDIX II.** Data for degradation analysis

Appendix I.  
NMR spectra

9.34  
9.34  
9.33  
9.33

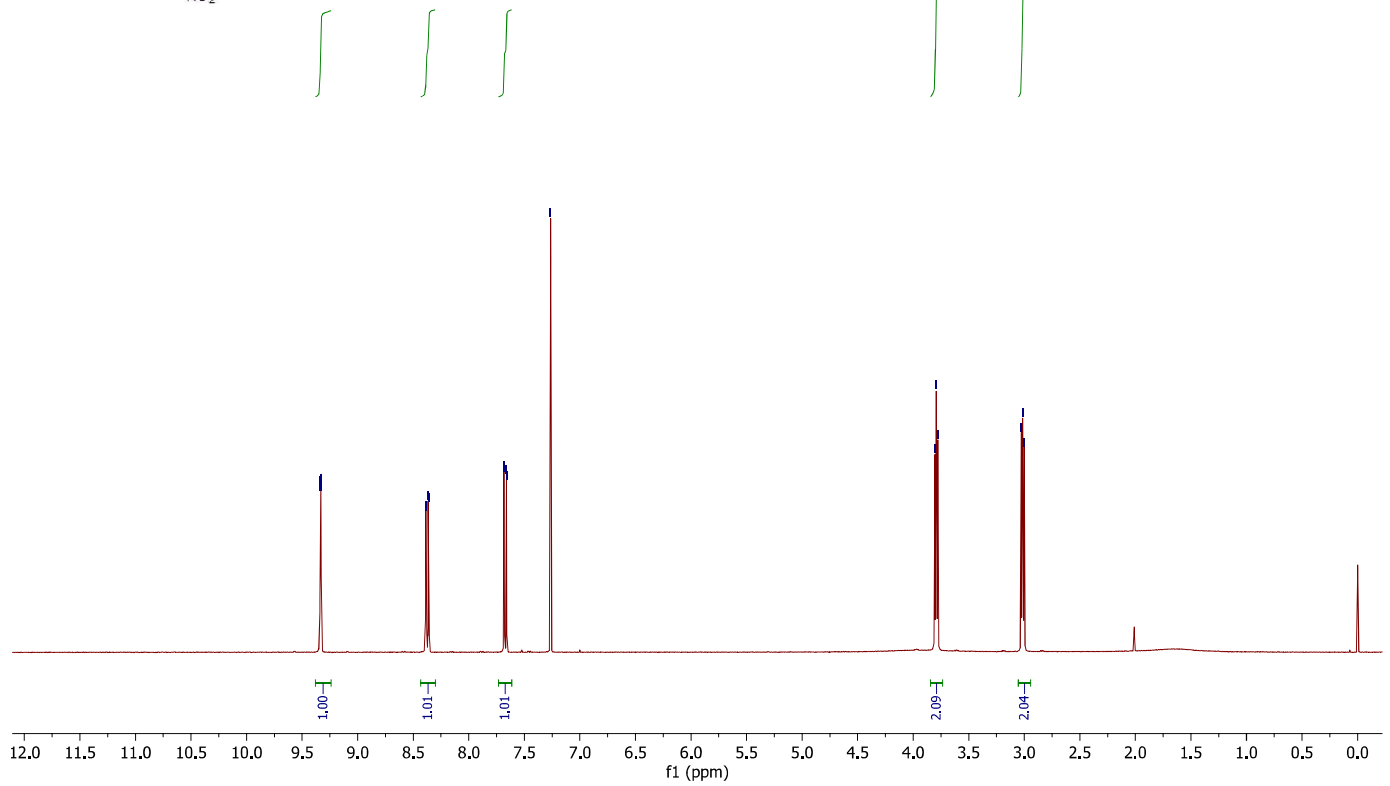
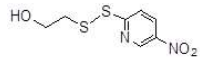
8.39  
8.38  
8.37  
8.36

7.68  
7.68  
7.66  
7.66  
7.26

3.81  
3.79  
3.78

3.03  
3.01  
3.00

2-(2-(5-Nitropyridin-2-yl)disulfanyl)ethanol (**1a**)



167.75

145.53  
142.73

131.59

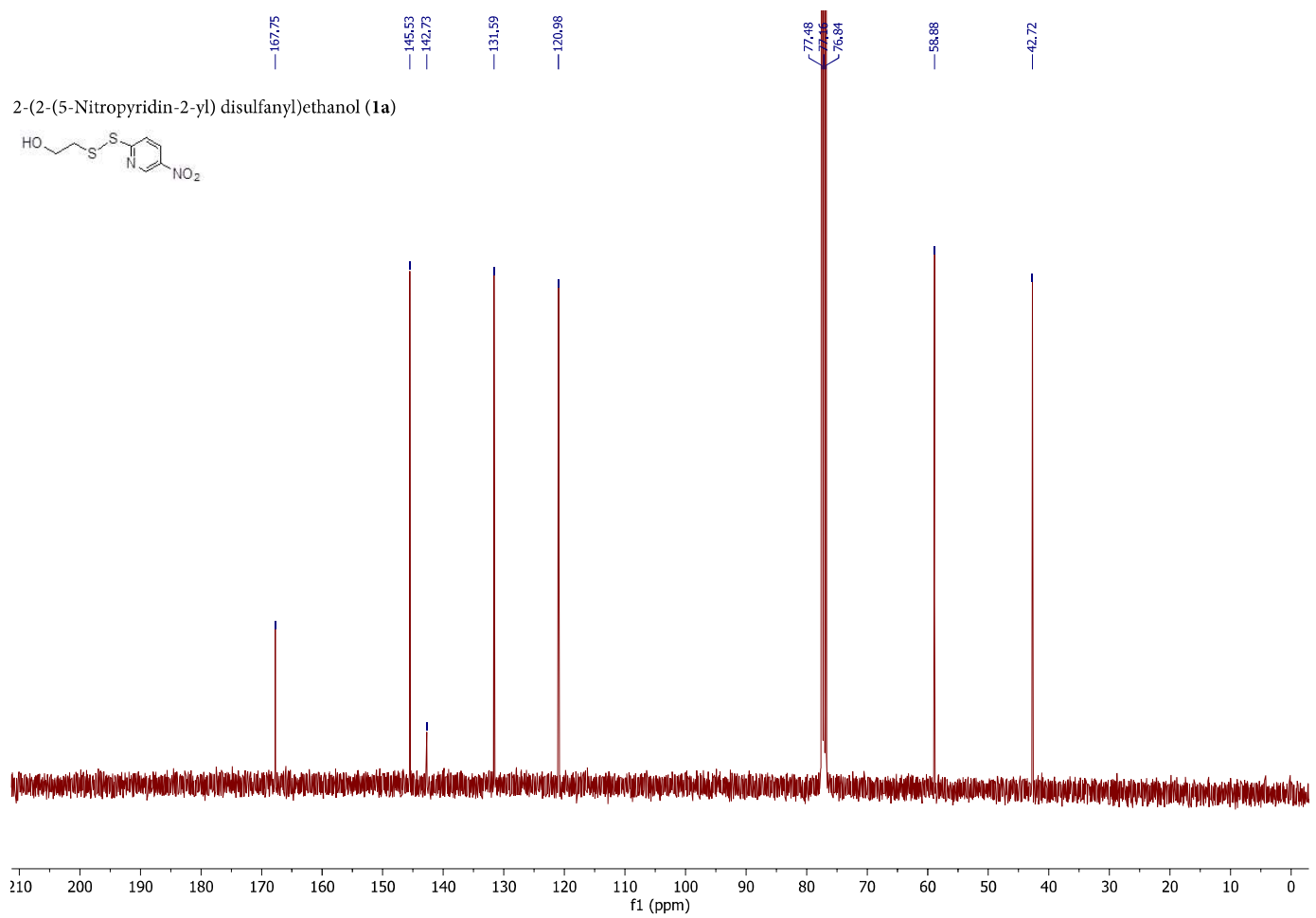
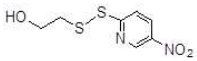
120.98

77.48  
77.46  
76.84

58.88

42.72

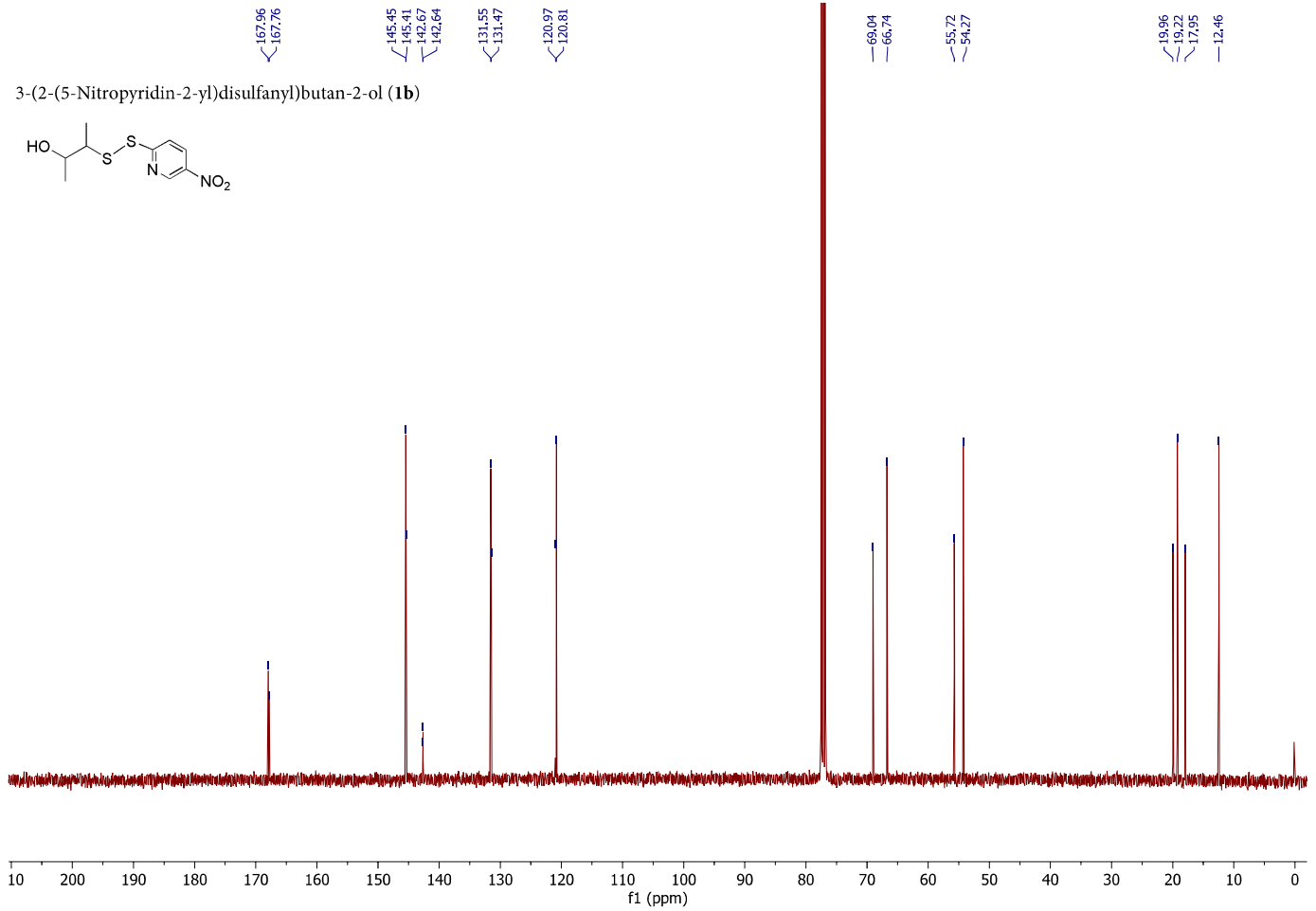
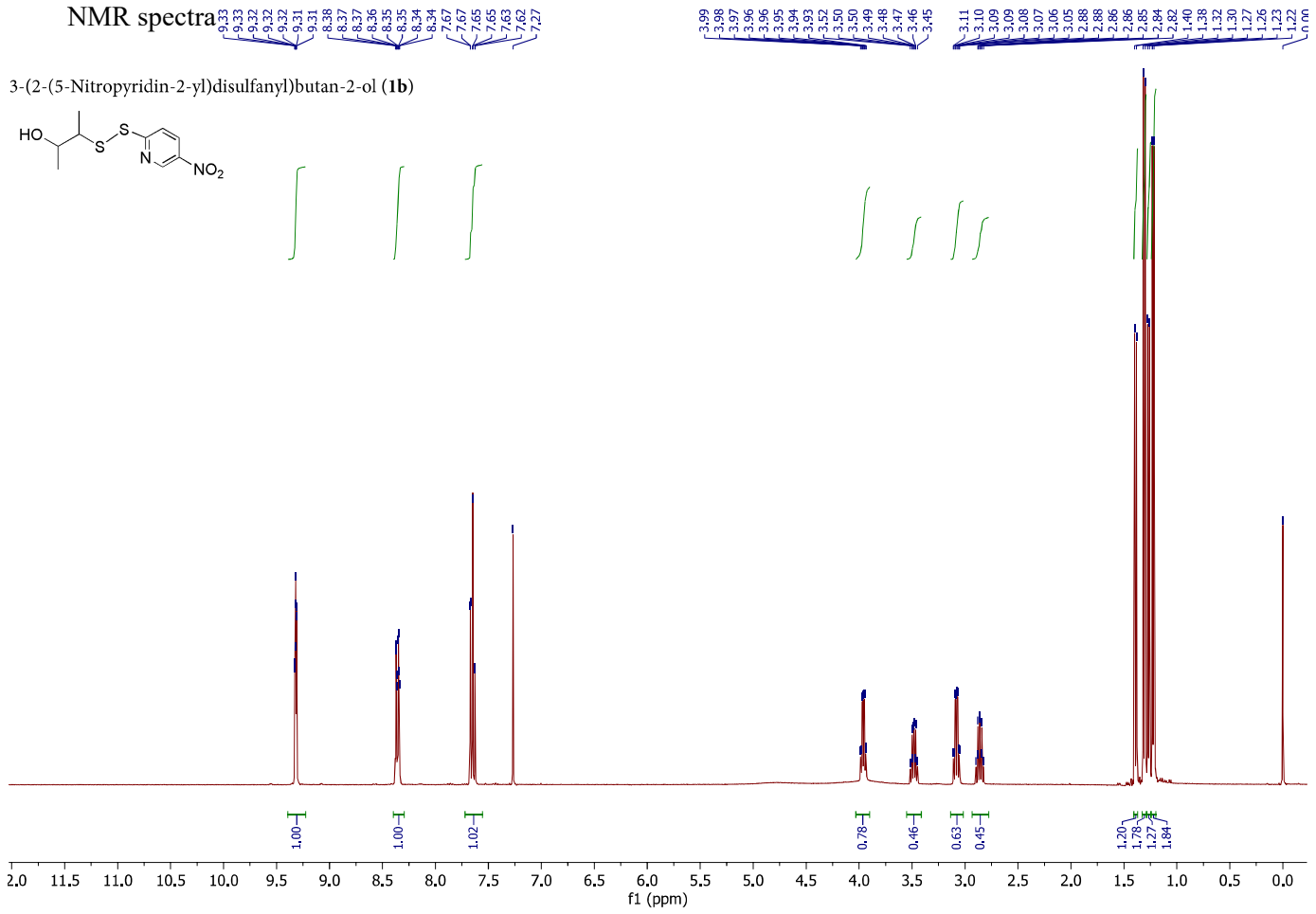
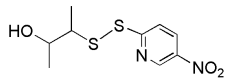
2-(2-(5-Nitropyridin-2-yl) disulfanyl)ethanol (**1a**)



Appendix I.

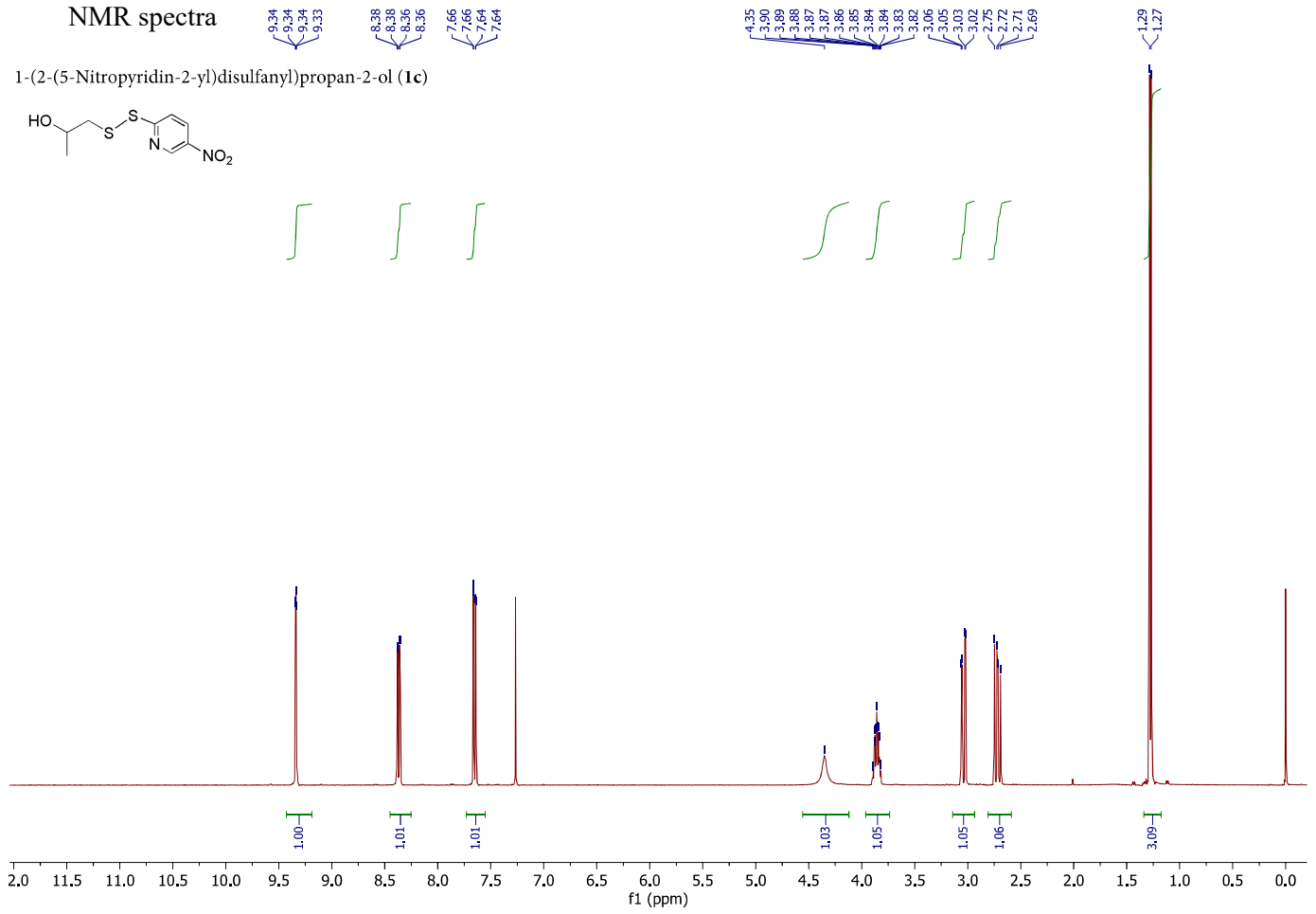
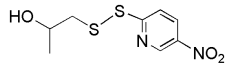
NMR spectra

3-(2-(5-Nitropyridin-2-yl)disulfanyl)butan-2-ol (**1b**)

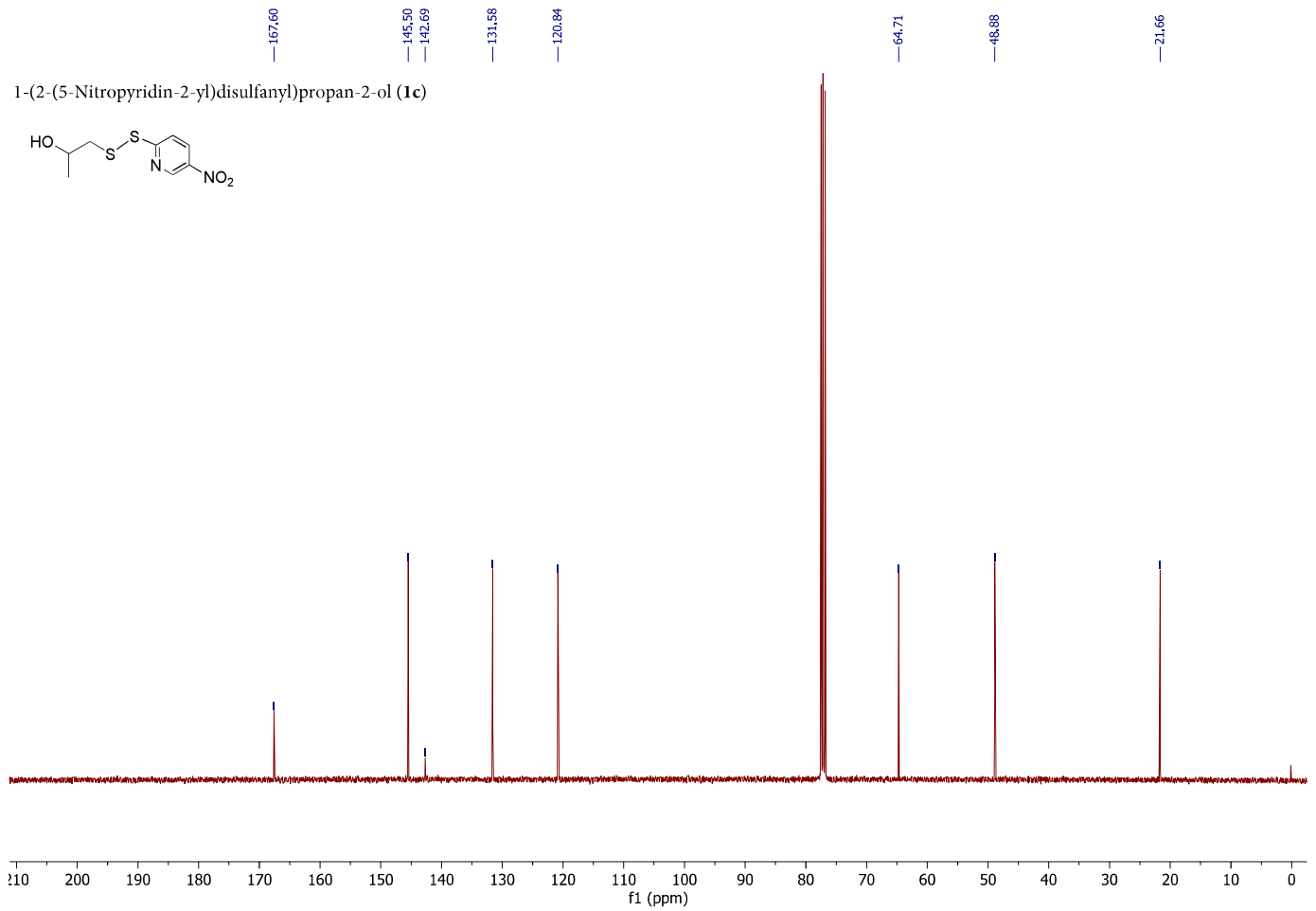
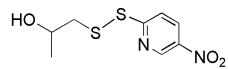


# Appendix I. NMR spectra

1-(2-(5-Nitropyridin-2-yl)disulfanyl)propan-2-ol (**1c**)



1-(2-(5-Nitropyridin-2-yl)disulfanyl)propan-2-ol (**1c**)



Appendix I.  
NMR spectra

9.22  
9.21

8.35  
8.33  
8.32

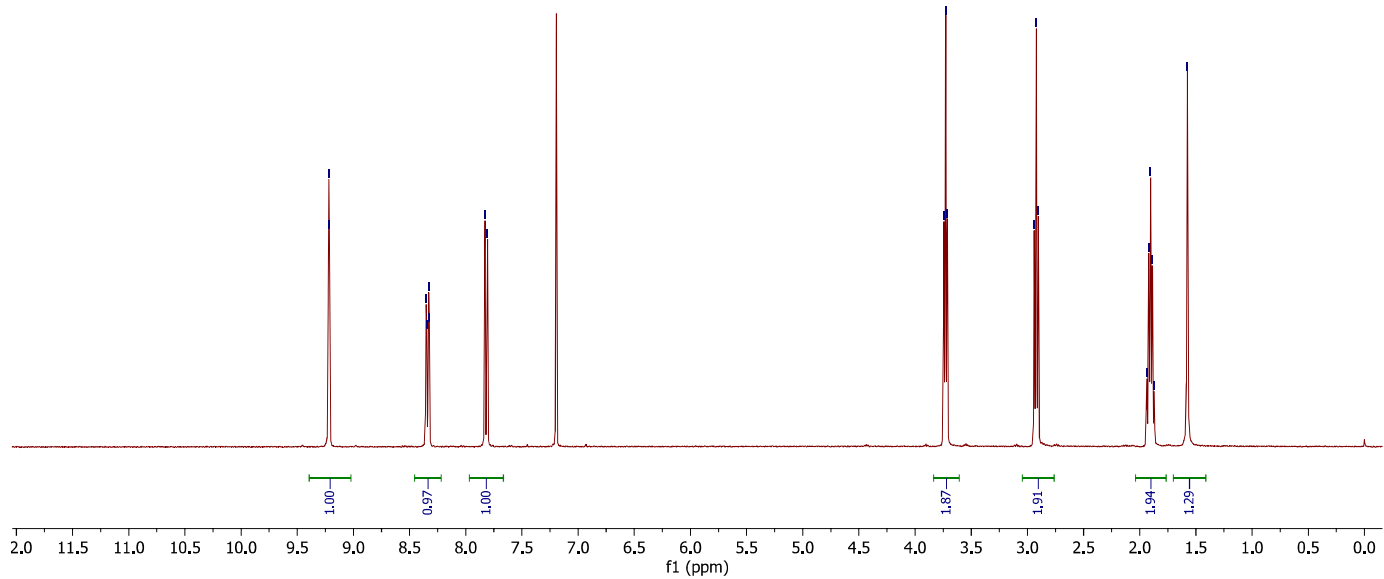
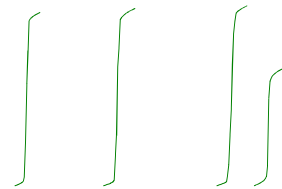
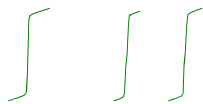
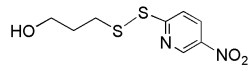
7.83  
7.81

3.74  
3.73  
3.71

2.94  
2.92  
2.90

1.94  
1.92  
1.90  
1.89  
1.87  
1.58

3-(2-(5-Nitropyridin-2-yl)disulfanyl)propan-1-ol (**1d**)



168.84

145.34  
142.21

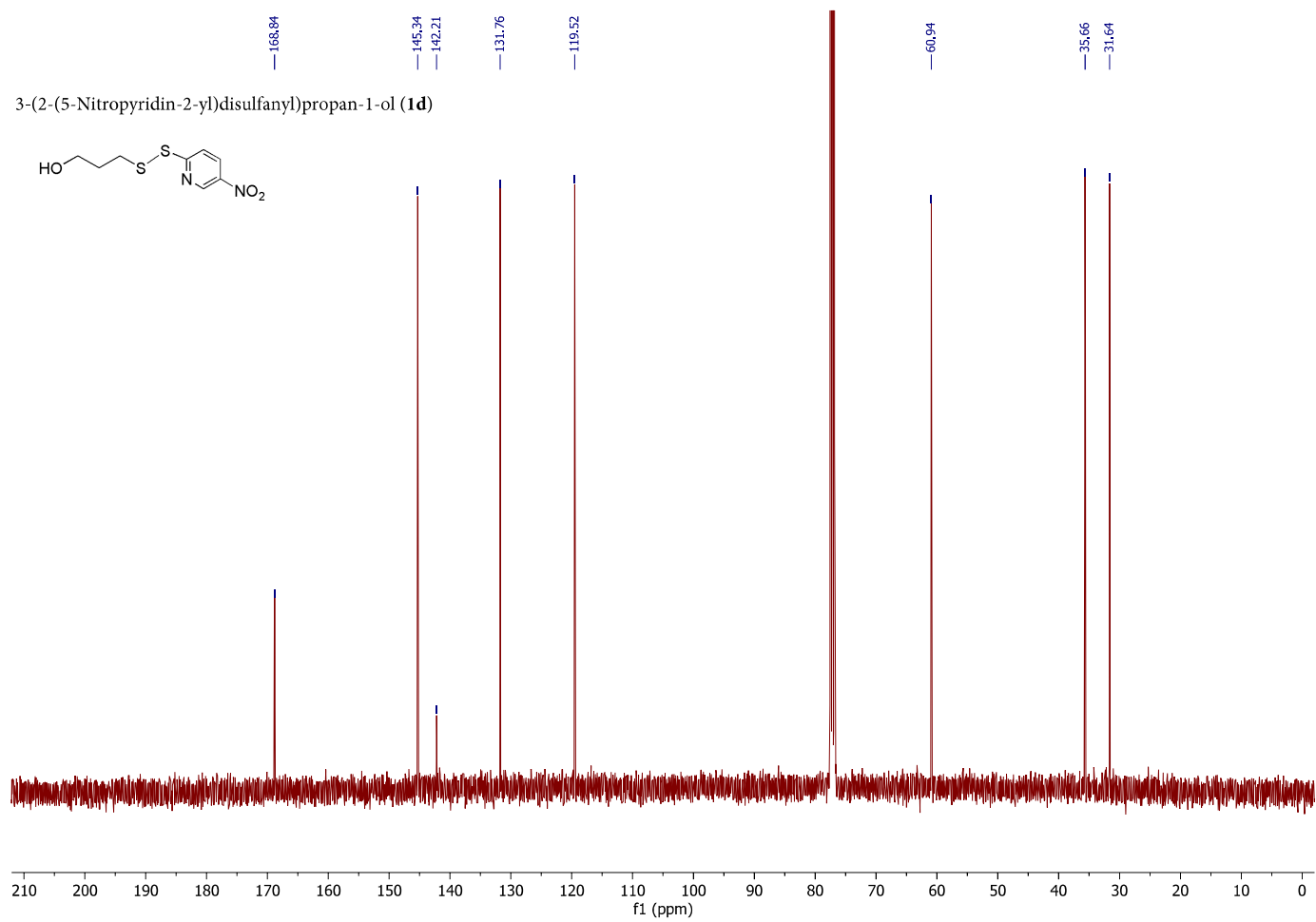
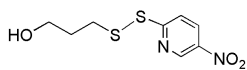
131.76

119.52

60.94

35.66  
31.64

3-(2-(5-Nitropyridin-2-yl)disulfanyl)propan-1-ol (**1d**)



Appendix I.  
NMR spectra

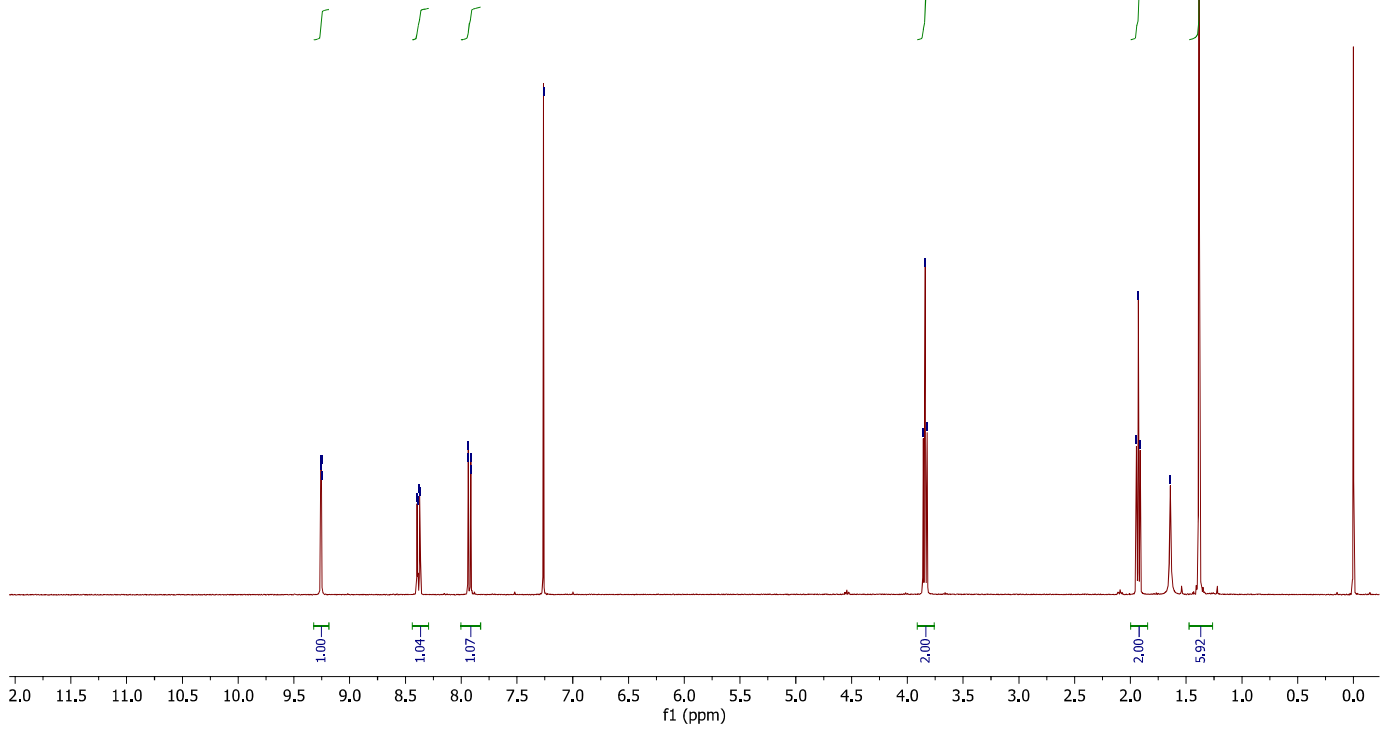
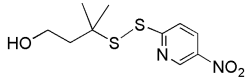
9.26  
9.26  
9.25  
9.25

8.40  
8.39  
8.37  
8.37

7.94  
7.94  
7.92  
7.91

— 7.26

3-Methyl-3-(2-(5-nitropyridin-2-yl)disulfanyl)butan-1-ol (**1e**)



— 169.72

— 145.03

— 142.18

— 131.57

— 119.72

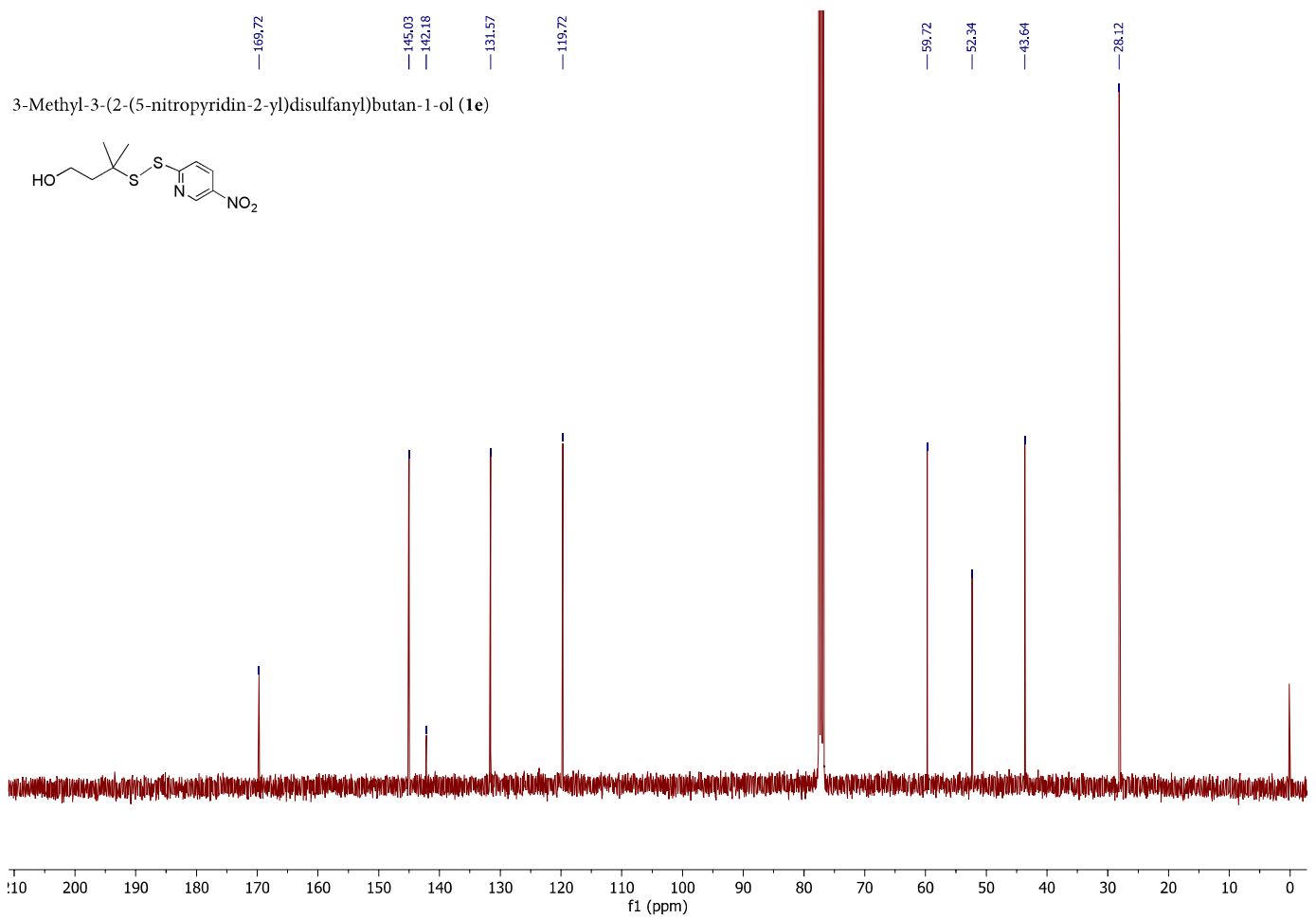
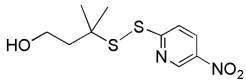
— 59.72

— 52.34

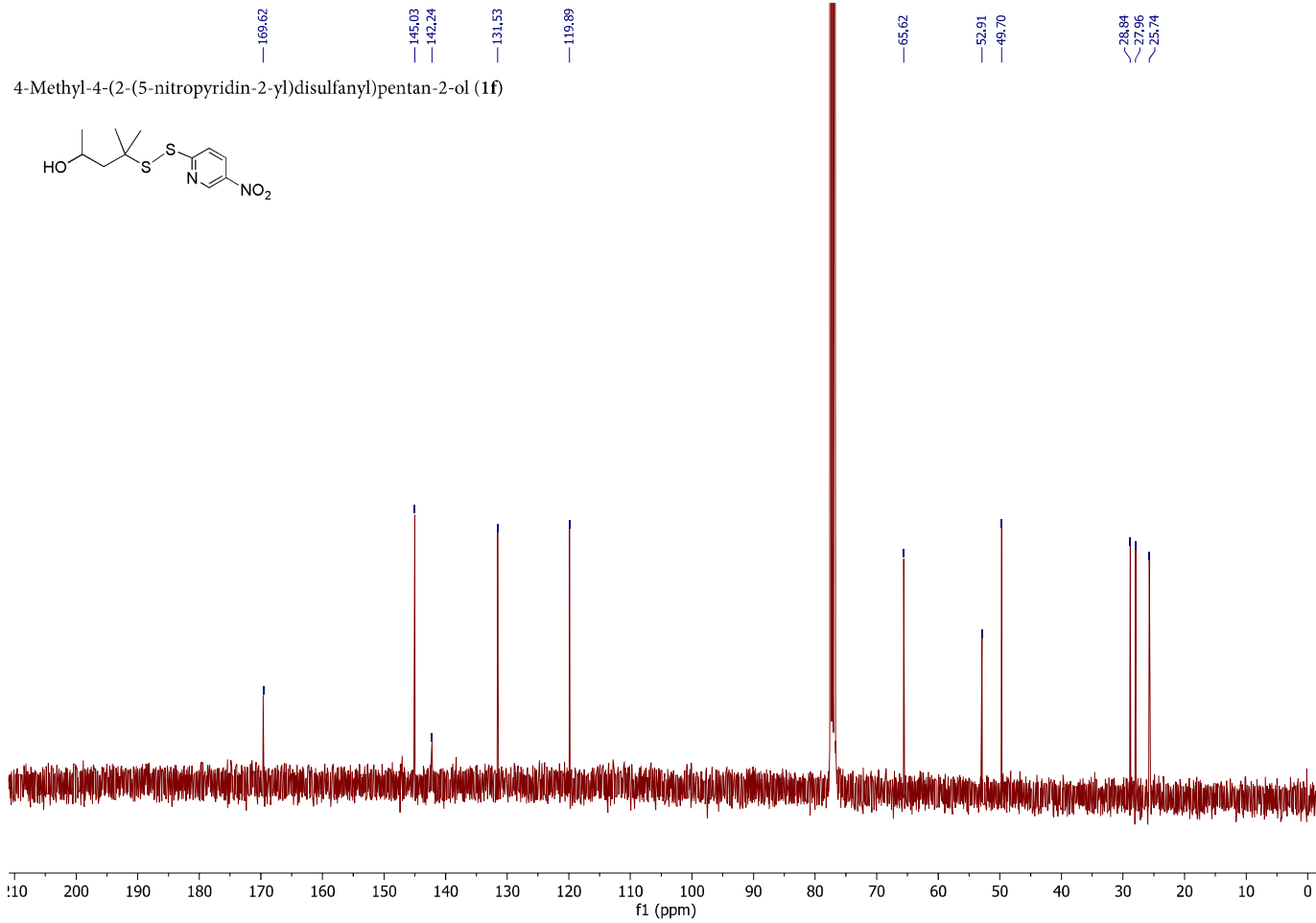
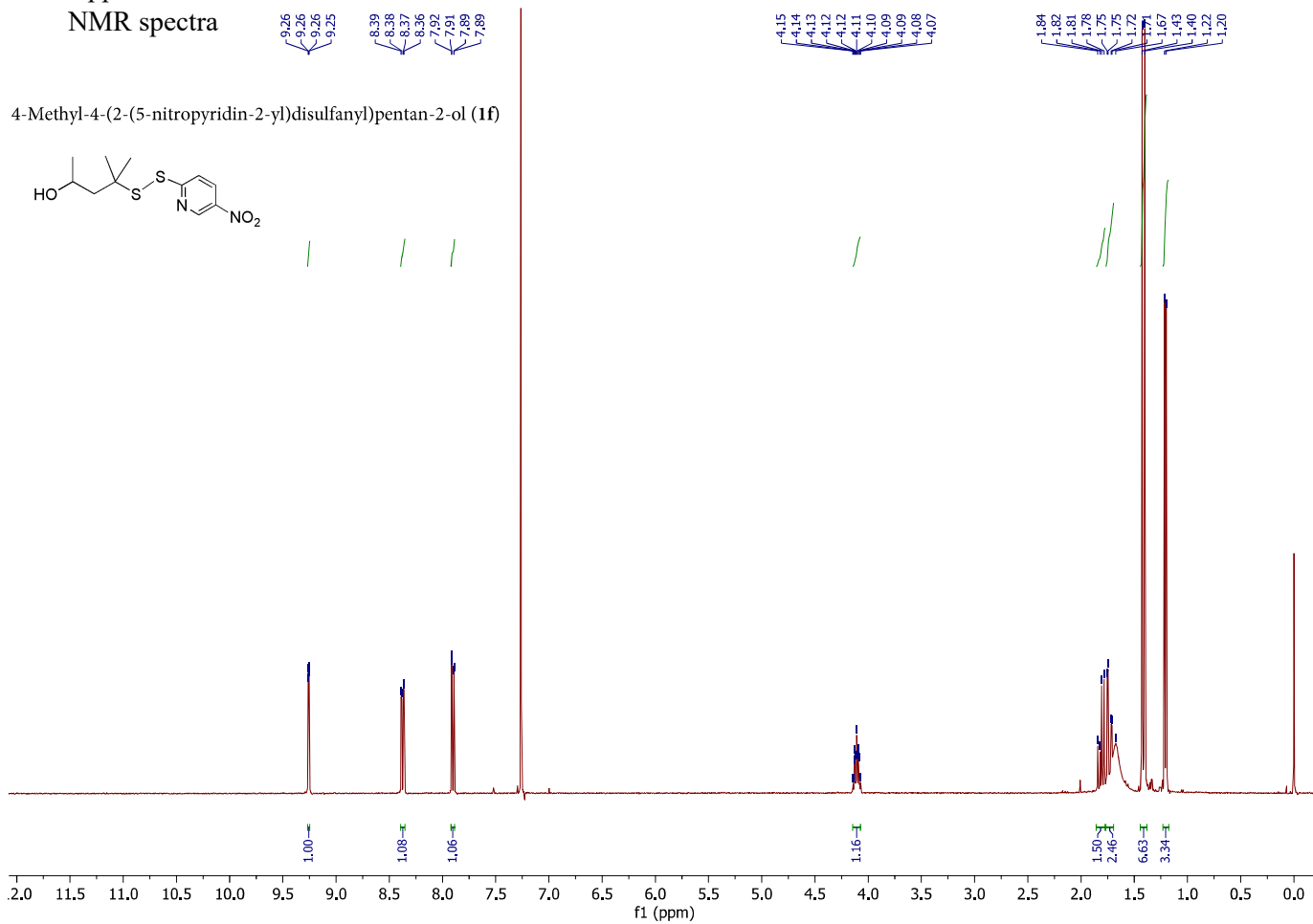
— 43.64

— 28.12

3-Methyl-3-(2-(5-nitropyridin-2-yl)disulfanyl)butan-1-ol (**1e**)



Appendix I.  
NMR spectra





Appendix I.  
NMR spectra

9.28  
9.28  
9.27  
9.27

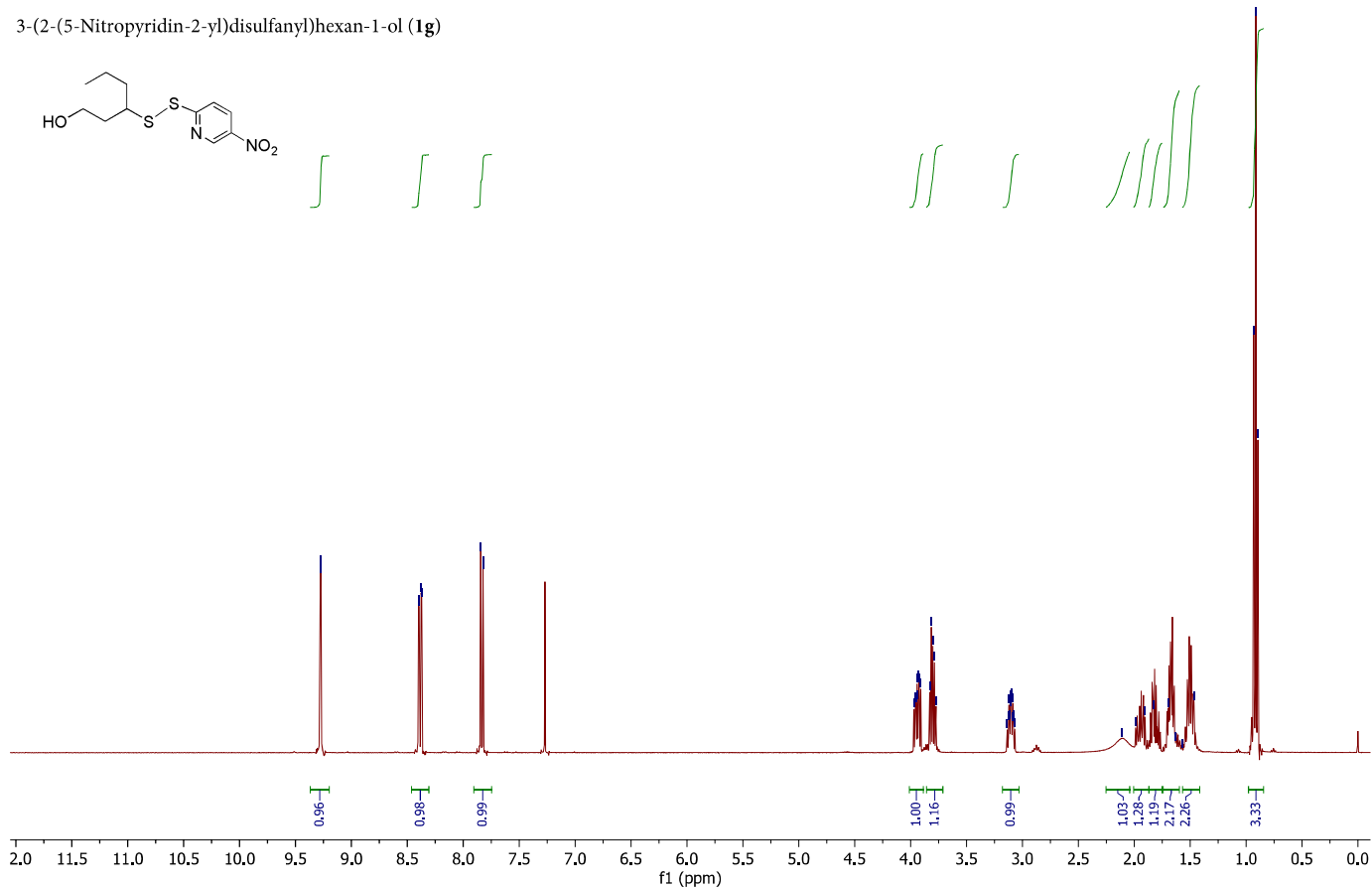
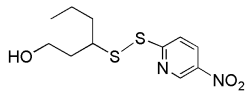
8.40  
8.39  
8.38  
8.37

7.84  
7.84  
7.82  
7.82

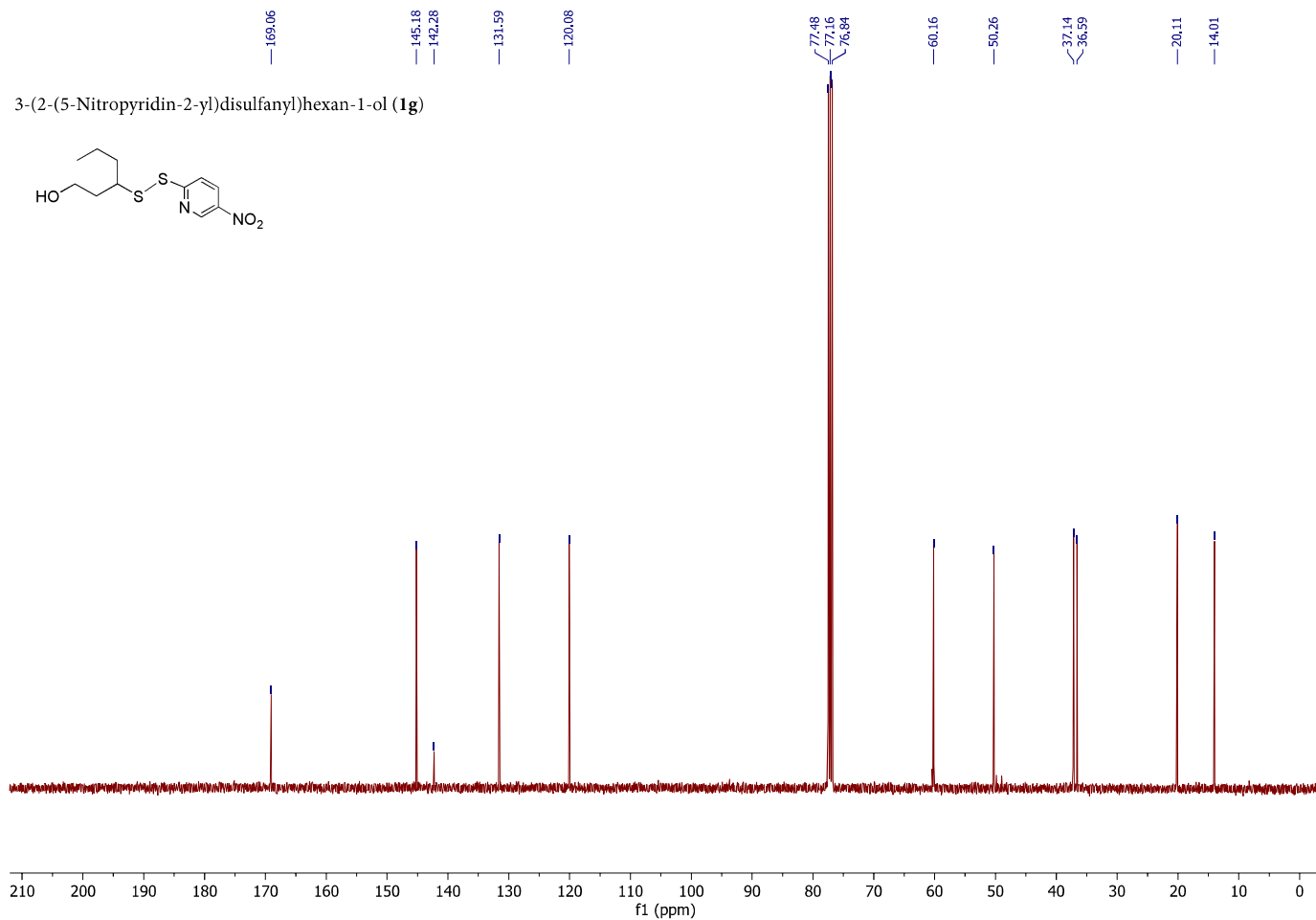
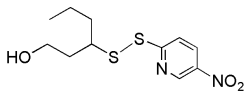
3.97  
3.96  
3.95  
3.94  
3.94  
3.93  
3.92  
3.91  
3.83  
3.81  
3.80  
3.79  
3.77  
3.14  
3.12  
3.11  
3.11  
3.10  
3.09  
3.08  
3.08  
3.07  
2.11  
1.99  
1.90  
1.83  
1.70  
1.63  
1.57  
1.47

0.93  
0.91  
0.89

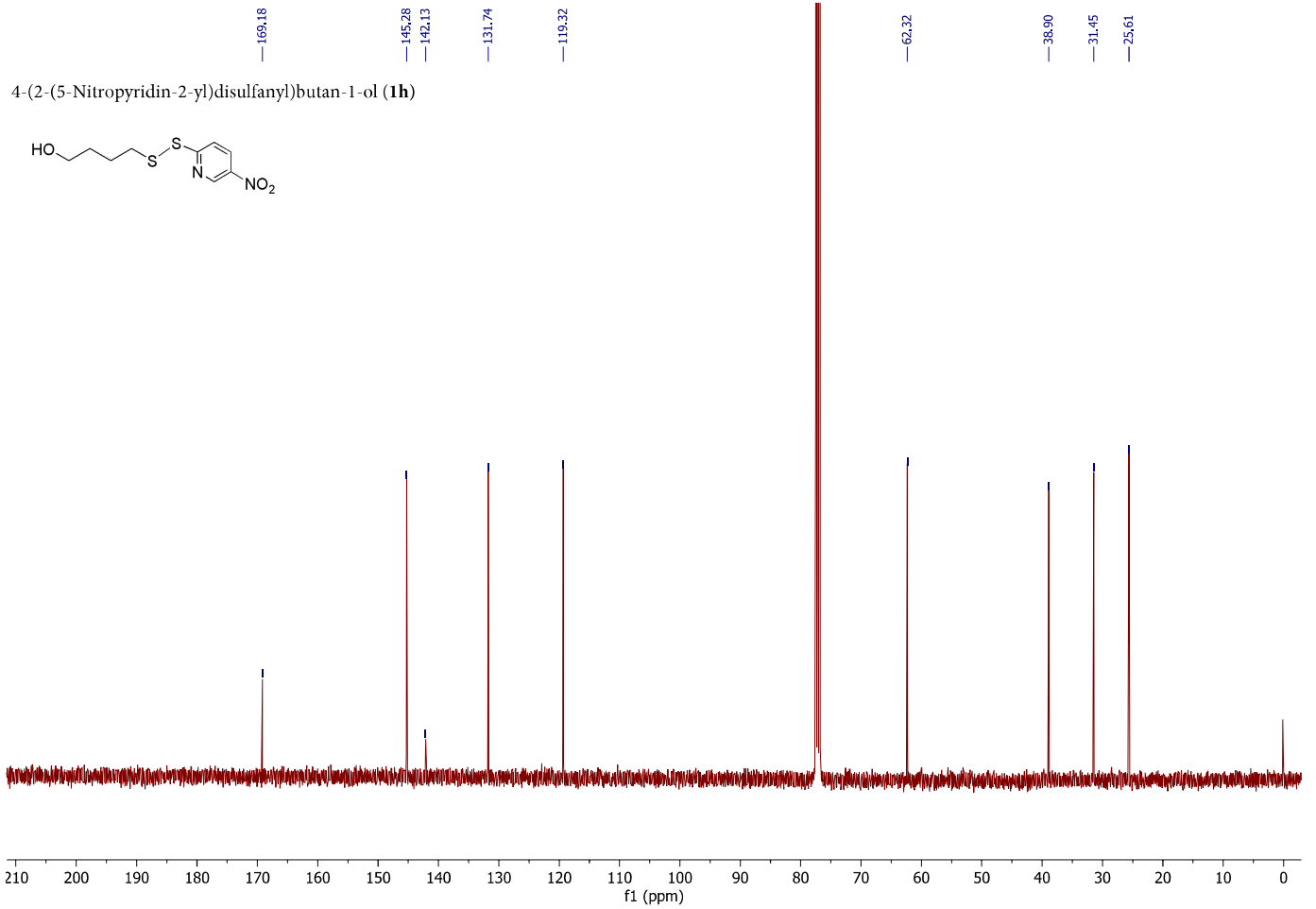
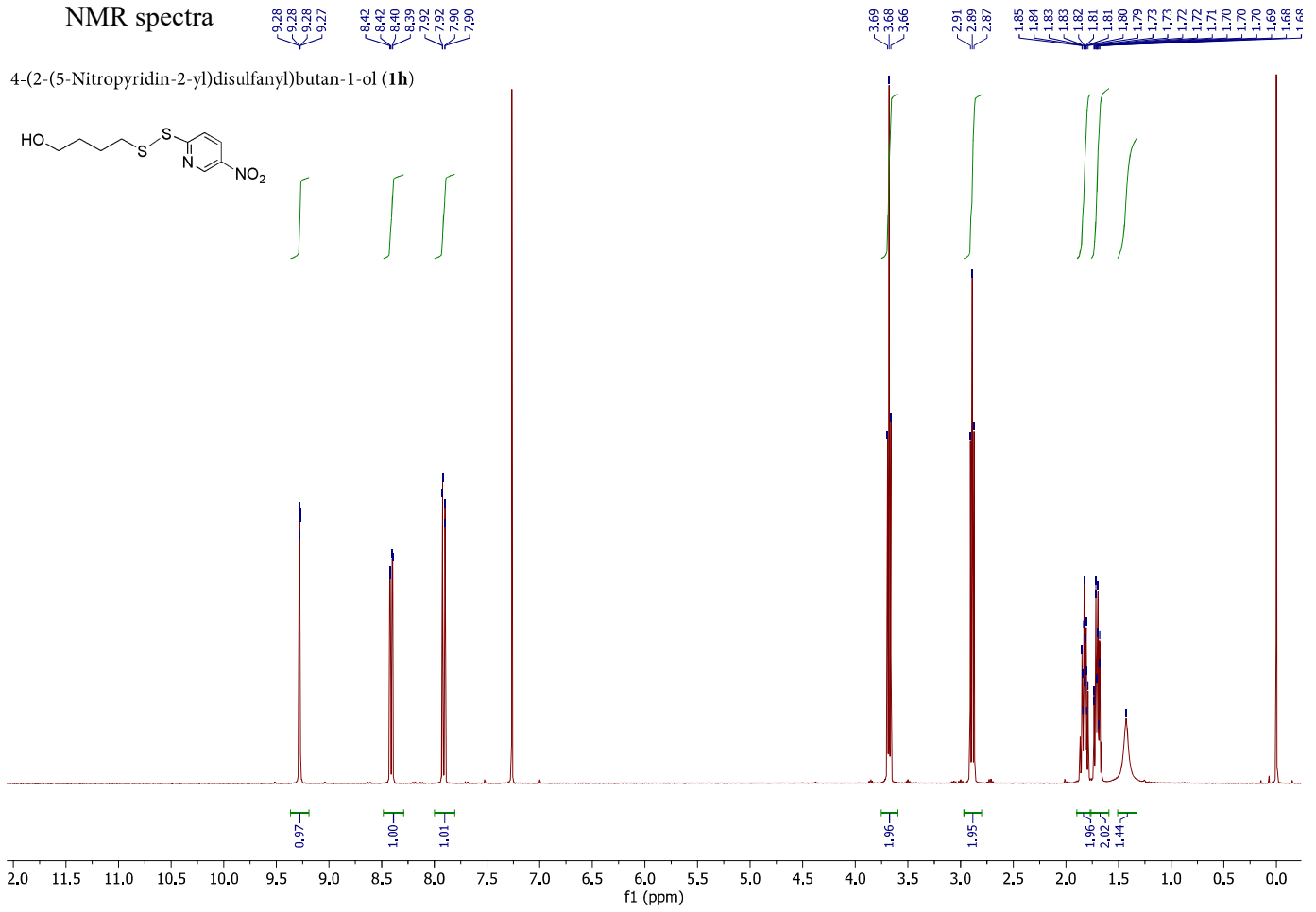
3-(2-(5-Nitropyridin-2-yl)disulfanyl)hexan-1-ol (**1g**)



3-(2-(5-Nitropyridin-2-yl)disulfanyl)hexan-1-ol (**1g**)

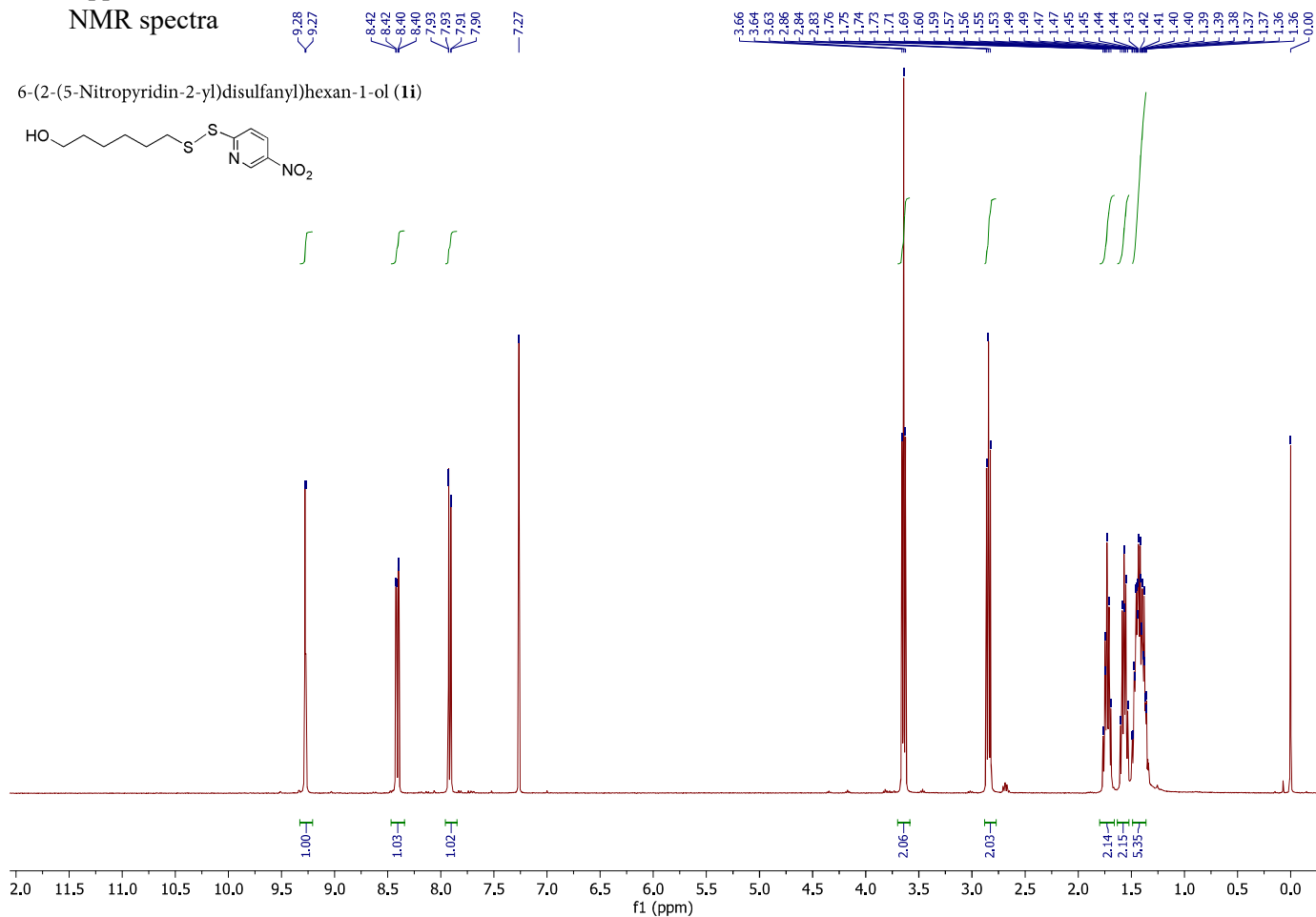
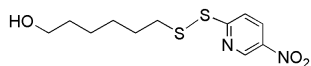


Appendix I.  
NMR spectra

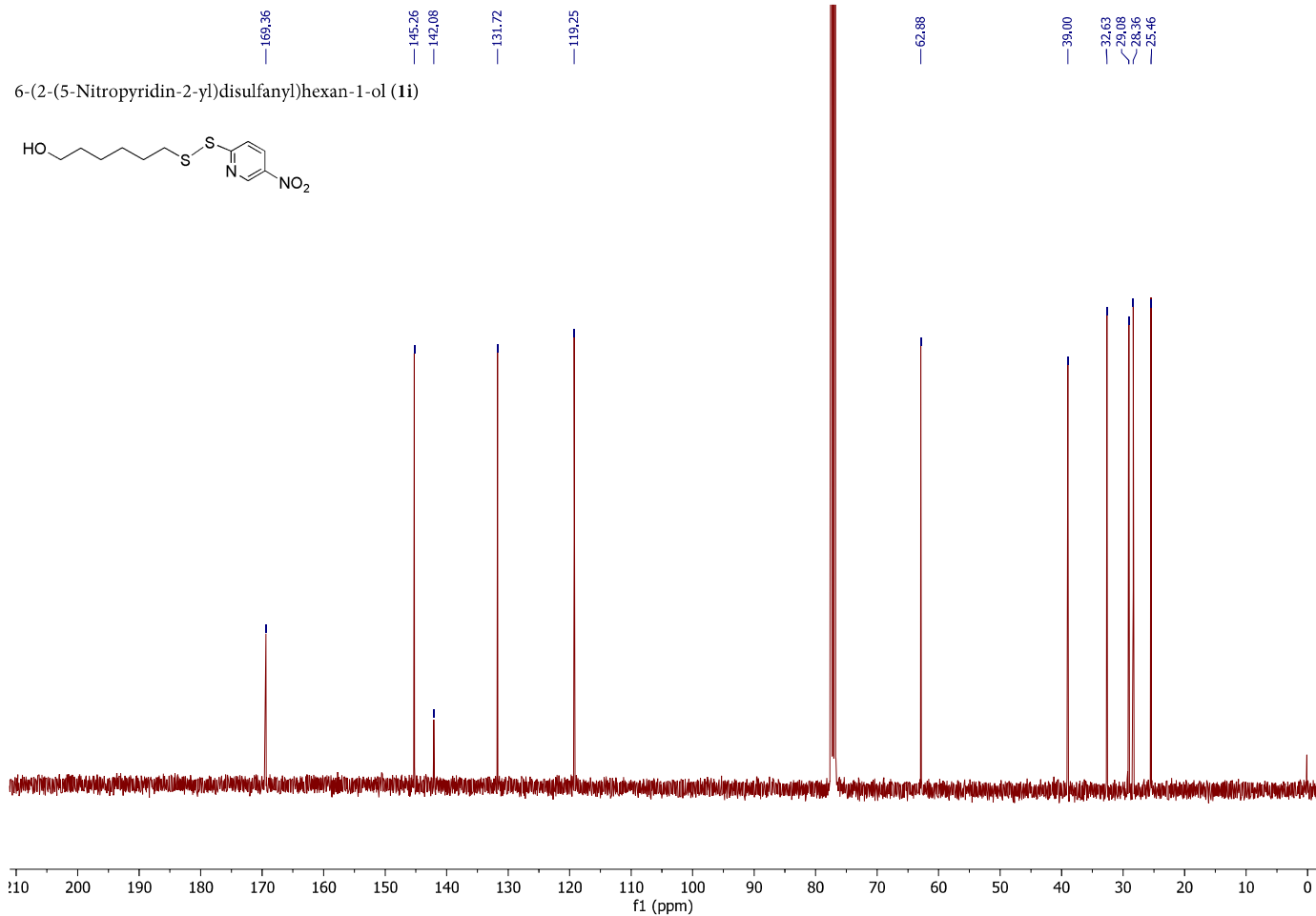
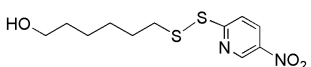


Appendix I.  
NMR spectra

6-(2-(5-Nitropyridin-2-yl)disulfanyl)hexan-1-ol (Ii)

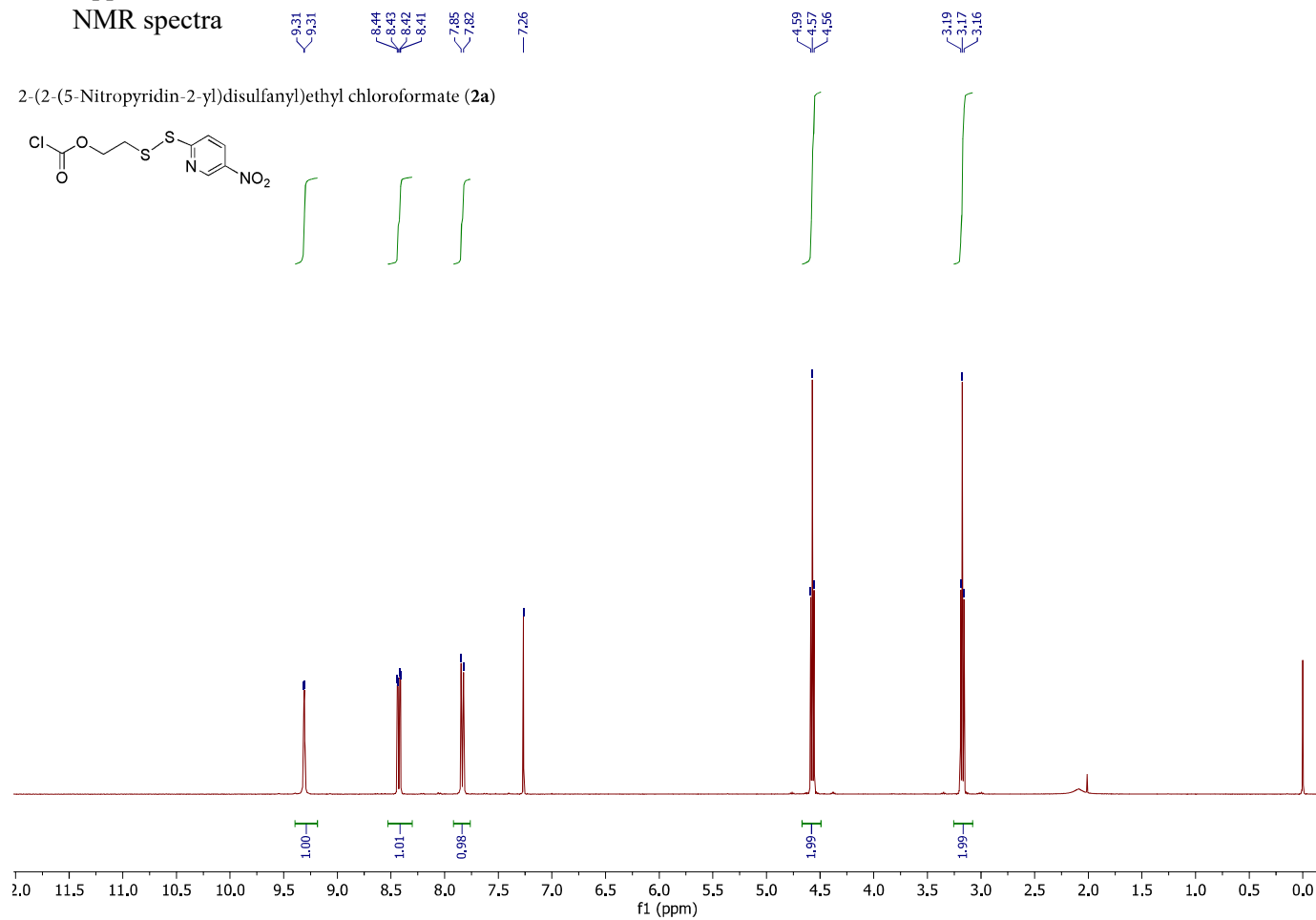
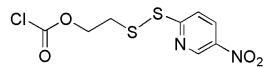


6-(2-(5-Nitropyridin-2-yl)disulfanyl)hexan-1-ol (Ii)

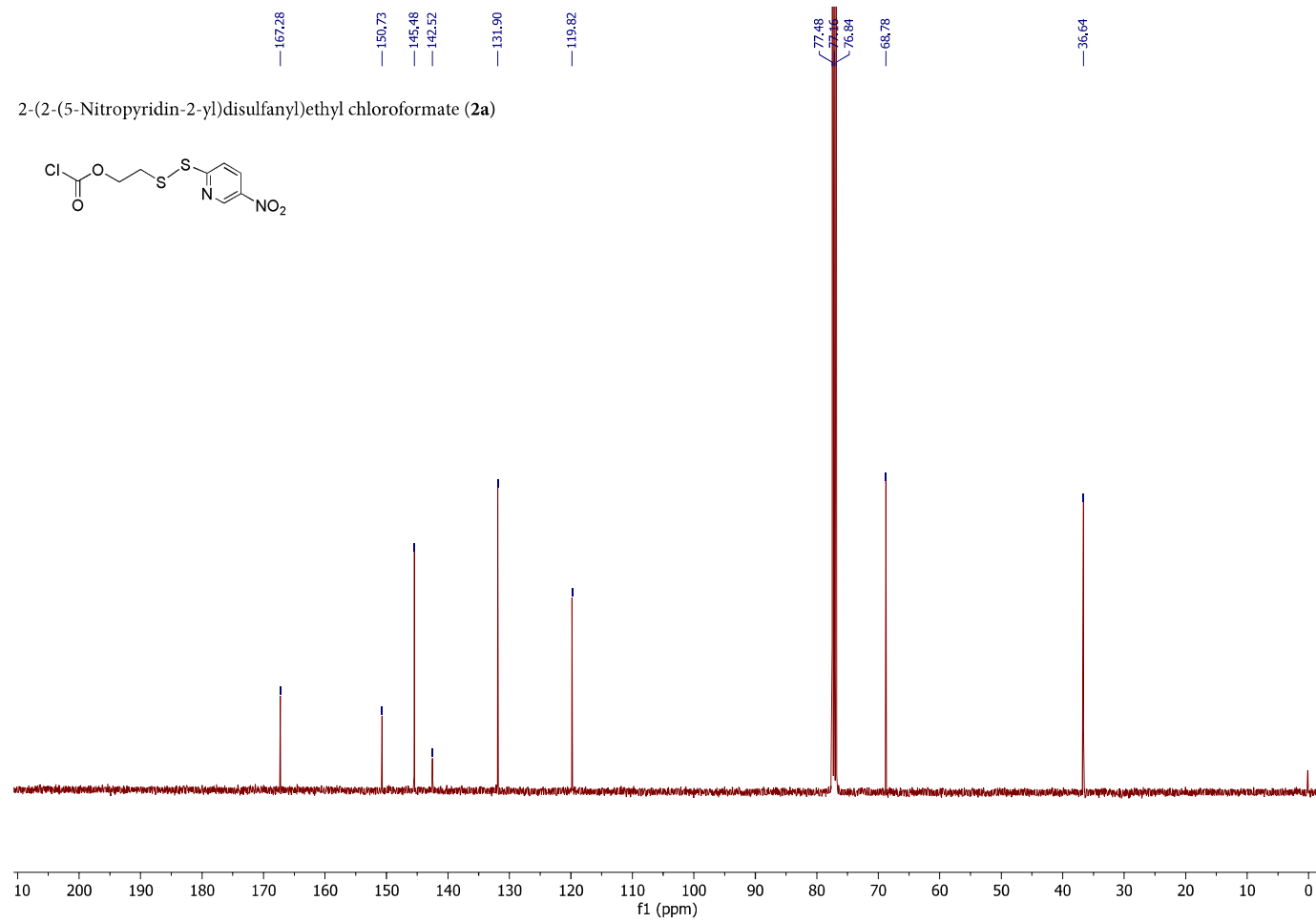
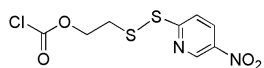


Appendix I.  
NMR spectra

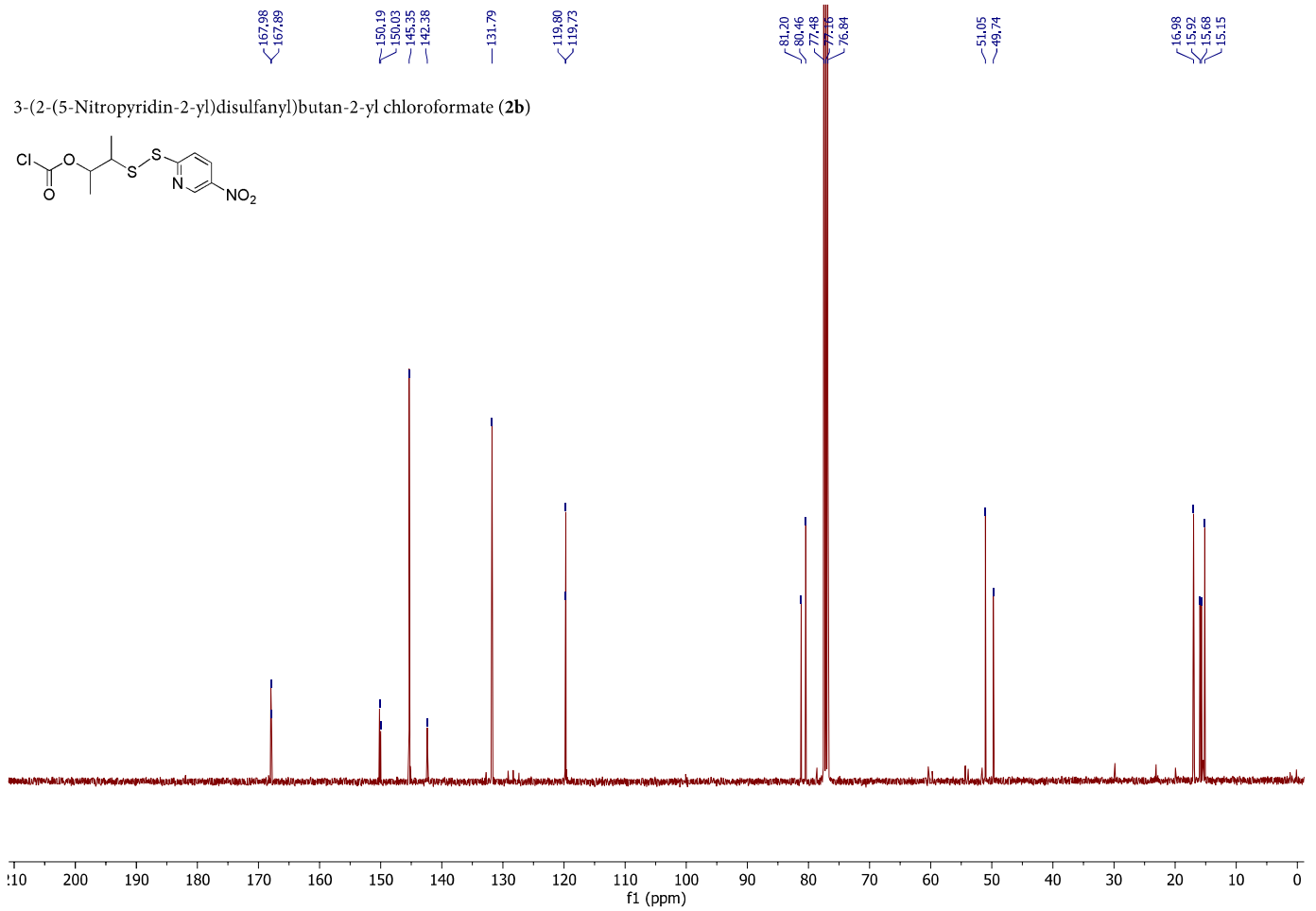
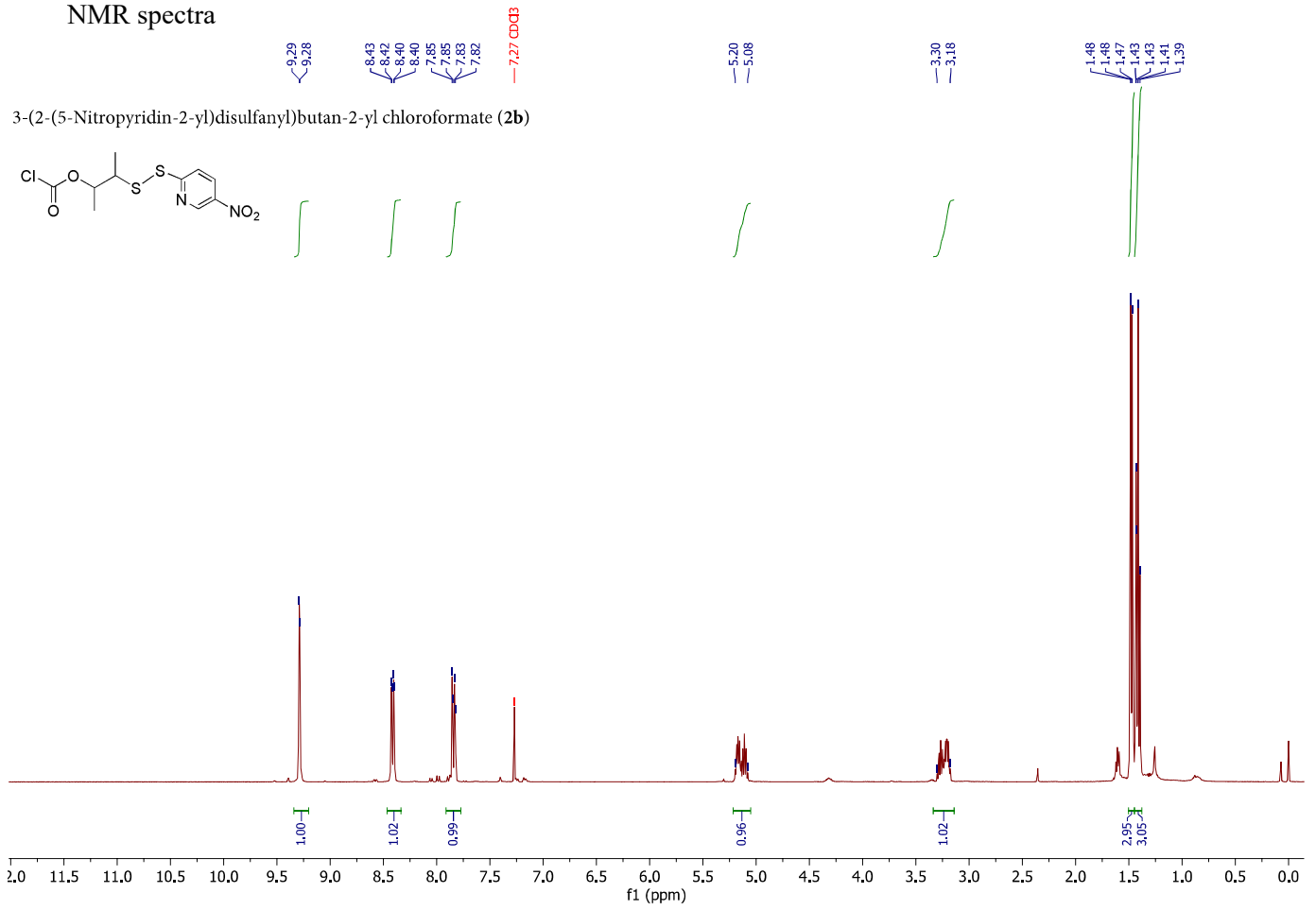
2-(2-(5-Nitropyridin-2-yl)disulfanyl)ethyl chloroformate (**2a**)



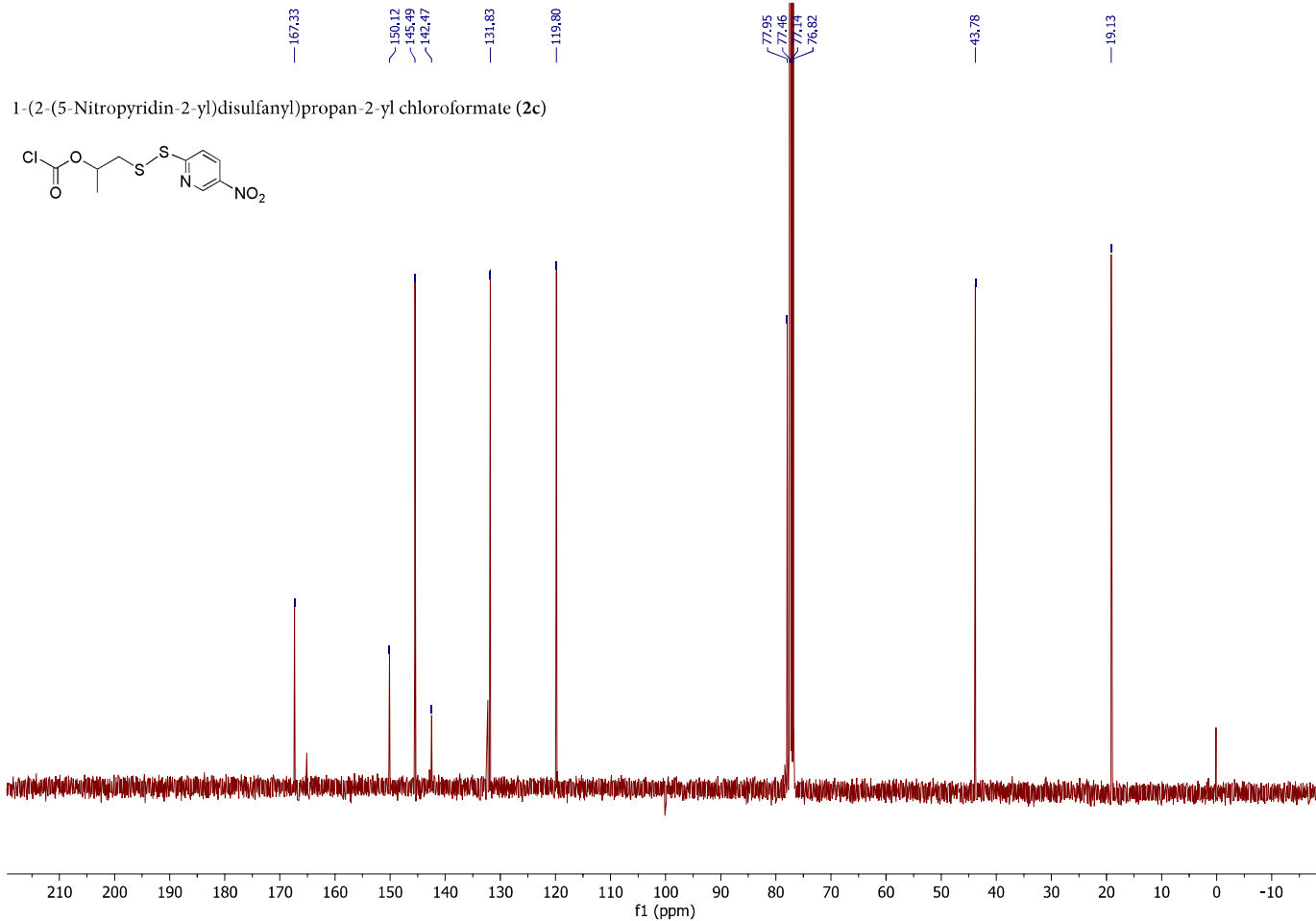
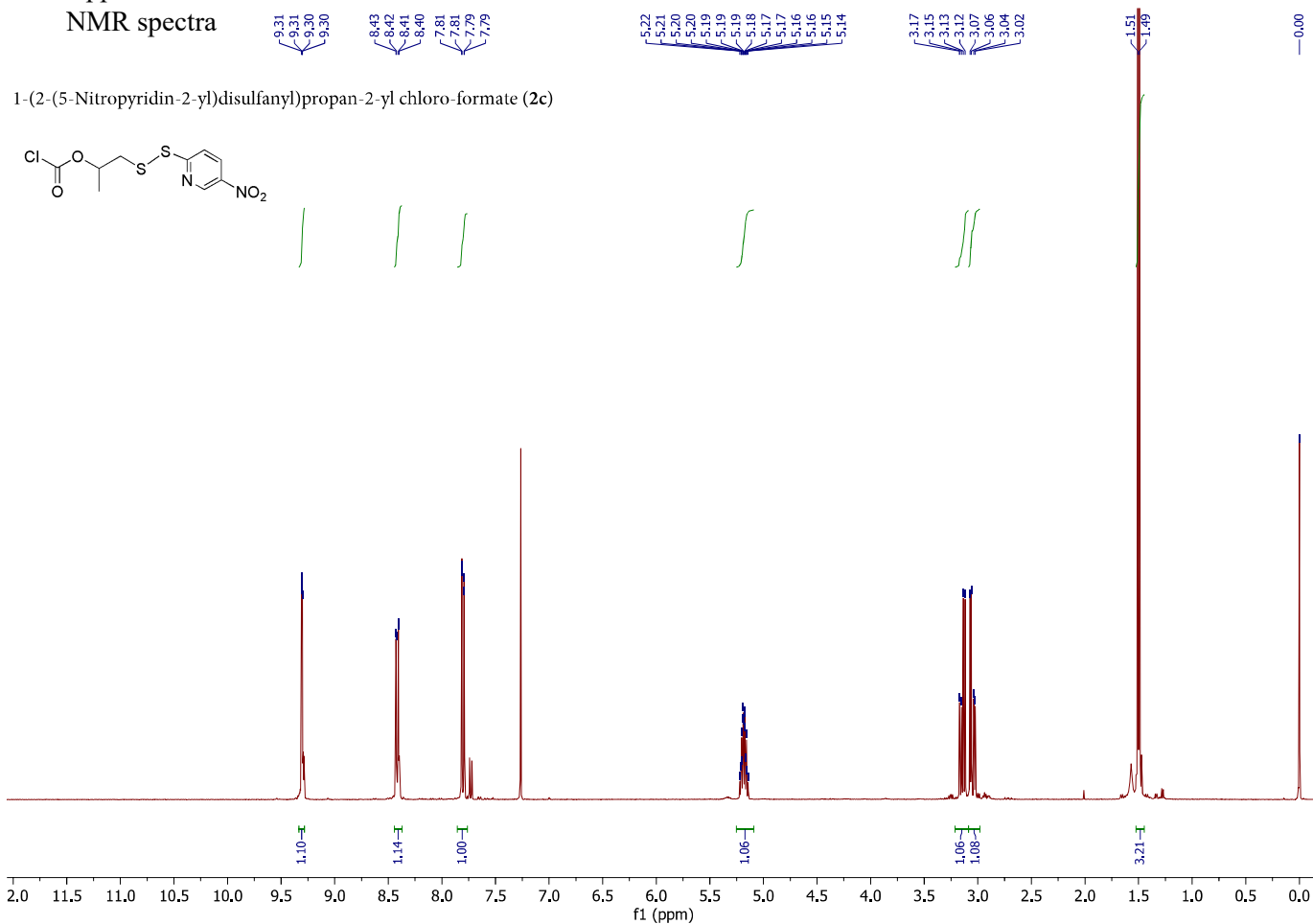
2-(2-(5-Nitropyridin-2-yl)disulfanyl)ethyl chloroformate (**2a**)



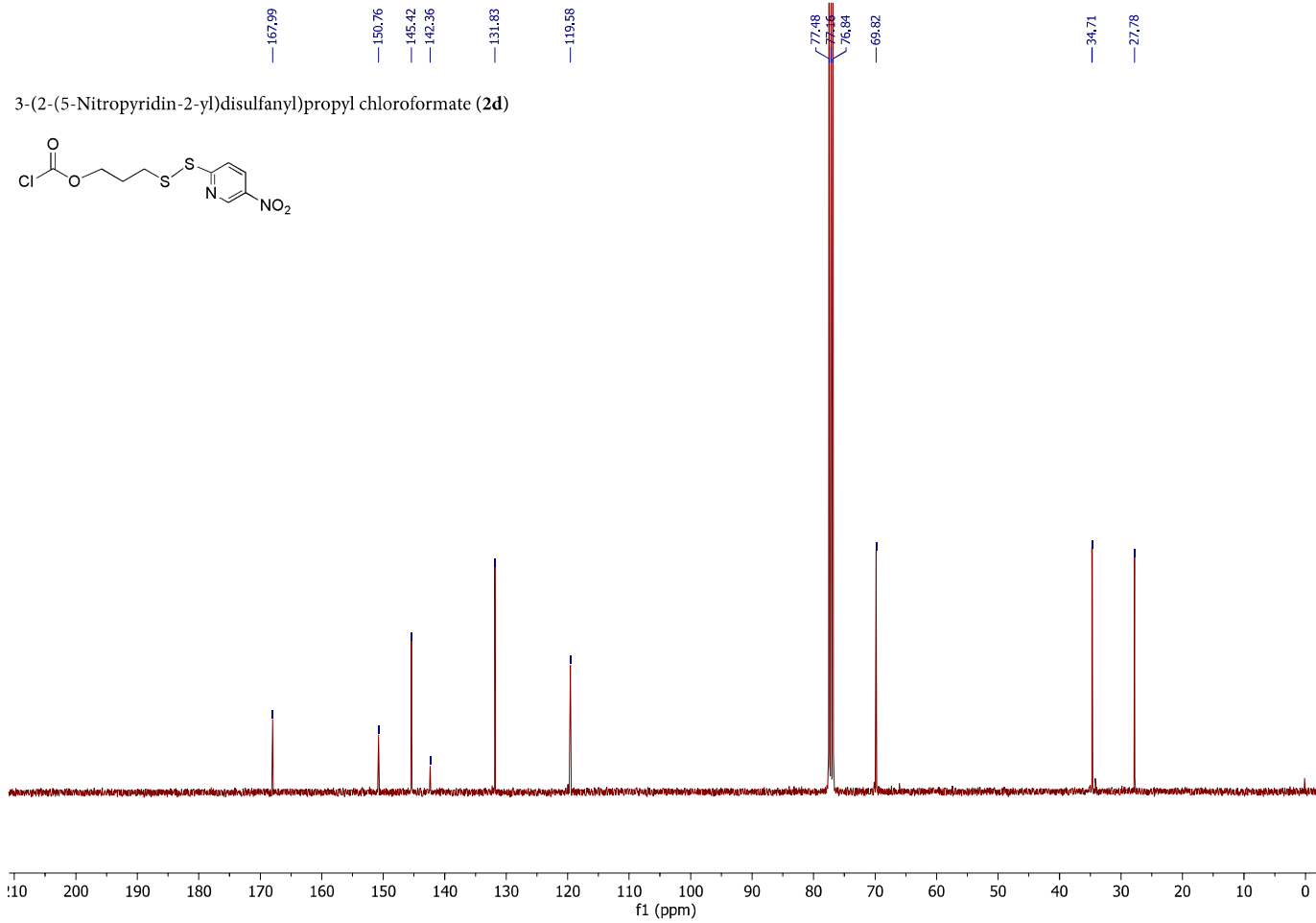
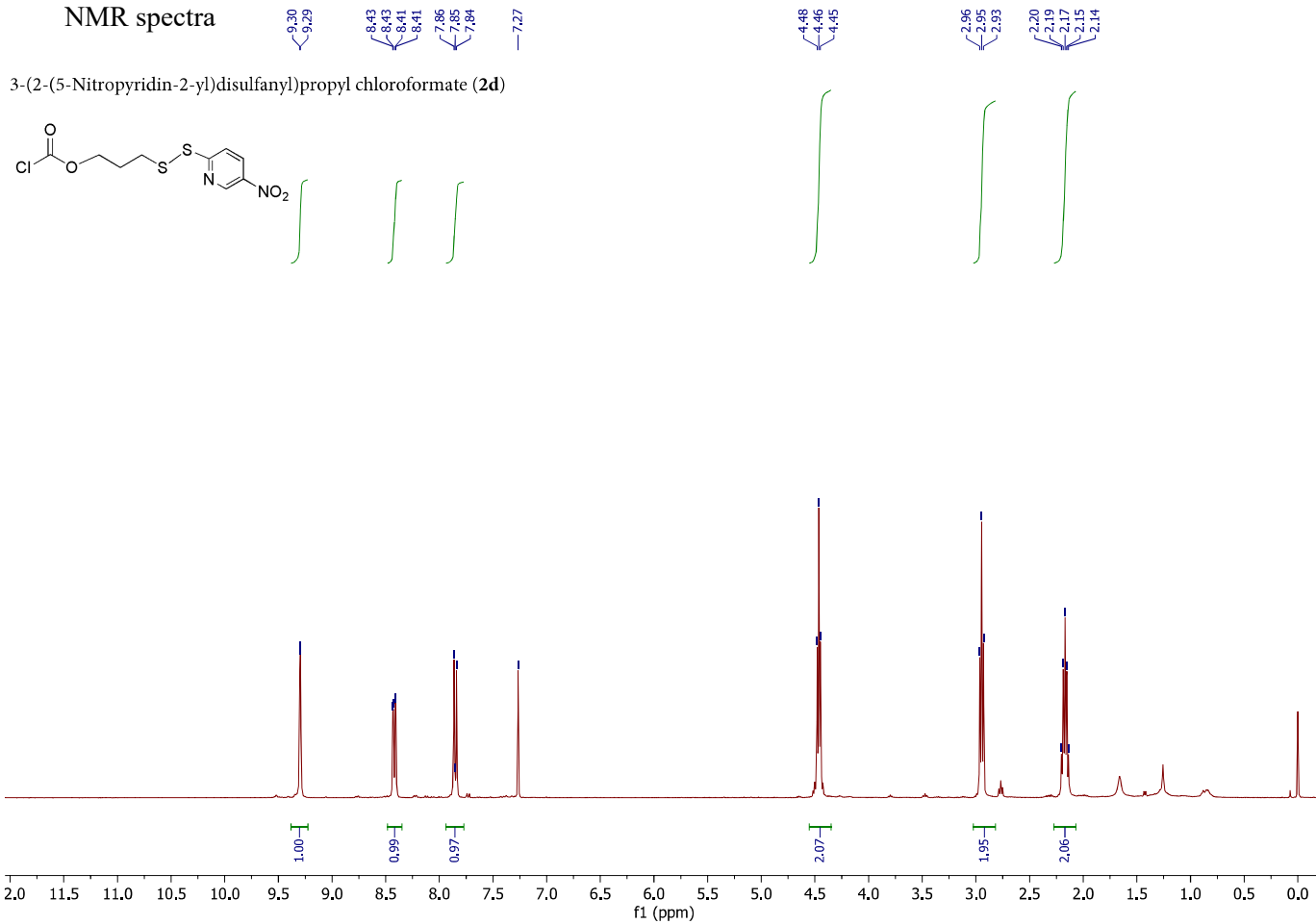
Appendix I.  
NMR spectra



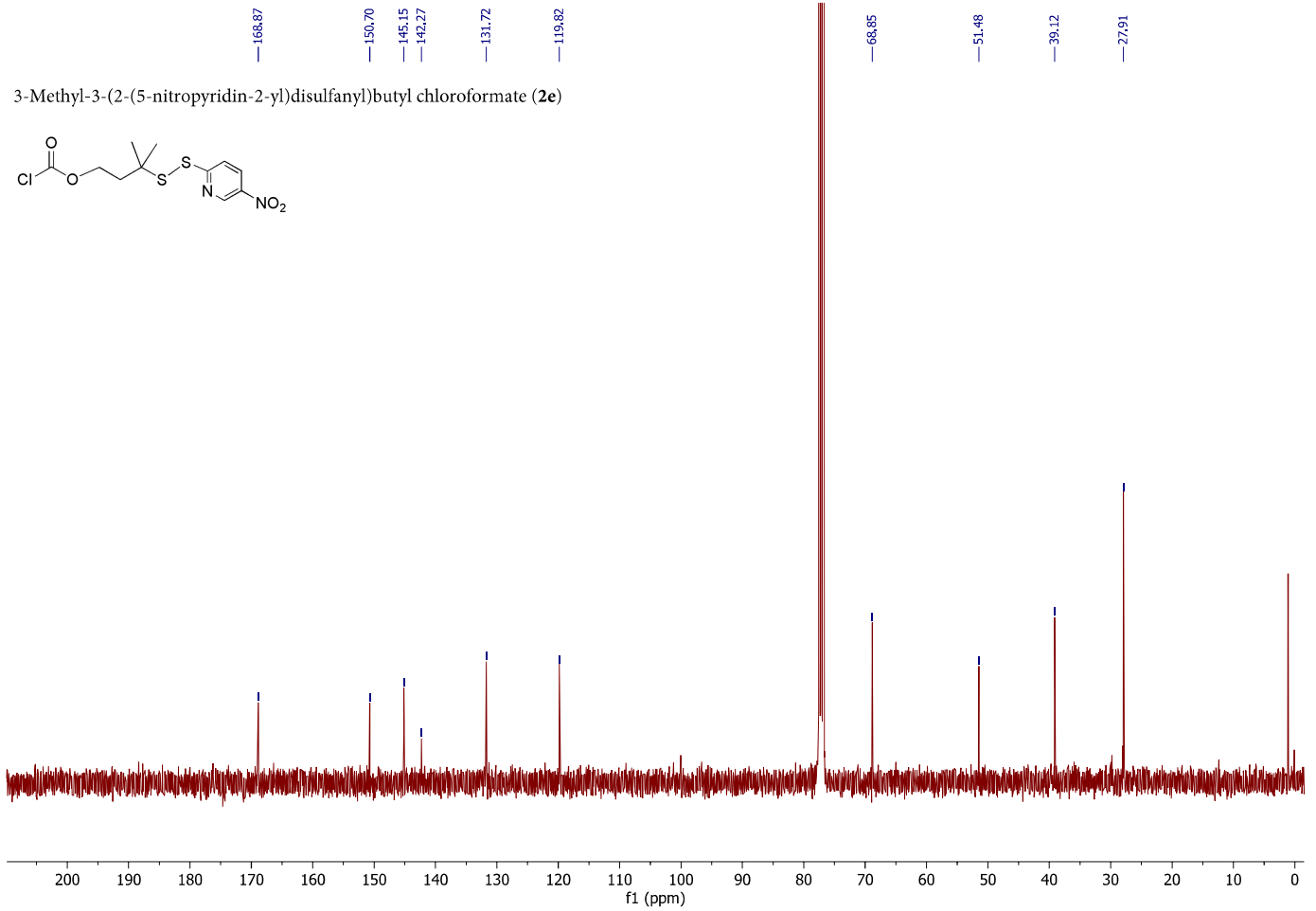
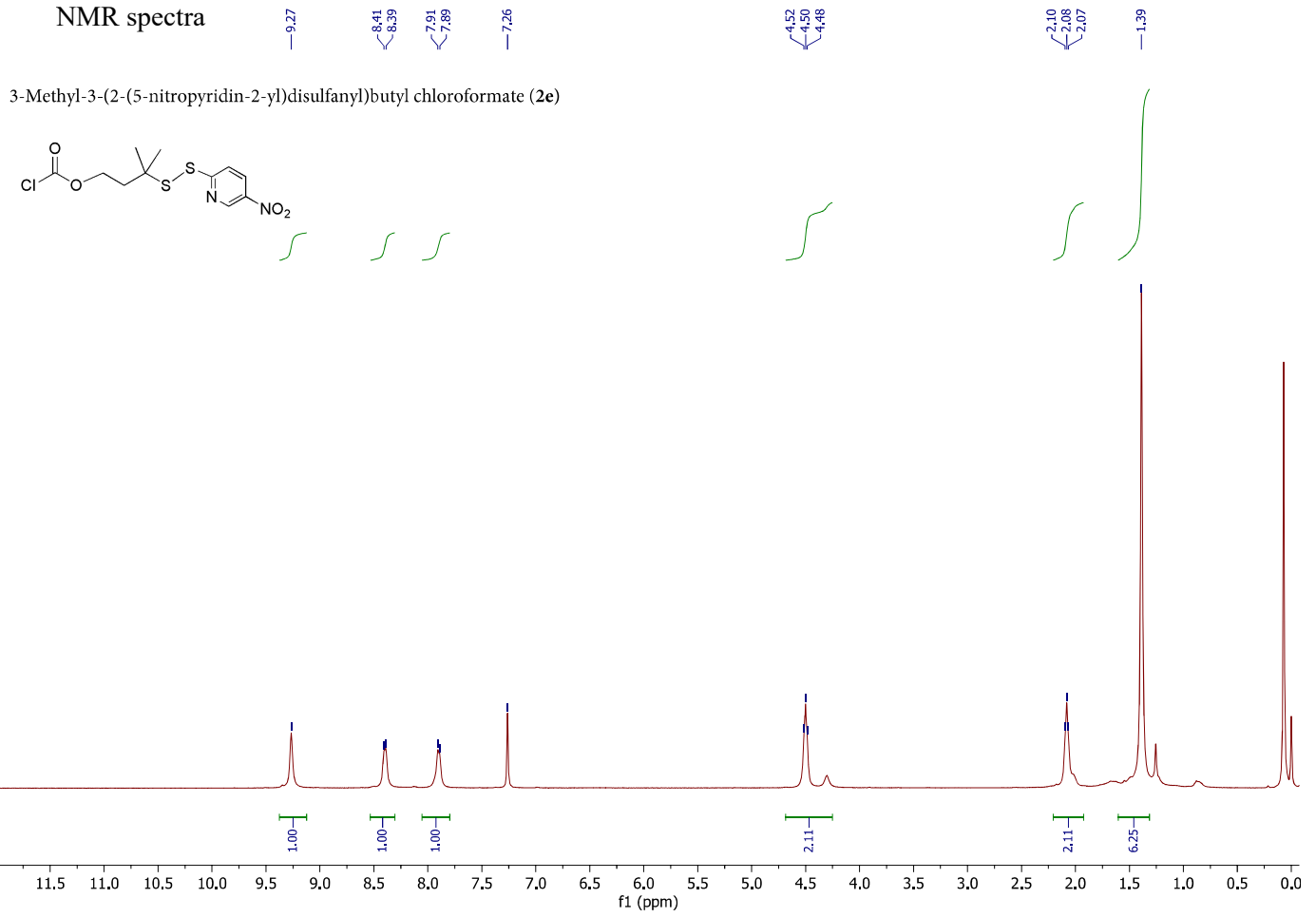
Appendix I.  
NMR spectra



Appendix I.  
NMR spectra

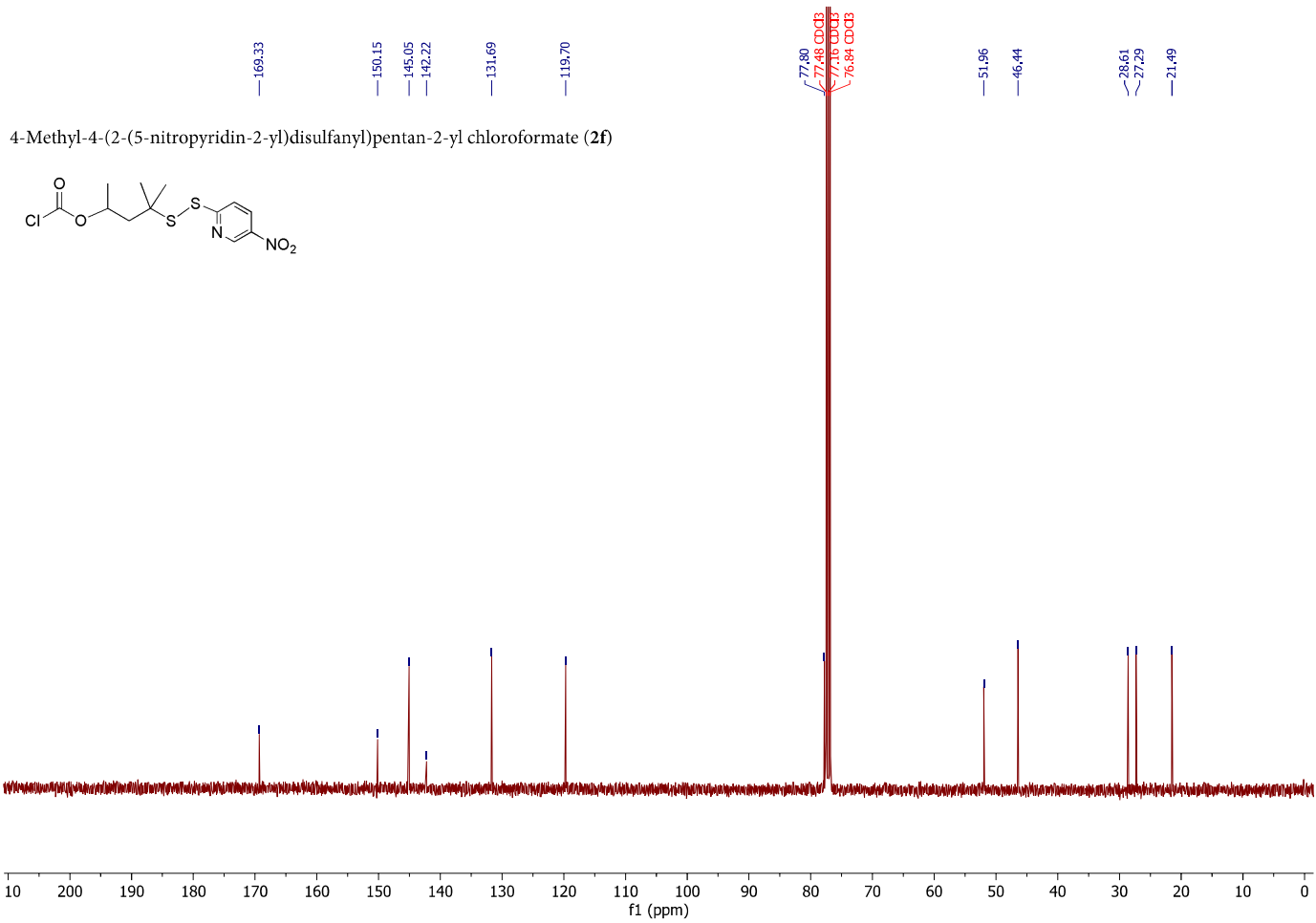
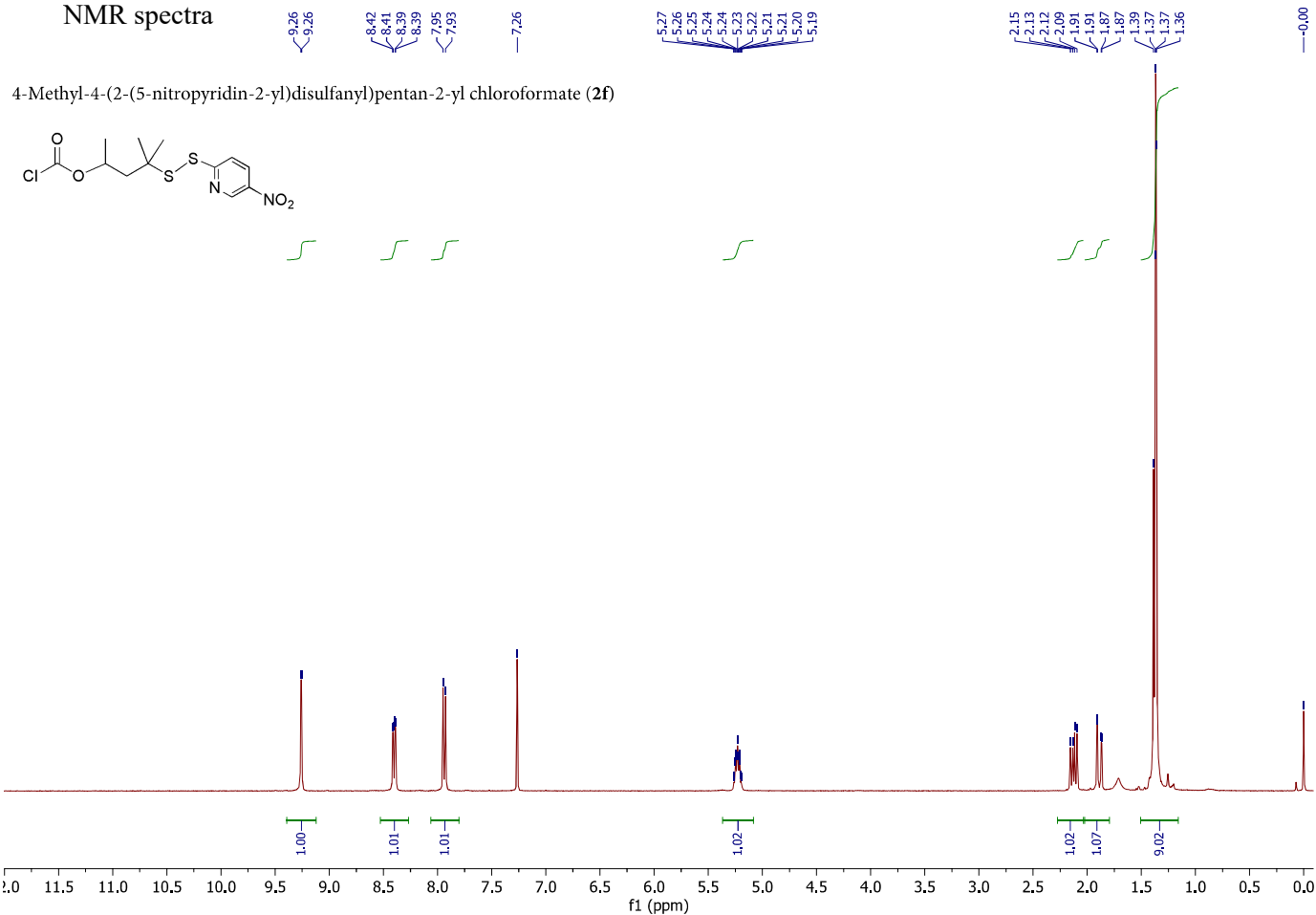


Appendix I.  
NMR spectra

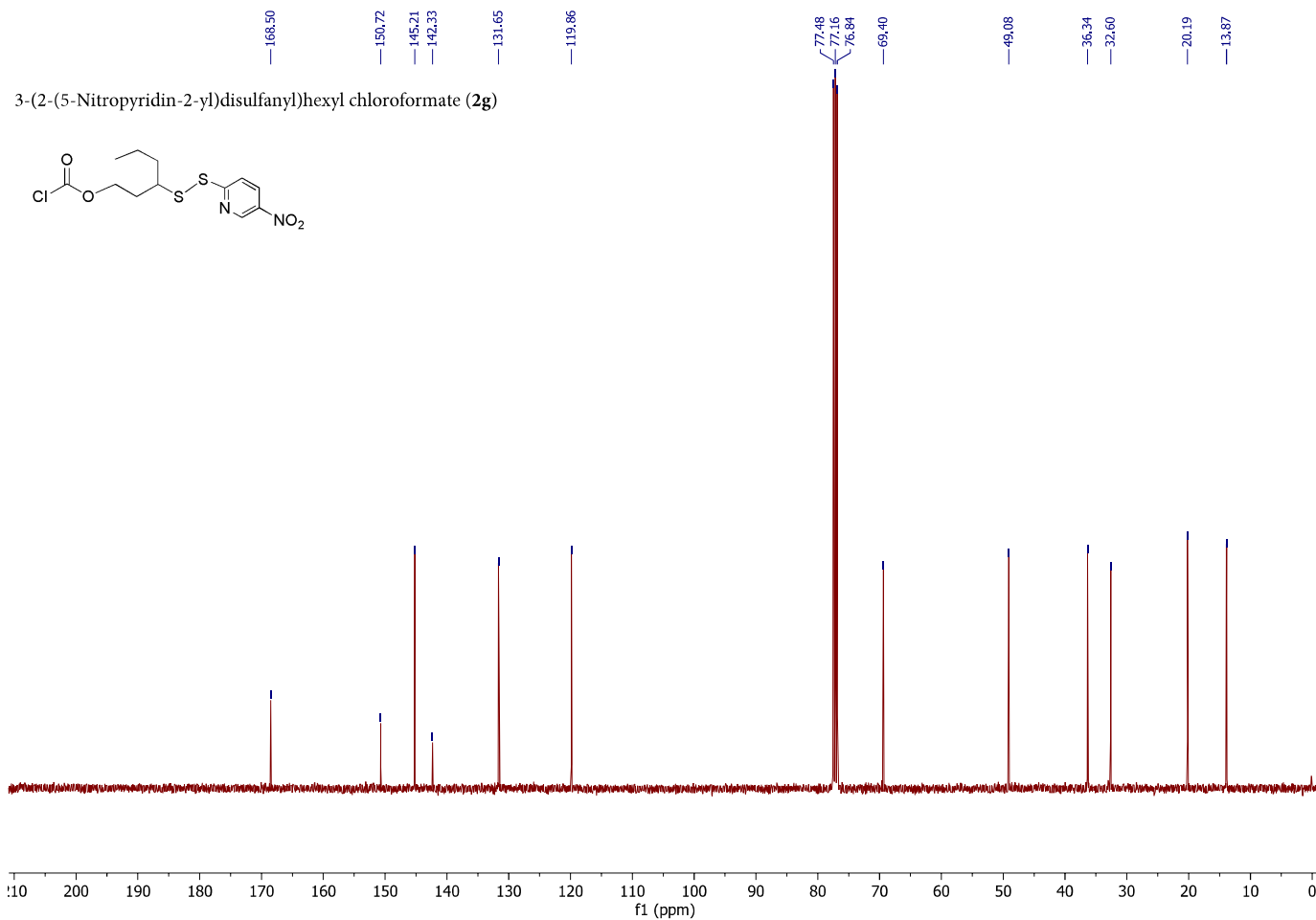
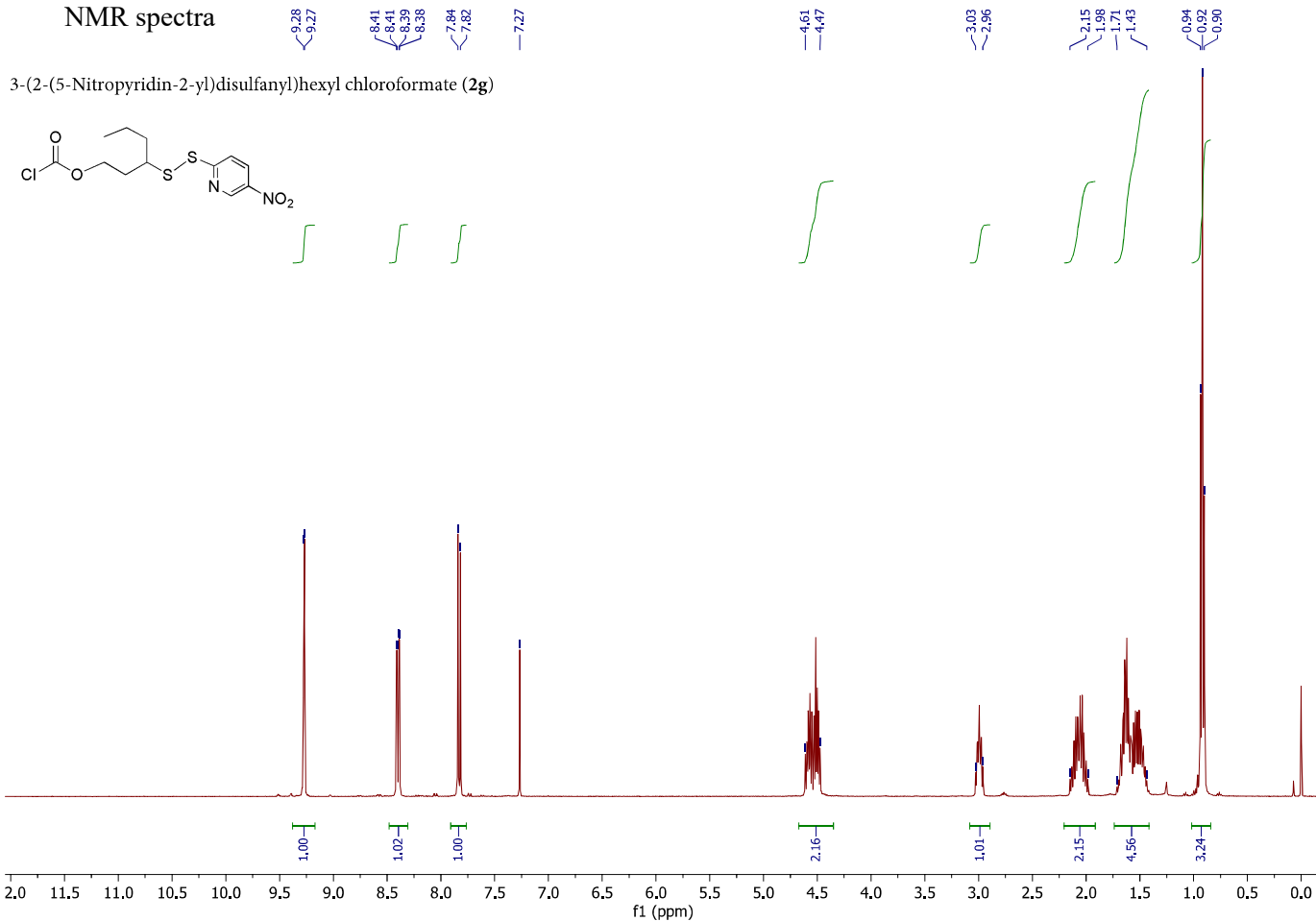




Appendix I.  
NMR spectra



Appendix I.  
NMR spectra

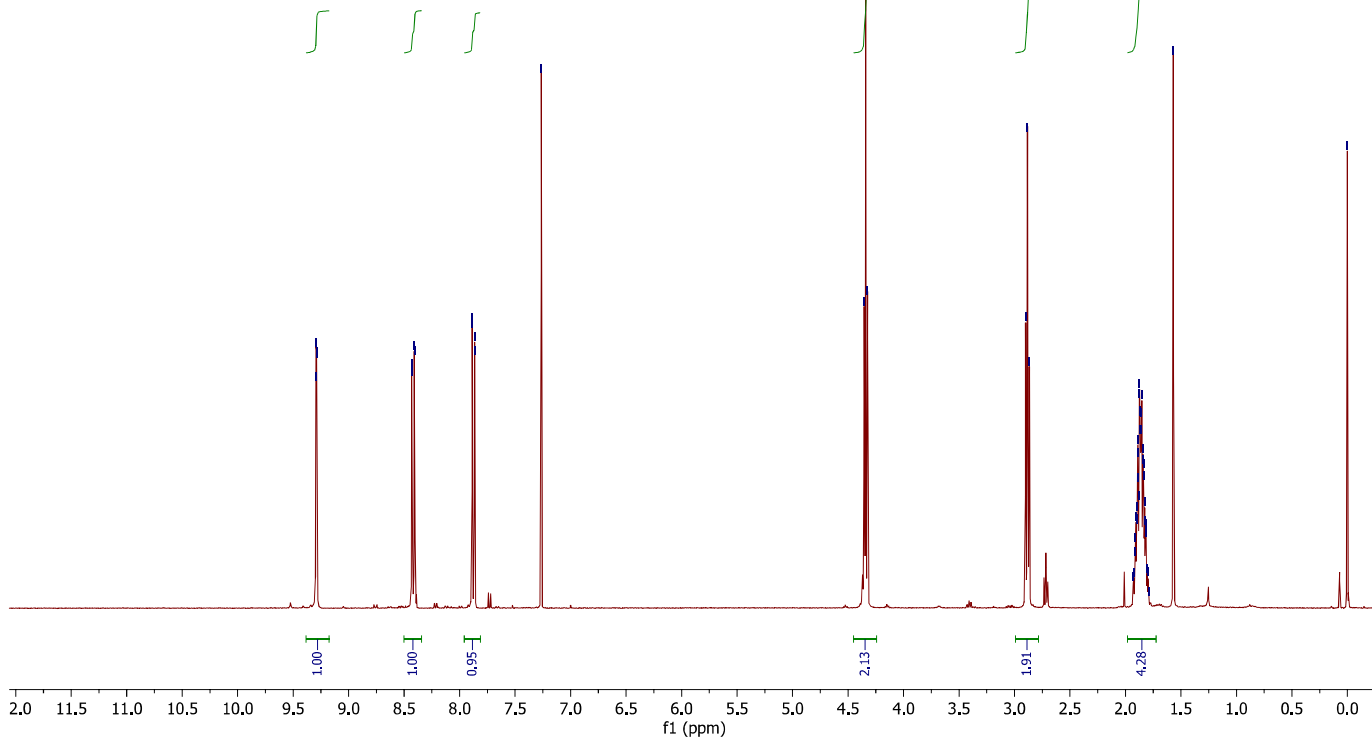
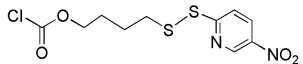


Appendix I.  
NMR spectra

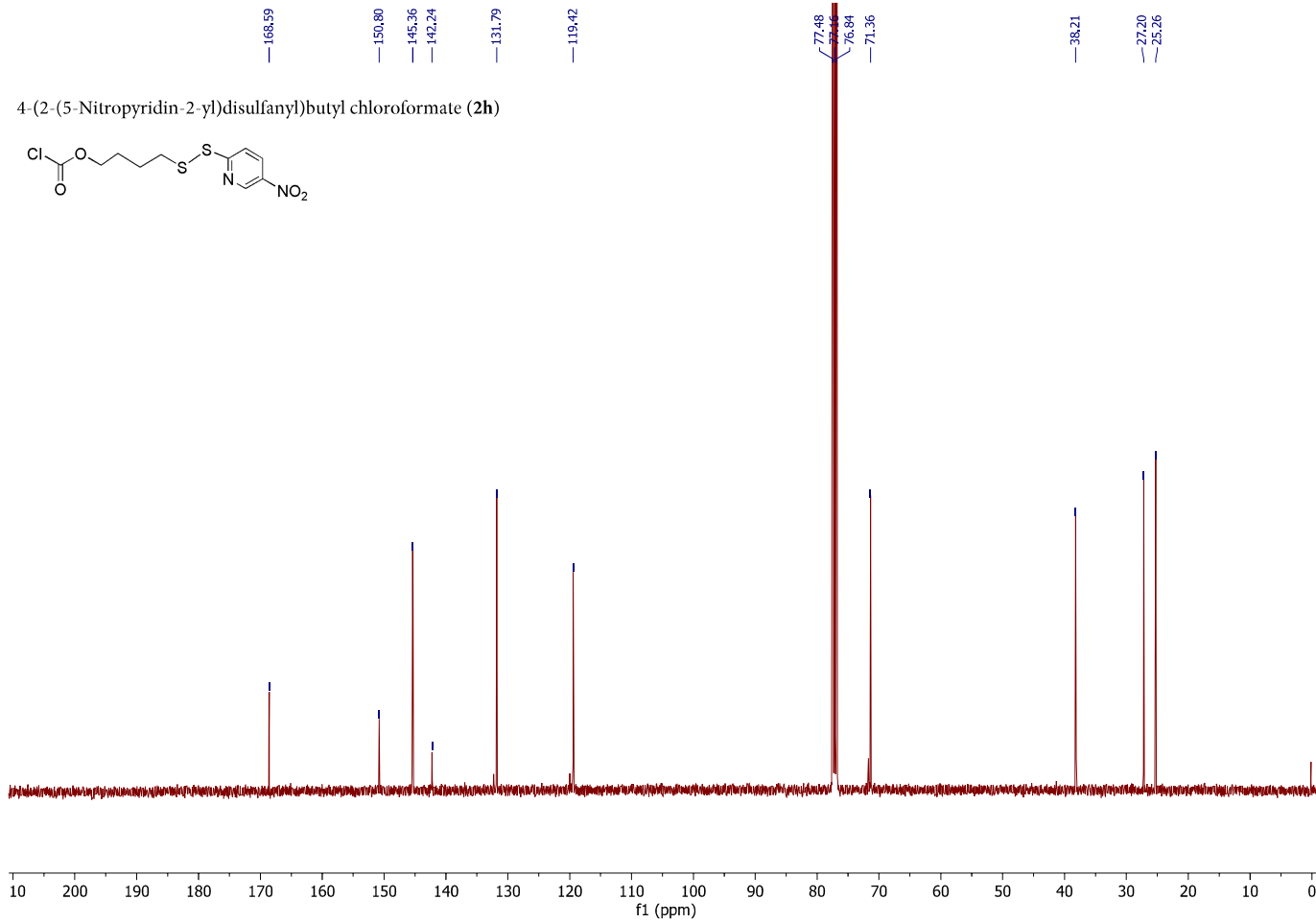
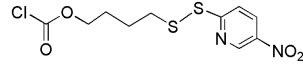
9.30  
9.29  
9.29  
8.43  
8.43  
8.41  
8.40  
7.89  
7.87  
7.86  
7.26

4.35  
4.34  
4.32  
2.90  
2.88  
2.87  
1.93  
1.92  
1.91  
1.91  
1.90  
1.90  
1.89  
1.89  
1.88  
1.88  
1.87  
1.87  
1.87  
1.86  
1.85  
1.85  
1.84  
1.84  
1.83  
1.83  
1.82  
1.82  
1.81  
1.81  
1.80  
1.80  
1.79  
1.57  
0.00

4-(2-(5-Nitropyridin-2-yl)disulfanyl)butyl chloroformate (**2h**)

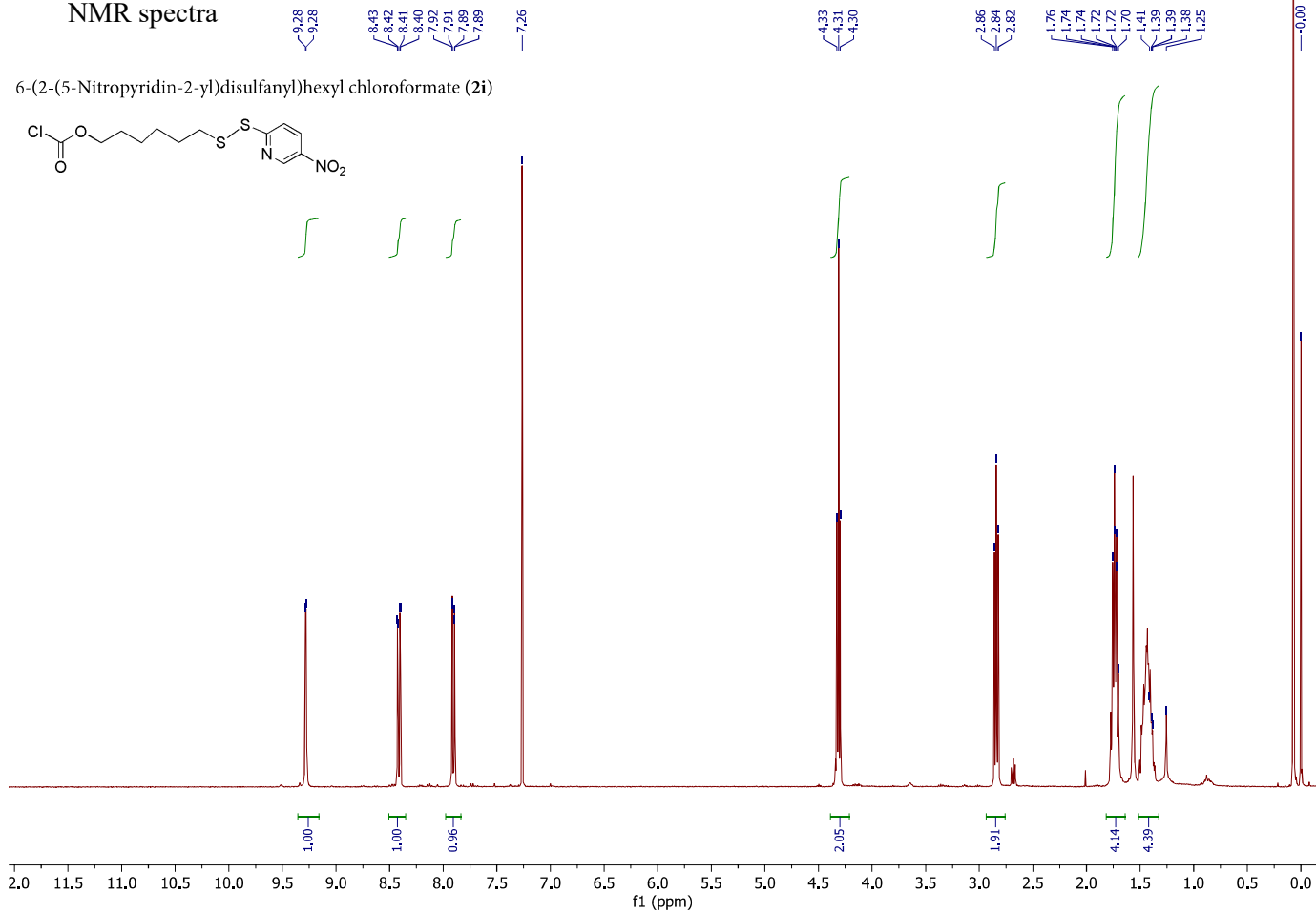


4-(2-(5-Nitropyridin-2-yl)disulfanyl)butyl chloroformate (**2h**)

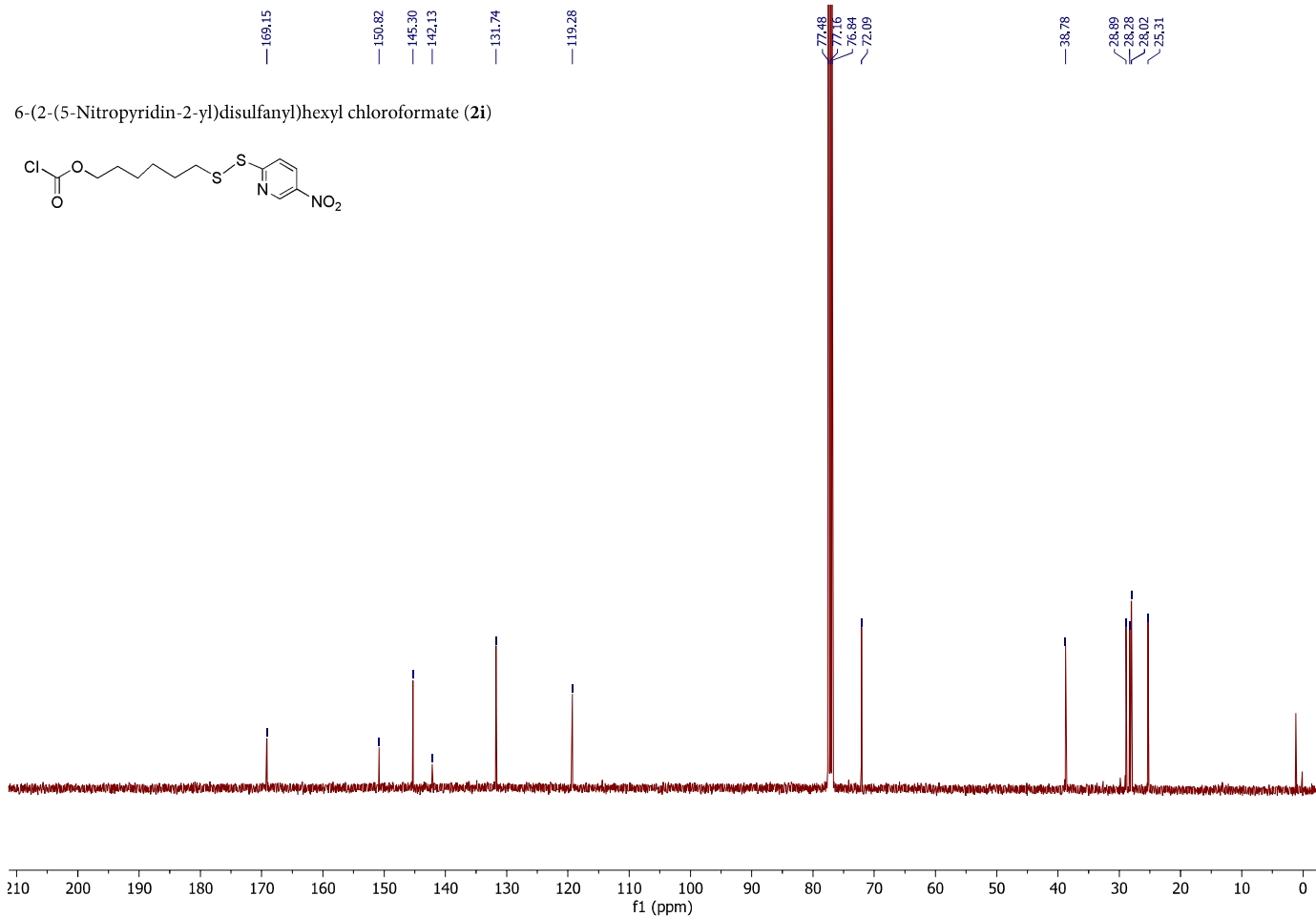


Appendix I.  
NMR spectra

6-(2-(5-Nitropyridin-2-yl)disulfanyl)hexyl chloroformate (**2i**)

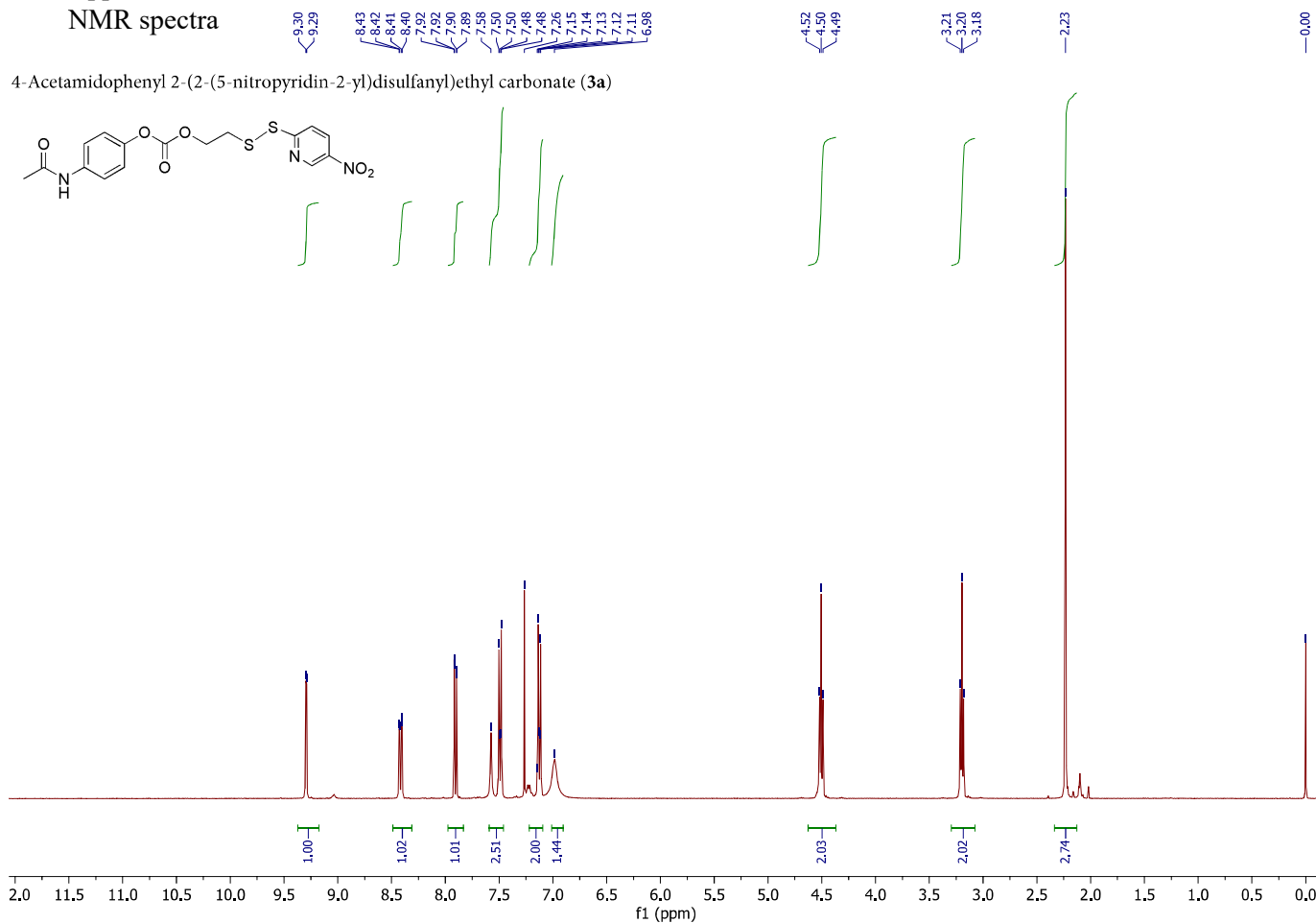
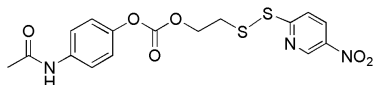


6-(2-(5-Nitropyridin-2-yl)disulfanyl)hexyl chloroformate (**2i**)

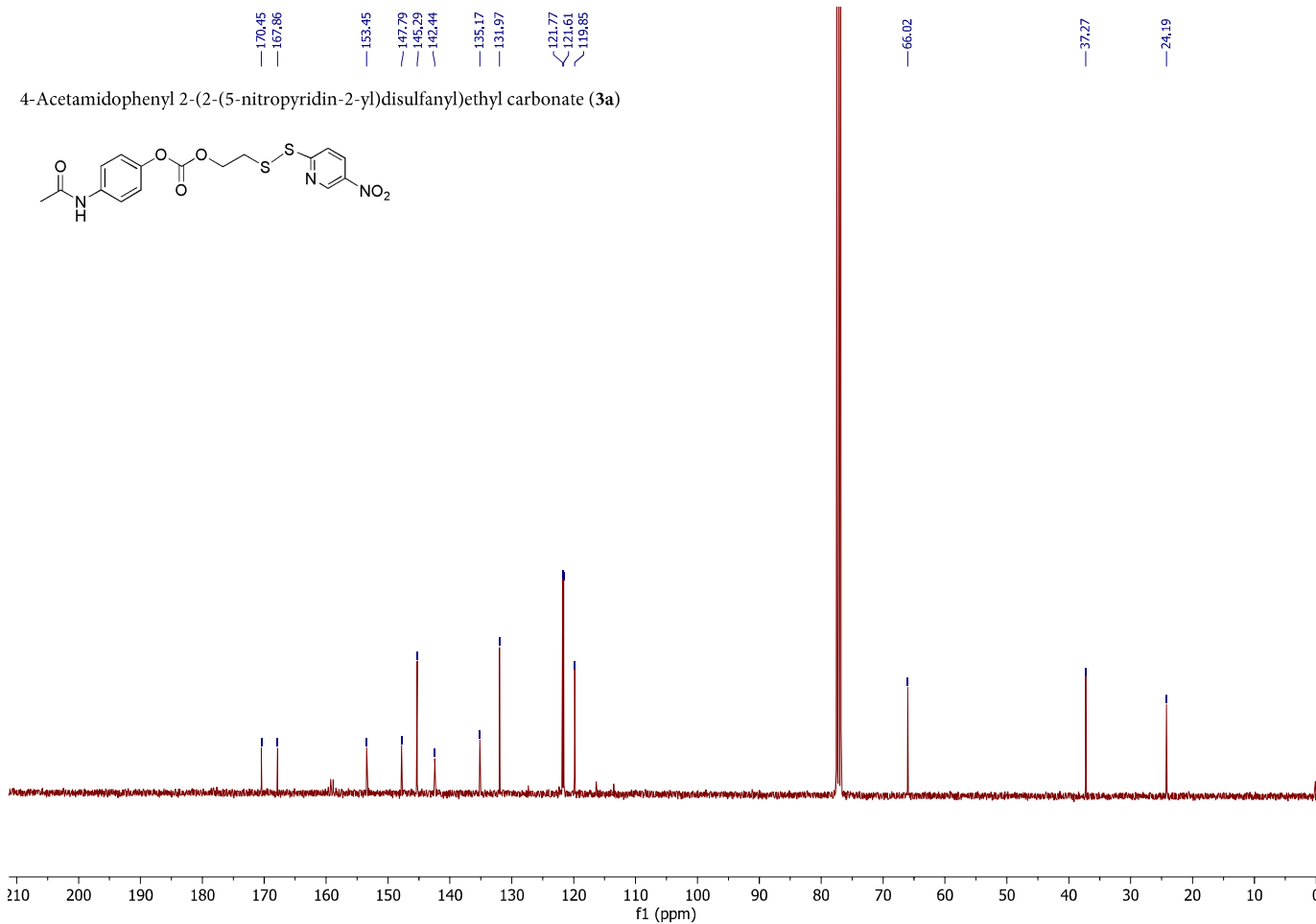
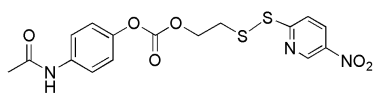


Appendix I.  
NMR spectra

4-Acetamidophenyl 2-(2-(5-nitropyridin-2-yl)disulfanyl)ethyl carbonate (3a)

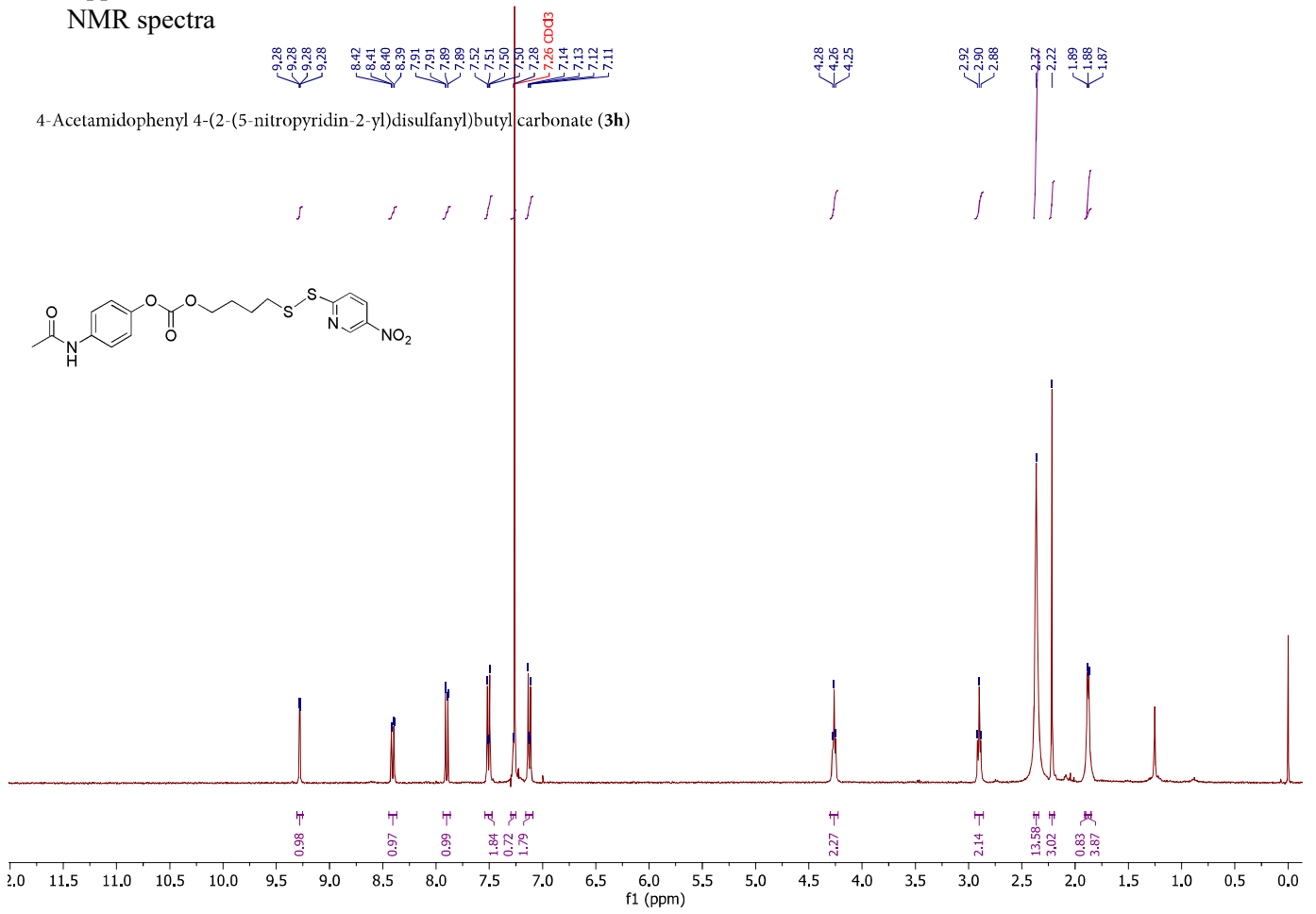


4-Acetamidophenyl 2-(2-(5-nitropyridin-2-yl)disulfanyl)ethyl carbonate (3a)

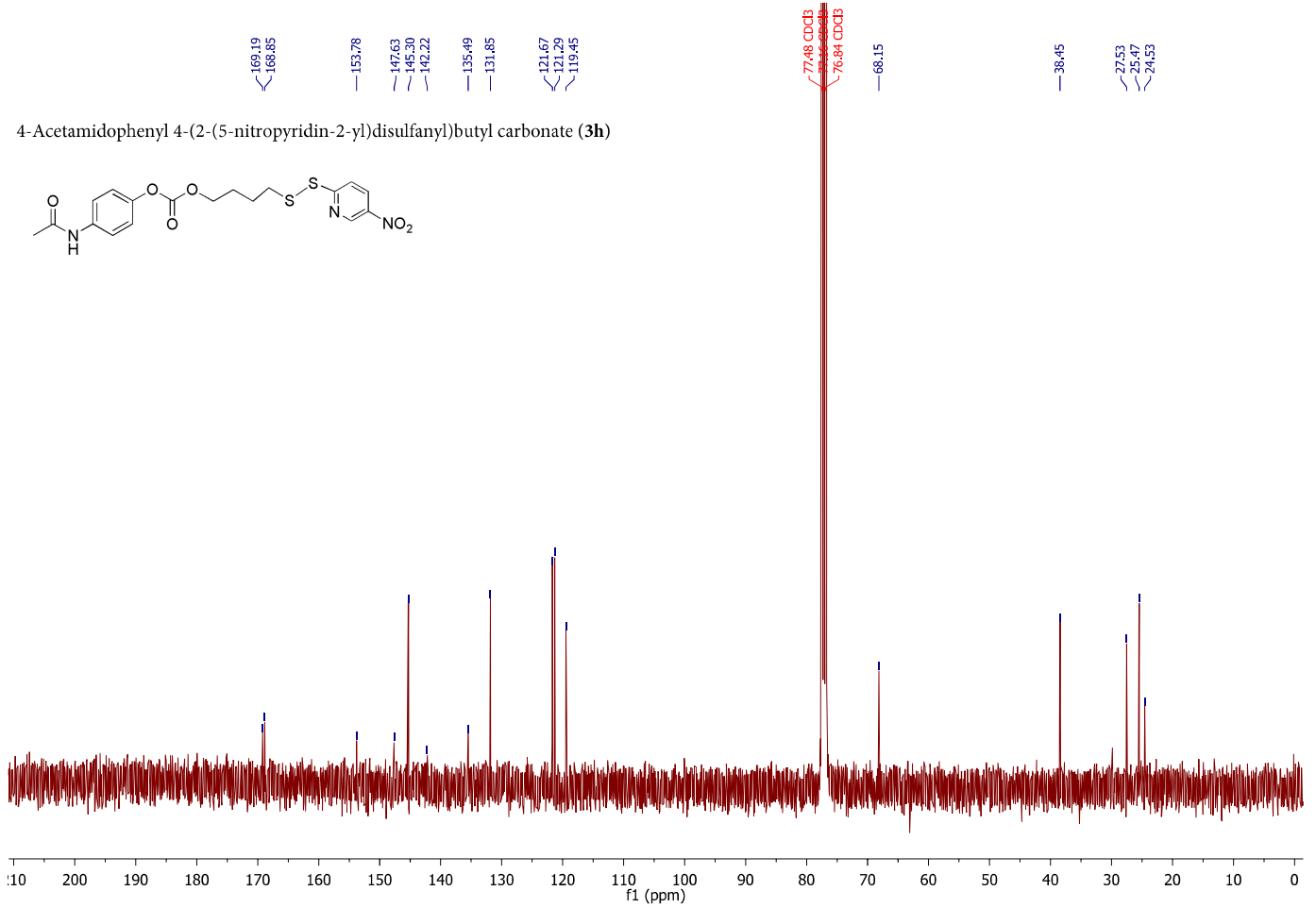


Appendix I.  
NMR spectra

4-Acetamidophenyl 4-(2-(5-nitropyridin-2-yl)disulfanyl)butyl carbonate (3h)



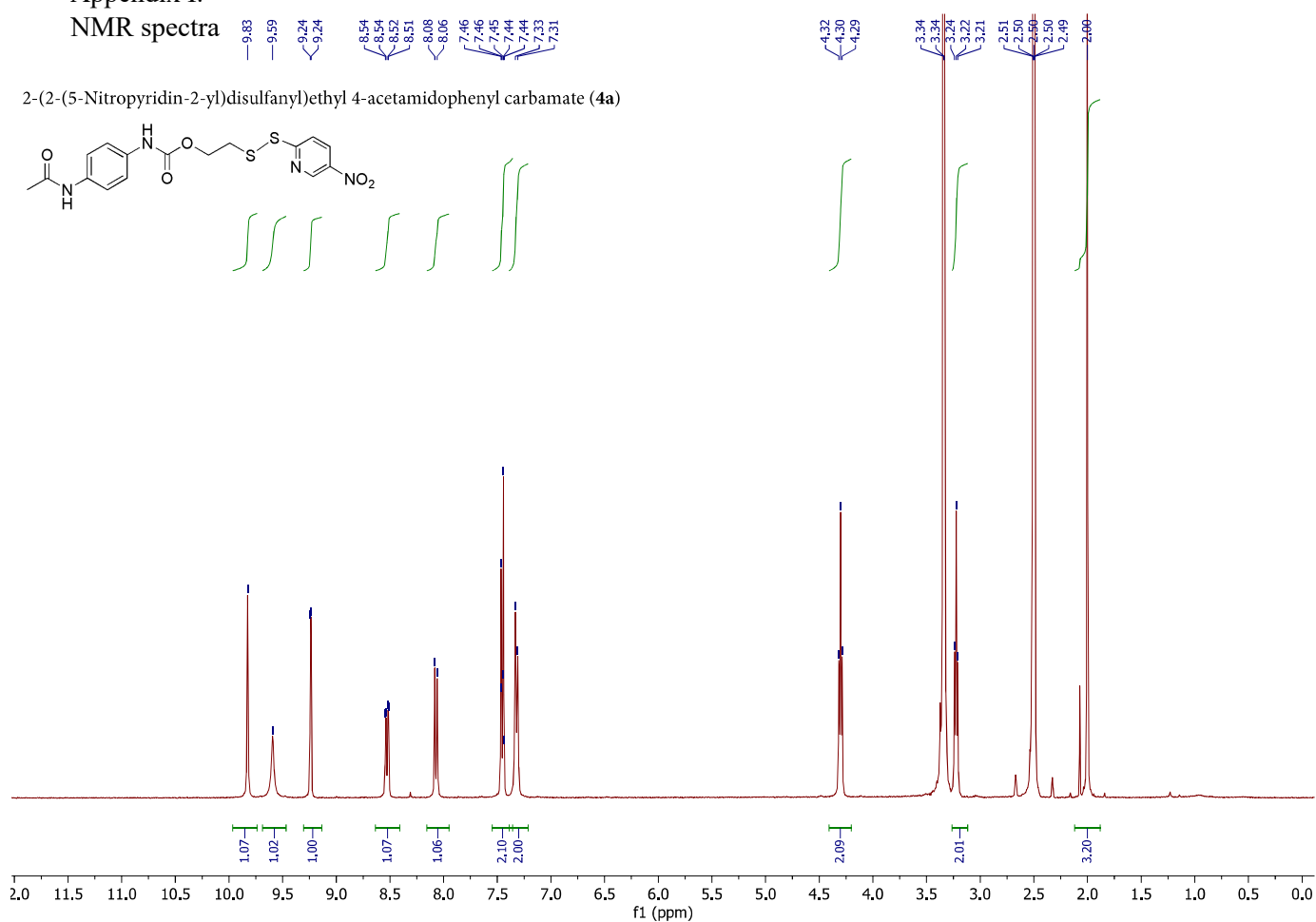
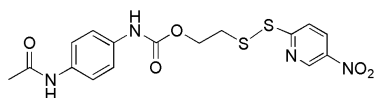
4-Acetamidophenyl 4-(2-(5-nitropyridin-2-yl)disulfanyl)butyl carbonate (3h)



Appendix I.  
NMR spectra

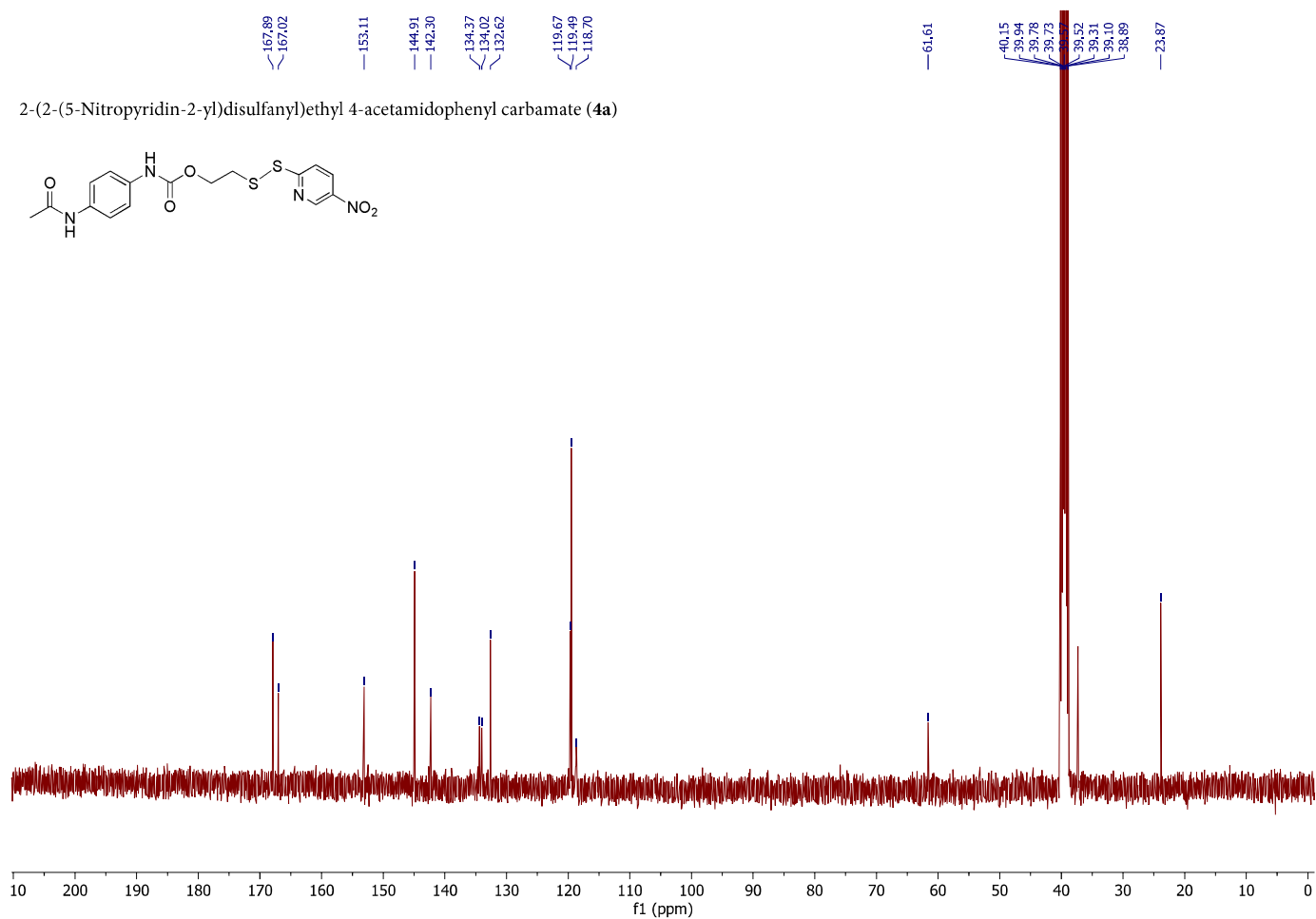
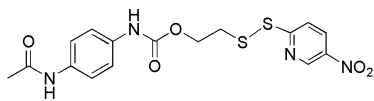
8.83 9.59 9.24 9.24 8.54 8.54 8.52 8.51 8.08 8.06 7.46 7.46 7.45 7.44 7.44 7.33 7.31

2-(2-(5-Nitropyridin-2-yl)disulfanyl)ethyl 4-acetamidophenyl carbamate (4a)



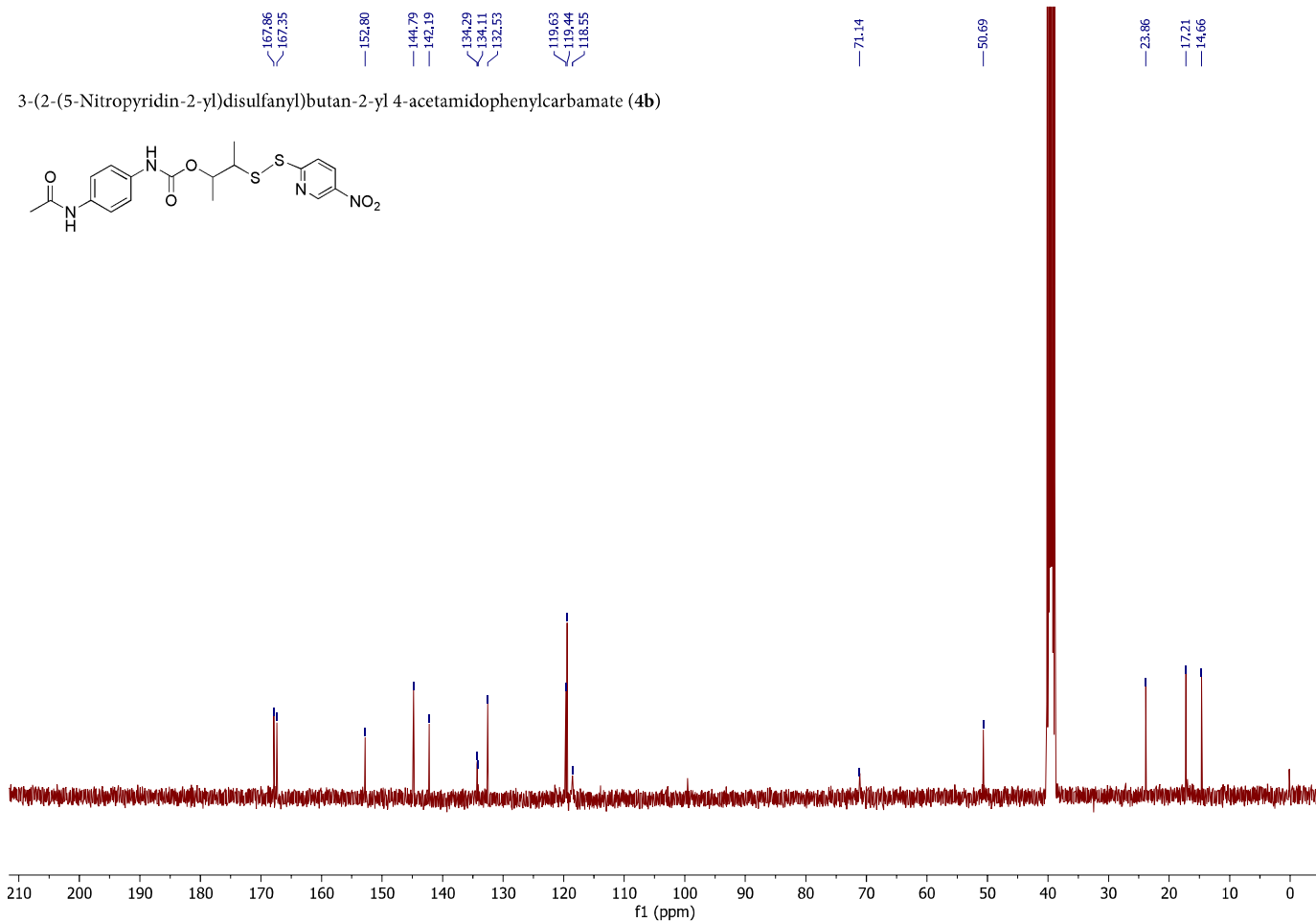
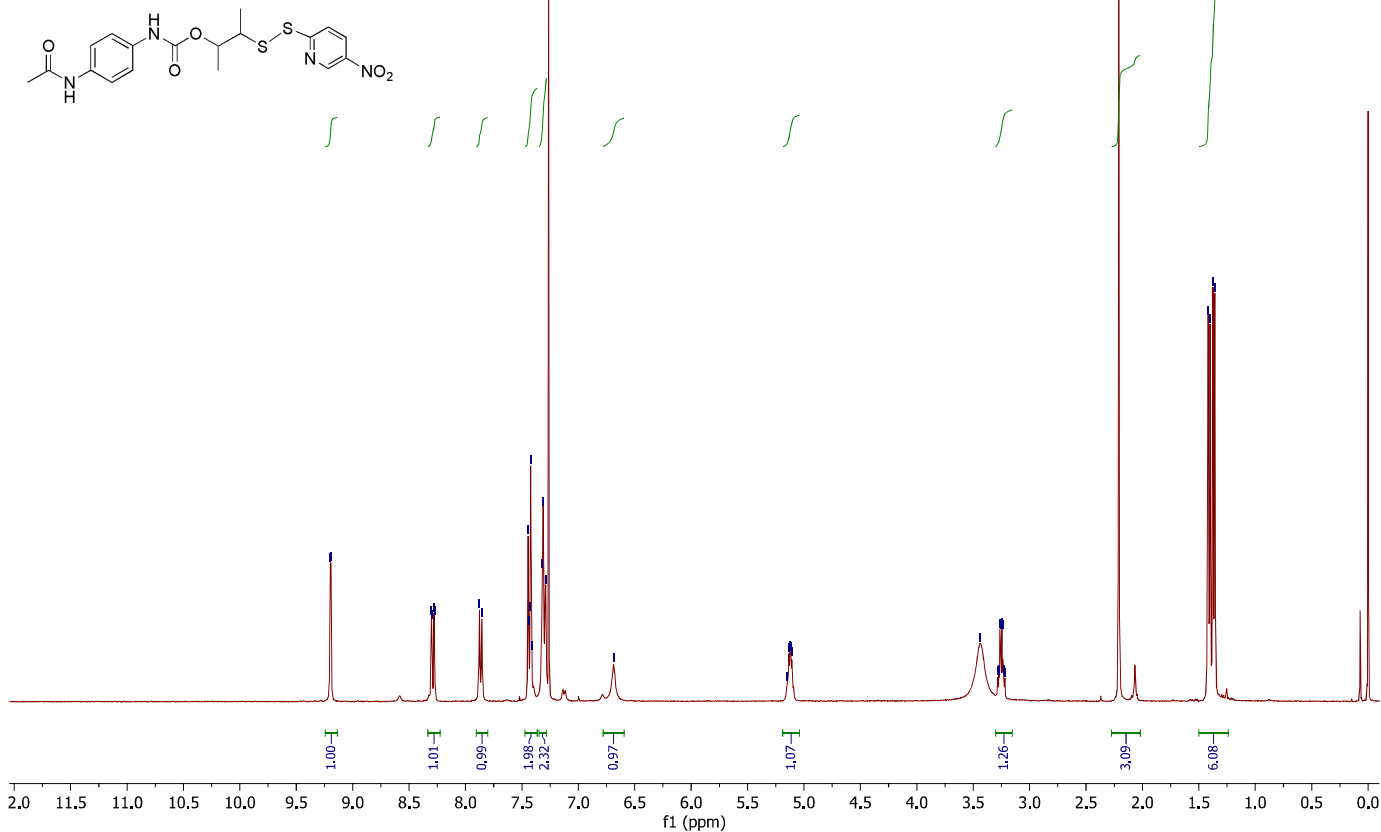
167.89 167.02 153.11 144.91 142.30 134.37 134.02 132.62 118.67 118.49 118.70 61.61 40.15 39.94 39.78 39.73 39.52 39.31 39.10 38.89 23.87

2-(2-(5-Nitropyridin-2-yl)disulfanyl)ethyl 4-acetamidophenyl carbamate (4a)



Appendix I.  
NMR spectra

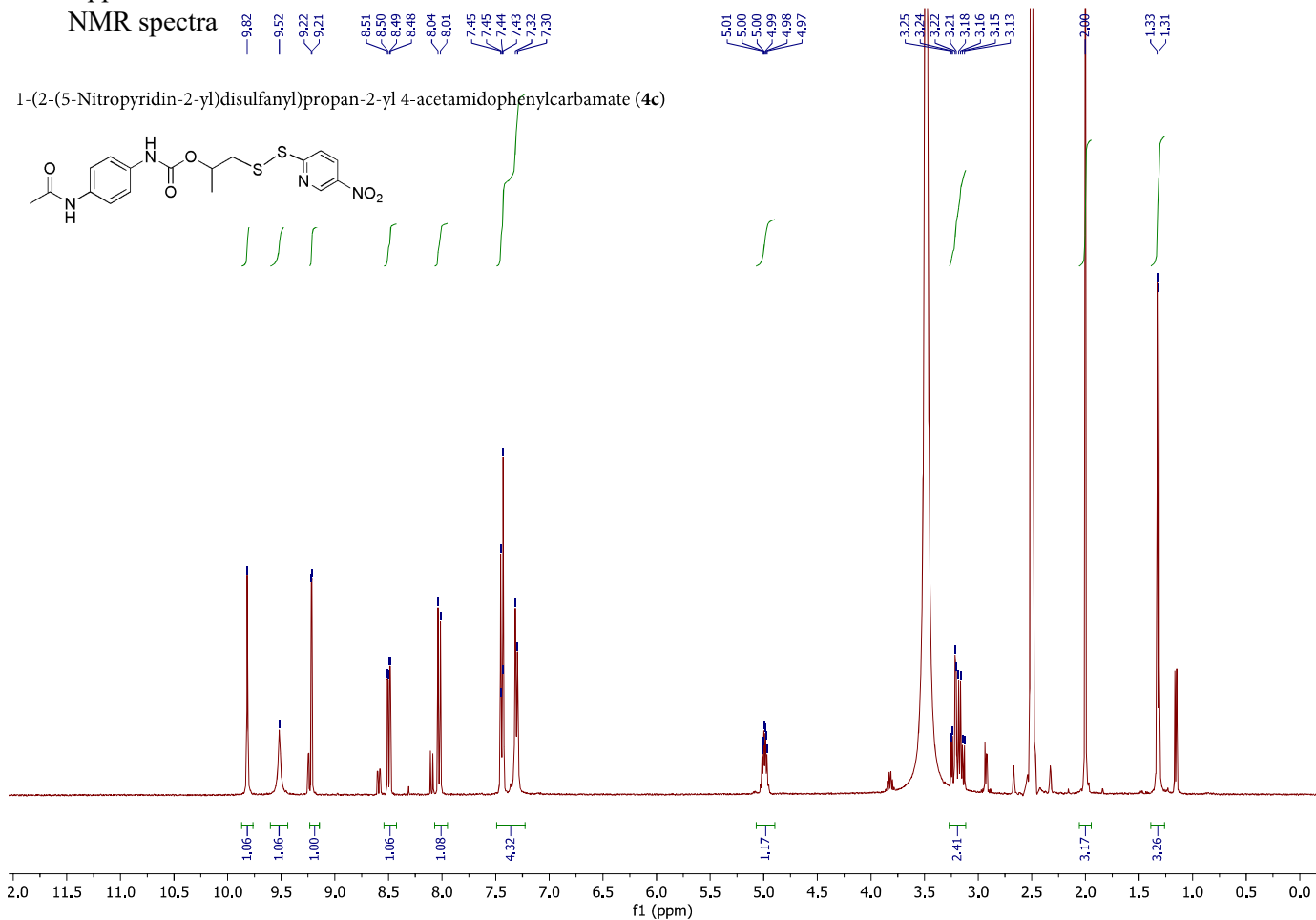
3-(2-(5-Nitropyridin-2-yl)disulfanyl)butan-2-yl 4-acetamidophenylcarbamate (**4b**)



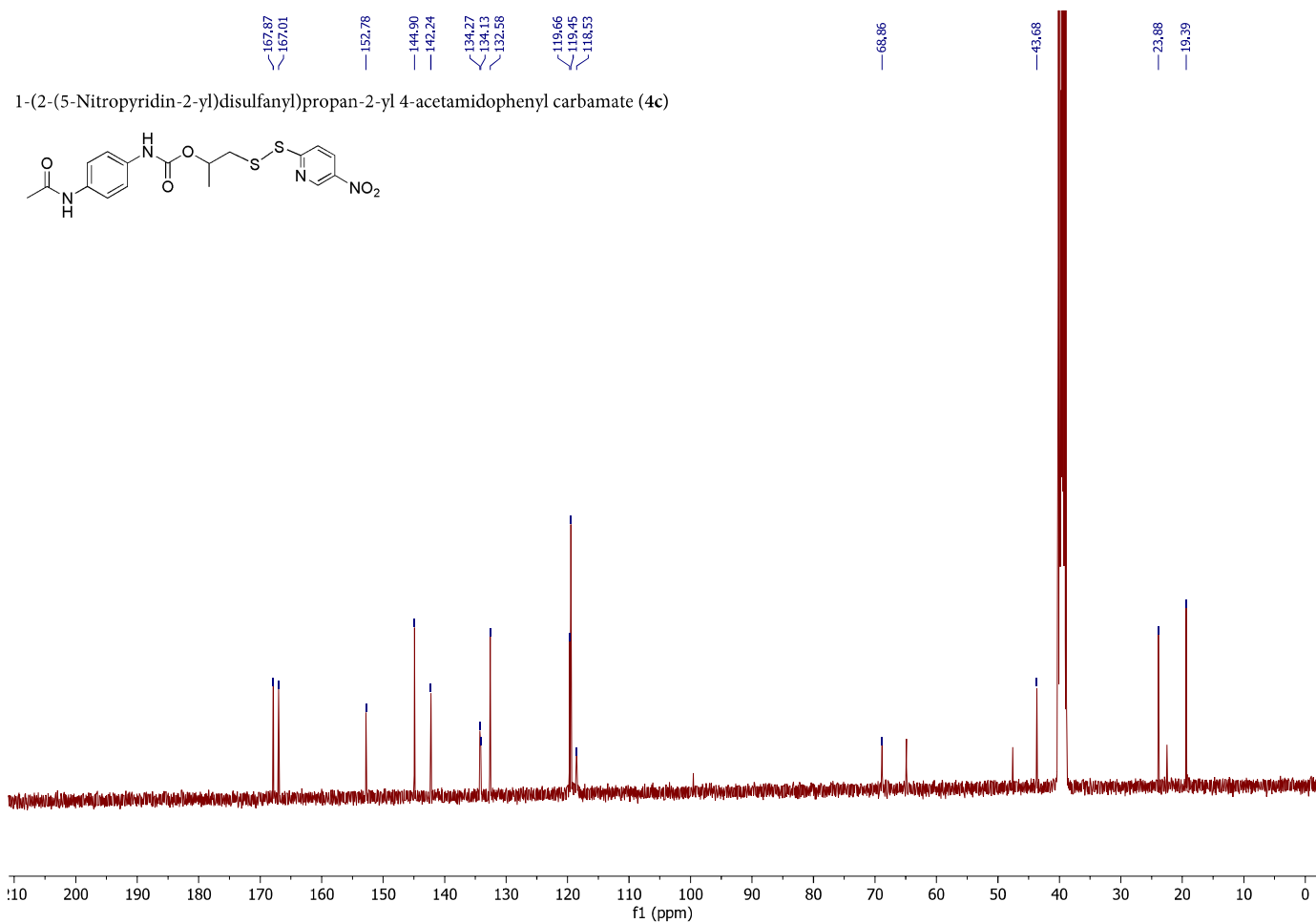


Appendix I.  
NMR spectra

1-(2-(5-Nitropyridin-2-yl)disulfanyl)propan-2-yl 4-acetamidophenyl carbamate (4c)

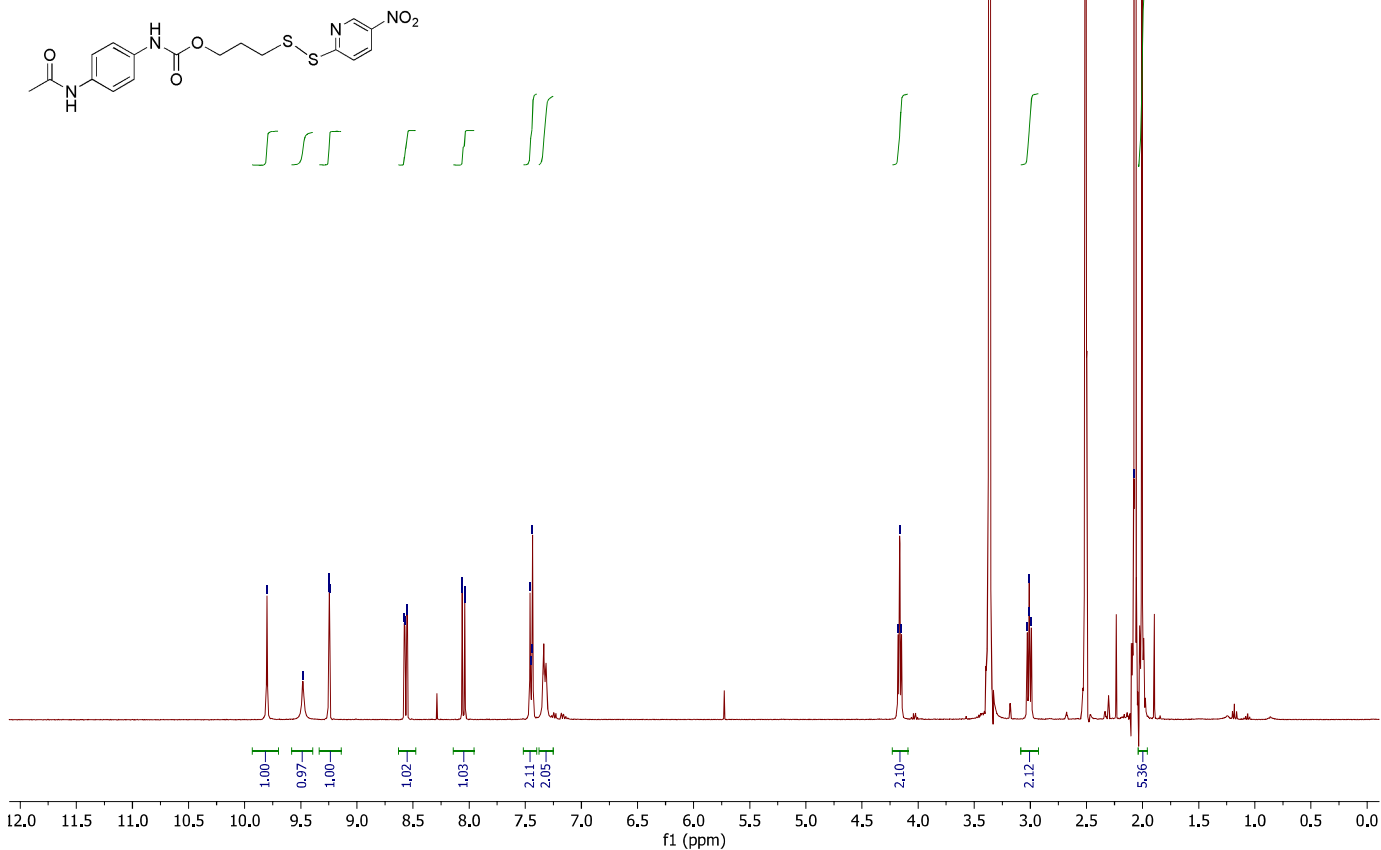


1-(2-(5-Nitropyridin-2-yl)disulfanyl)propan-2-yl 4-acetamidophenyl carbamate (4c)

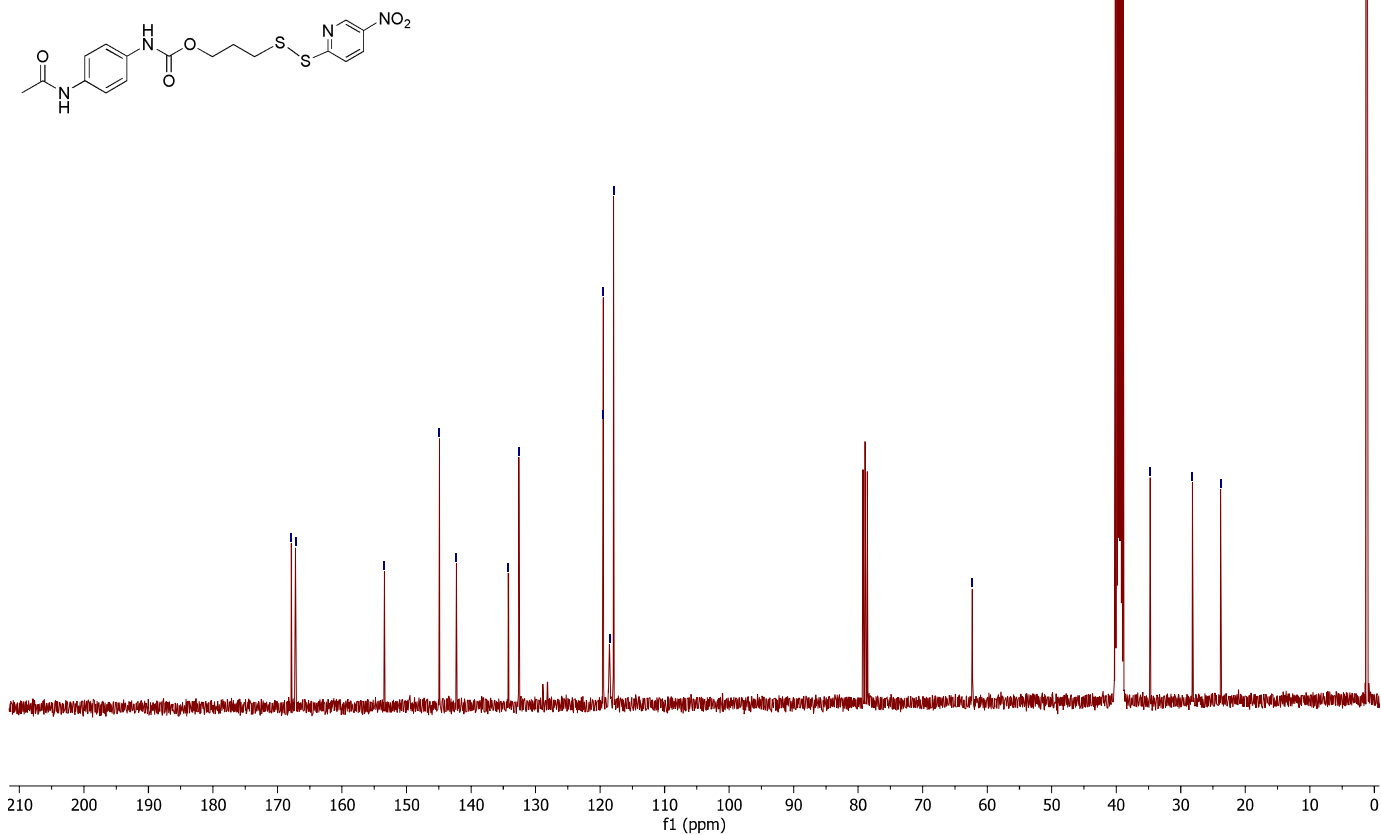


Appendix I.  
NMR spectra

3-(2-(5-Nitropyridin-2-yl)disulfanyl)propyl 4-acetamidophenyl carbamate (4d)

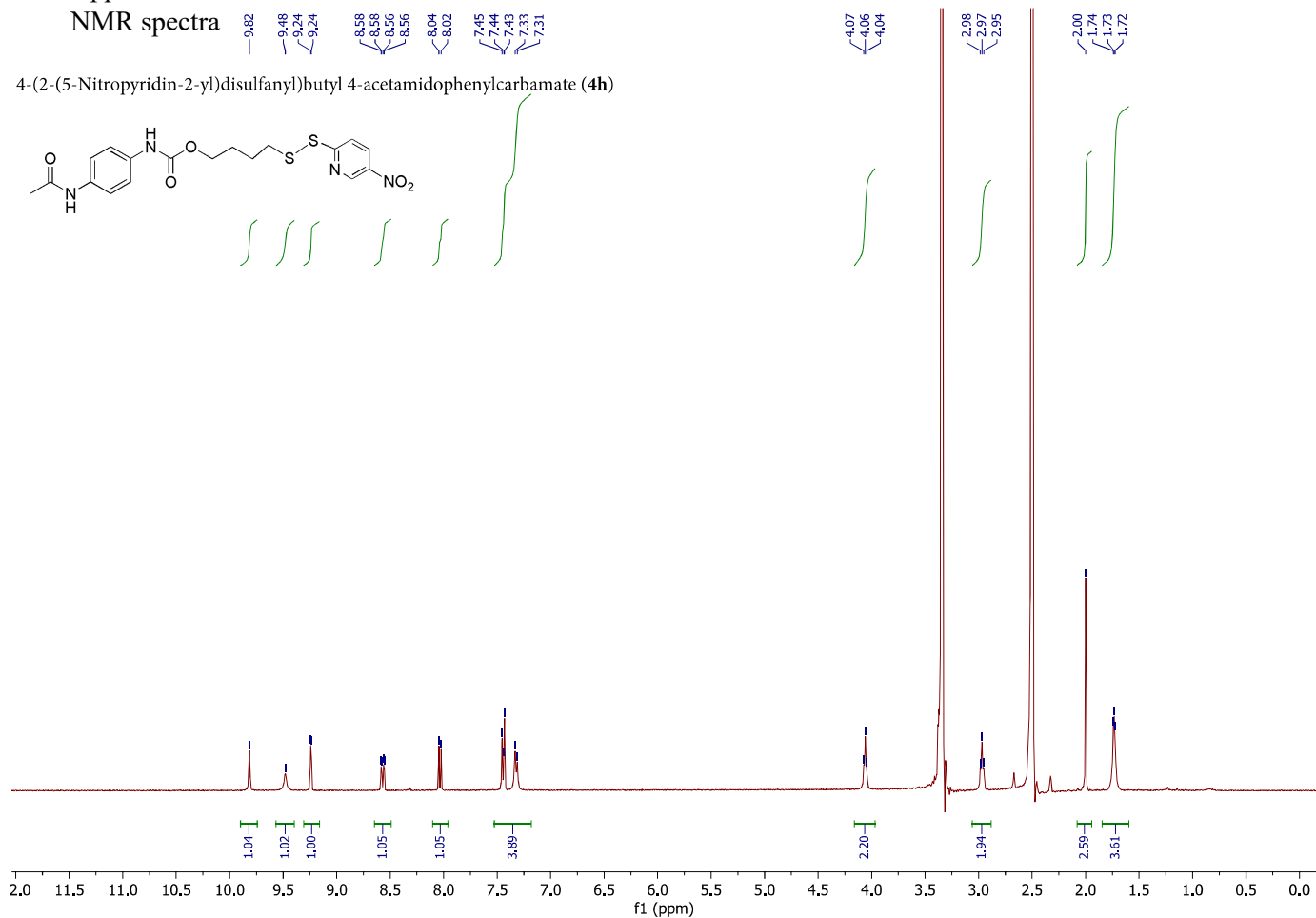


3-(2-(5-Nitropyridin-2-yl)disulfanyl)propyl 4-acetamidophenyl carbamate (4d)

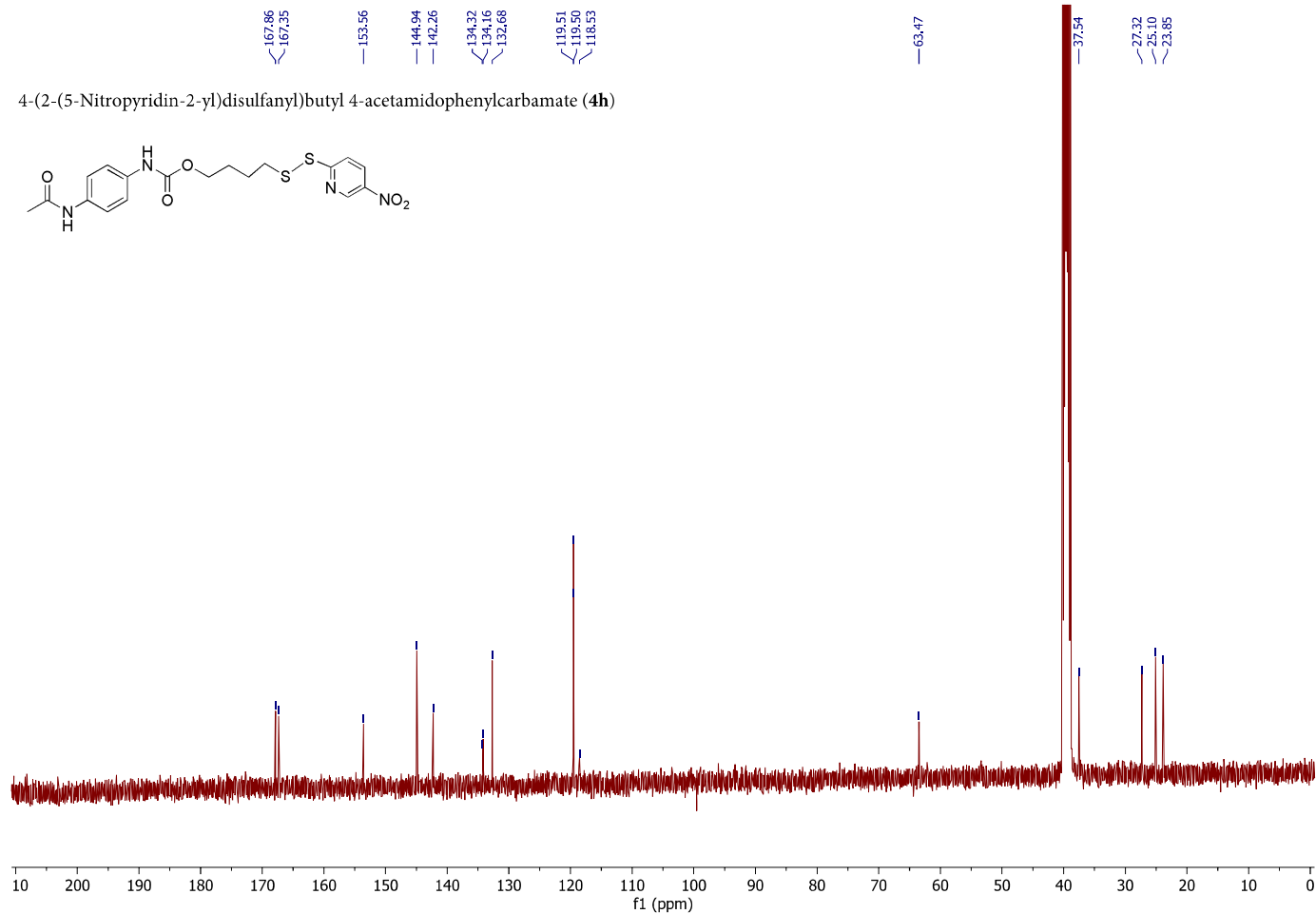


Appendix I.  
NMR spectra

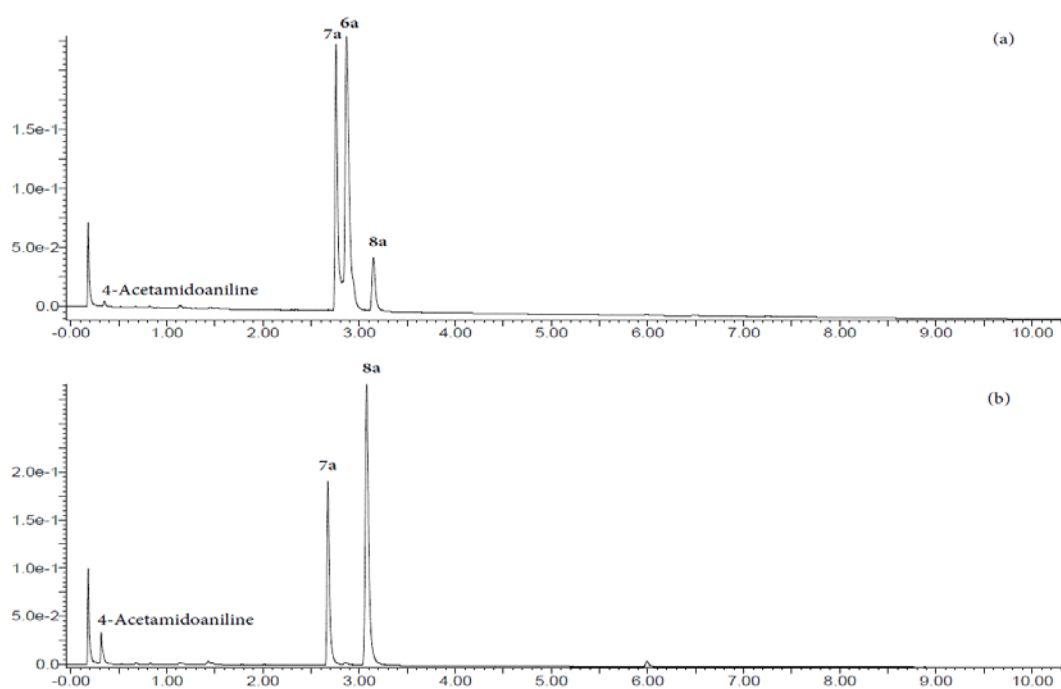
4-(2-(5-Nitropyridin-2-yl)disulfanyl)butyl 4-acetamidophenylcarbamate (**4h**)



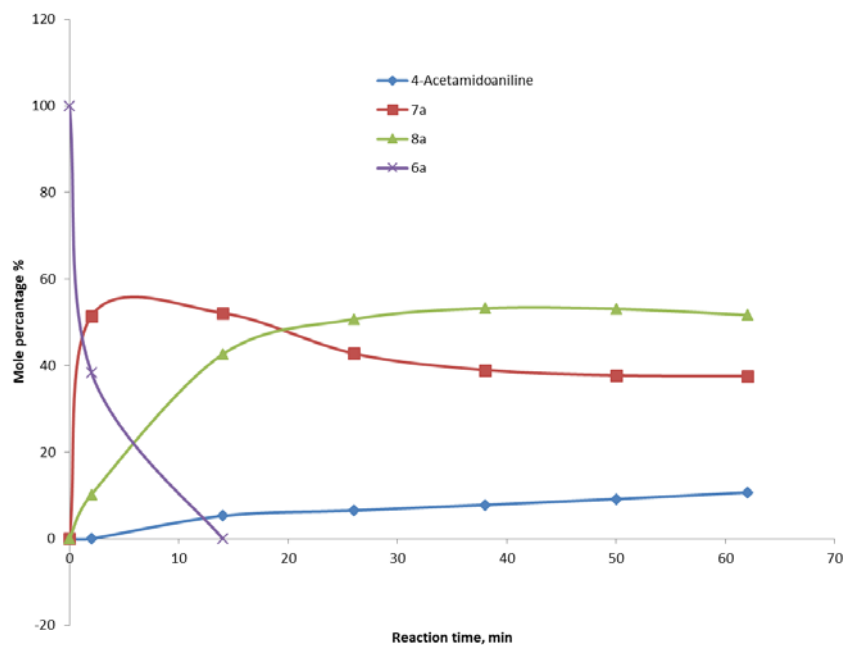
4-(2-(5-Nitropyridin-2-yl)disulfanyl)butyl 4-acetamidophenylcarbamate (**4h**)



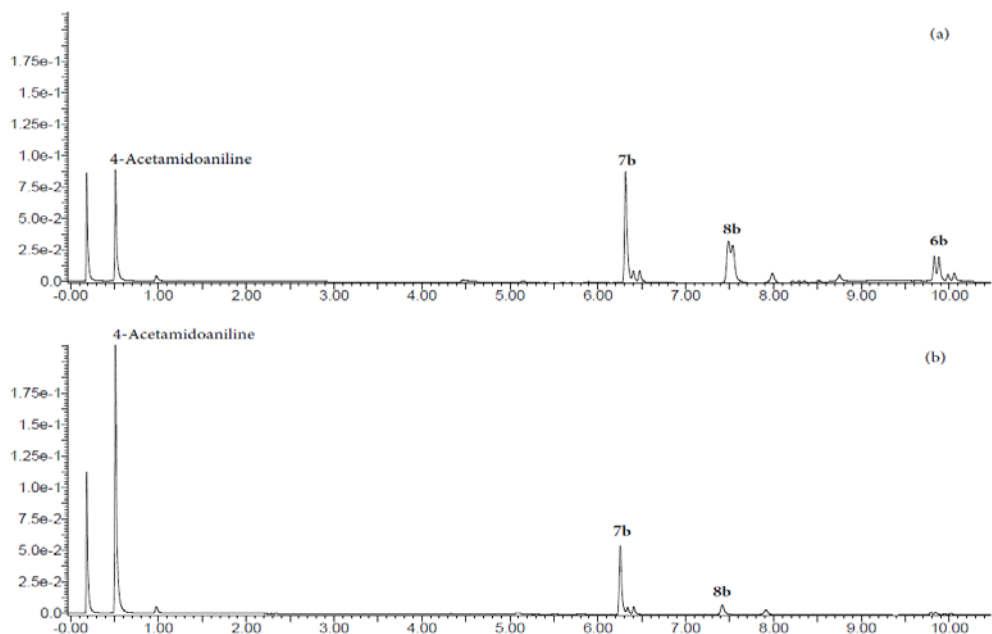
## Appendix II. Degradation analysis



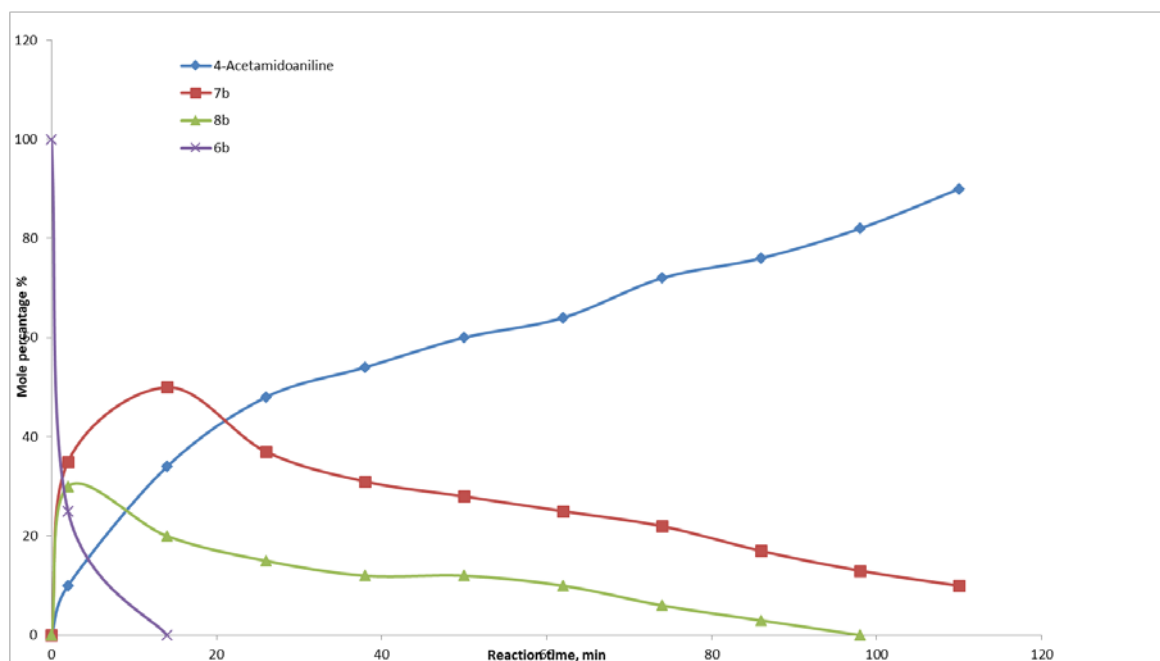
**Appendix II - Figure A1.** UPLC analysis of the degradation products from **6a**. Gradient: acetonitrile 5% to 50% in water in 10 min. a) after 2 min b) after 62 min



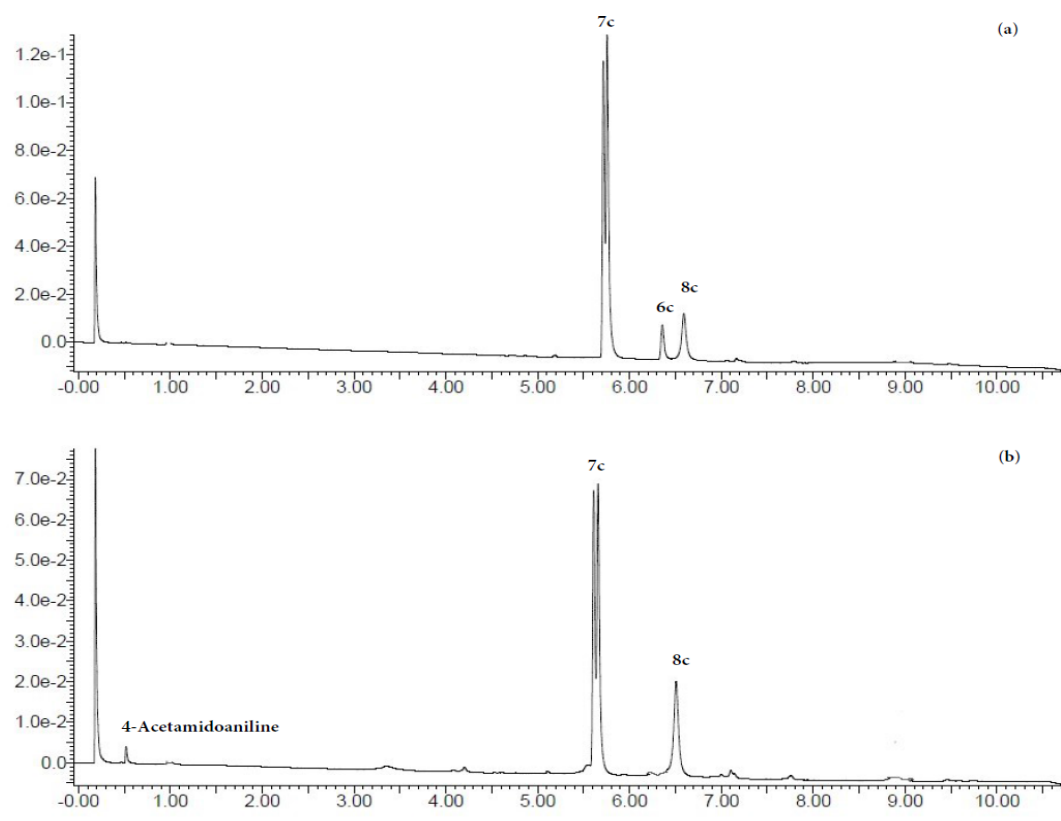
**Appendix II- Figure A2.** Distribution of cargo-containing products as function of time for the reaction between glutathione and **6a**



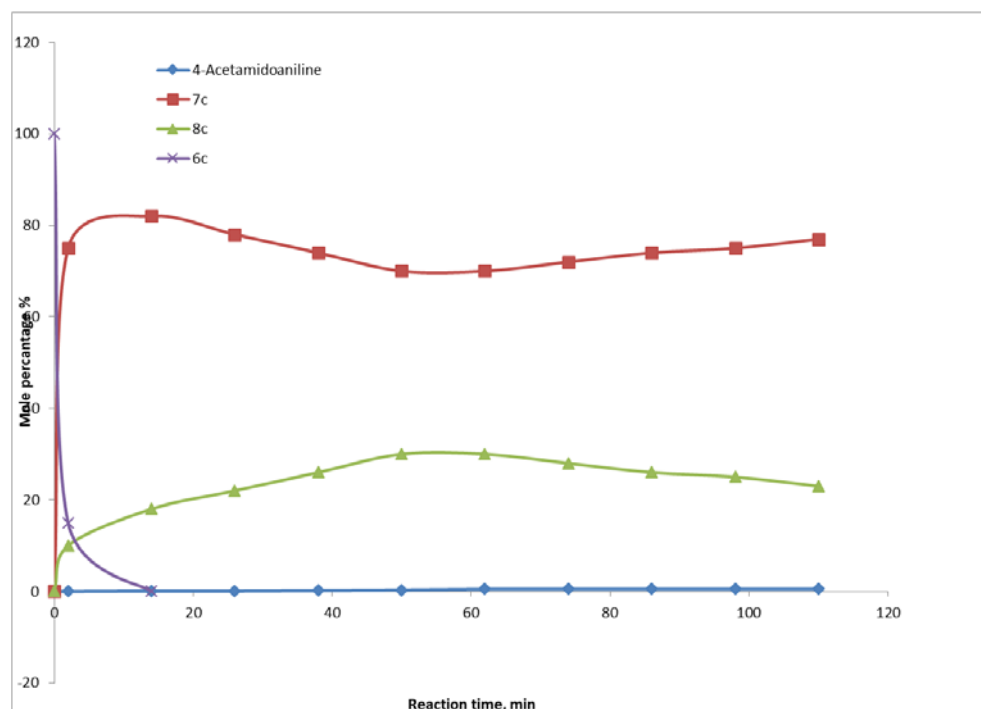
**Appendix II - Figure A3.** UPLC analysis of the degradation products from **6b**. Gradient: acetonitrile 0% to 30% in water in 10 min. a) after 2 min b) after 62 min.



**Appendix II - Figure A4.** Distribution of cargo-containing products as function of time for the reaction between glutathione and **6b**

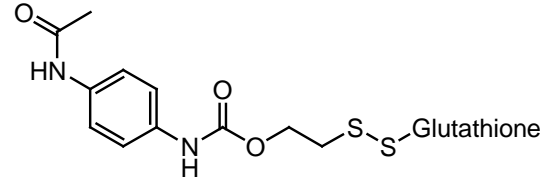
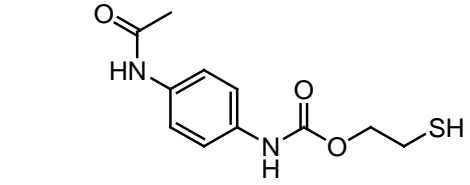
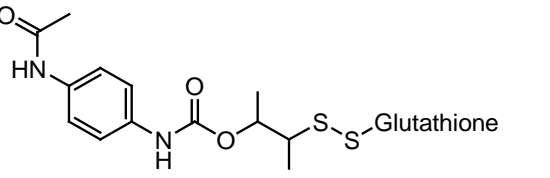
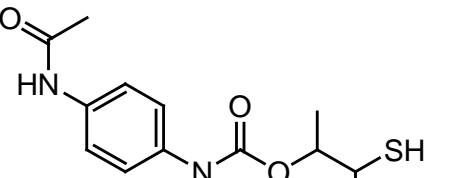
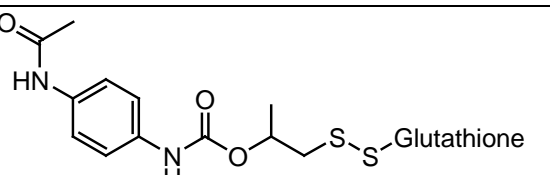
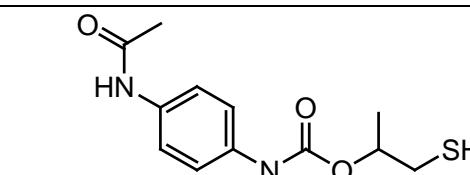


**Appendix II - Figure A5.** UPLC analysis of the degradation products from **6c**. Gradient: acetonitrile 0% to 30% in water in 10 min. a) after 2 min b) after 90 min.



**Appendix II - Figure A6.** Distribution of cargo-containing products as function of time for the reaction between glutathione and **6c**

**Appendix II - Table A1.** Mass spectral data for products of the glutathione-triggered degradation of conjugates **6a-6c**

C-L-glutathione	(C-L)-thiol
 <p style="text-align: center;"><b>7a</b></p> <p>Calcd for <math>C_{21}H_{30}N_5O_9S_2^+</math>  <math>[M+H]^+</math> 560.1485, found 560.1479</p>	 <p style="text-align: center;"><b>8a</b></p> <p>Calcd for <math>C_{11}H_{15}N_2O_3S^+</math> <math>[M+H]^+</math> 255.0803,  found 255.0799,  Calcd for <math>C_{11}H_{14}NaN_2O_3S^+</math> <math>[M+Na]^+</math> 277.0623  found 277.0612</p>
 <p style="text-align: center;"><b>7b</b></p> <p>Calcd for <math>C_{23}H_{34}N_5O_9S_2^+</math> <math>[M+H]^+</math> 588.1798,  found 588.1798</p>	 <p style="text-align: center;"><b>8b</b></p> <p>Calcd for <math>C_{13}H_{19}N_2O_3S^+</math> <math>[M+H]^+</math> 283.1116,  found 283.1116;  Calcd for <math>C_{13}H_{18}NaN_2O_3S^+</math> <math>[M+Na]^+</math> 305.0936,  found 305.0944</p>
 <p style="text-align: center;"><b>7c</b></p> <p>Calcd for <math>C_{22}H_{32}N_5O_9S_2^+</math> <math>[M+H]^+</math> 574.1641,  found 574.1650</p>	 <p style="text-align: center;"><b>8c</b></p> <p>Calcd for <math>C_{12}H_{17}N_2O_3S^+</math> <math>[M+H]^+</math> 269.0960  found 269.0971;  Calcd for <math>C_{12}H_{16}NaN_2O_3S^+</math> <math>[M+Na]^+</math> 291.0780,  found 291.0787</p>







